SCUOLA DI DOTTORATO

UNIVERSITÀ DEGLI STUDI DI MILANO-BICOCCA

Department of Earth and Environmental Sciences

PhD program in Chemical, Geological and Environmental Science Cycle XXXV

Chemistry Curriculum

DEVELOPMENT OF NEW "GENERAL PURPOSE" METHODS TO INTRODUCE FLUORINE-18 IN BIOLOGICALLY ACTIVE MOLECULES

Surname IANNONE

Name MARCO NICOLA

Registration number 854386

Tutor: CRISTINA AIROLDI

Supervisor: SERGIO TODDE

ACADEMIC YEAR 2021-2022

CONTENTS

CHAPTER I

GENERAL INTRODUCTION

1.1 MOLECULAR IMAGING

Screening, characterization and monitoring of biologic processes within living subjects is what we call "Molecular Imaging", which is gaining a constantly growing interest and importance in diagnosis and treatment of a large variety of diseases. Using this methodology, early and advanced phase diseases can be detected without invasive interventions. Well established techniques like X-ray, magnetic resonance (MRI) and computerized tomography (TC) are very useful, but limited to provide images of anatomical biological structures [1]. On the contrary, techniques such as Single Photon Emission Tomography (SPECT) and Positron Emission Tomography (PET), which are based on radiopharmaceuticals administration to patients, are capable to provide information about "functional" status of an organ/tissue, thus allowing, in combination with anatomical imaging techniques, to have a full set of diagnostic information. Thus, Molecular Imaging instruments are strategic in order to detect diseases with accuracy, and to drive the correct treatment and follow-up [2][3][4].

1.2 PET

Positron Emission Tomography (PET) is the most used and the most accurate functional imaging technique. For instance, with PET it is possible to detect and quantify glucose metabolism, in vivo, using [^{18}F]fluorodeoxy-D-glucose as a radiotracer, that allows for cancer diagnosis because most of malignant cells have a higher glucose consumption compared with healthy tissues. In general, PET imaging is often successfully used in cancer diagnosis, evaluation of cancer treatment, and detecting recurrence of tumors in early phase compared with other diagnostic modalities [5]. However, PET may also be useful in the evaluation of other pathologies, such as cardiologic (e.g. stroke) and neurologic diseases (e.g. Alzheimer disease, Parkinson disease) [2].
PET/SPECT work taking advantage of the "signals" emitted by the radioactive decay of radionuclides which are incorporated into suitable molecular structures, and that allow for detection of biochemical changes in organ or tissue [5][6].
In particular, PET works by using a scanning device to detect photons (γ rays) generated by the annihilation of the emitted positrons with surrounding electrons. Emitted photons have very precise physical characteristics (same direction and intensity, opposite verse), whose acquisition allows the software to create an accurate map of the tissue under study (Figure 1) [7][8].

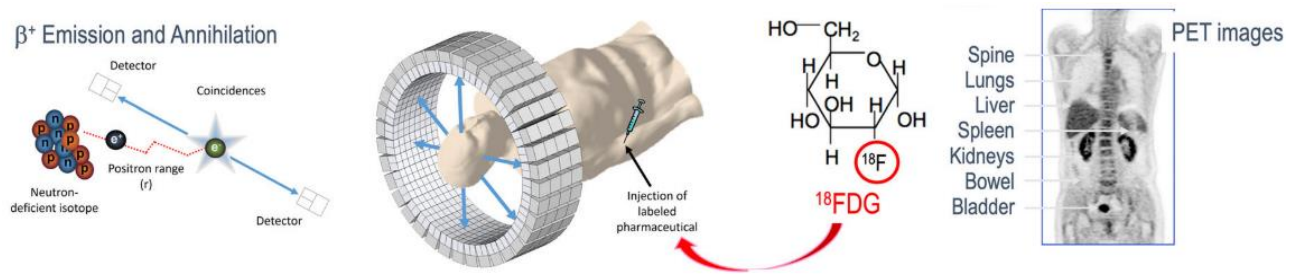

Figure 1.1: *Principle of PET functioning*

A high number of useful radiopharmaceuticals for the diagnosis of various diseases have been developed, to date, the most used of which is still [^{18}F]Fluorodeoxyglucose (FDG).

1.3 RADIONUCLIDES AND RADIOPHARMACEUTICALS

As above mentioned, PET imaging is based on the administration of radioactive substances to the patients, and subsequent reconstruction of images depending on the *in vivo* distribution pattern of the radiopharmaceutical. Radioactivity is a natural phenomenon where an unstable nucleus is spontaneously transformed into a more stable one, due to the emission of particles, often associated with the emission of high energy photons.

There are four different ways a nucleus may release its excess energy and "decay":

1) Emission of α-particles: α decay usually occurs for unstable nuclei with a high atomic number (Z>80). A high energy Helium-4 (^{4}He) particle is emitted and a ${}^{A}_{Z}X$ is transformed into a ${}^{A-4}_{Z-2}Y$ nucleus.
2) Emission of β^- particles: β^- decay occurs when a nucleus has an excess of neutrons. In this type of decay, a neutron is converted to a proton emitting β-particle, which may be considered as a high energy electron, bearing the same electric charge and having the same mass.
3) Emission of β^+ particles (positrons): β^+, decay occurs when a nucleus has an excess of protons. The equation is as follows:

$$ {}^{A}_{Z}X \rightarrow {}_{Z-1}{}^{A}Y + {}_{+1}{}^{0}\beta + \nu $$

$$ {}^{18}_{9}F \rightarrow {}^{18}_{8}O + \beta^+ $$

Figure 1.2: general equation for *β^+ decay and fluorine-18 decay example*

4) Emission by Electron Capture (EC): a nucleus may also relax to a more stable one by capturing one electron from the orbital closest to the nucleus itself, turning a proton into a neutron. The void left by the captured electron is then filled by and electron "falling" from higher energy levels, with simultaneous release of X-ray photons [9]. EC is also typical of nucleus with excess protons and radionuclides that decay with mixed EC/ β^+ are often encountered.
5) Moreover, γ and x-rays may also be emitted during the decay when nuclei are at an intermediate energy level, in the so called "metastable" status. In this case daughter nucleus will have the same atomic and mass number of mother nucleus. An example of this phenomenon, which is called isomeric transition, is provided by the well-known radionuclide technetium-99m, which decays to technetium-99 with a half-life of 6 hours [7][10].

Every radionuclide is unique, and can be differentiated from any other based on its physical characteristics (emitted particle, their relative abundance, half-life, emitted particle energy, type of decay, etc.) that need to be kept into account in order to find the most suitable radionuclide for a particular clinical use.
For example, a relatively short half-life is typical for radionuclides to be used in imaging (e.g. fluorine-18, gallium-68, carbon-11, technetium-99m), while a long half-life is usually mandatory for therapeutic purposes (e.g. iodine-131, lutetium-177, etc.) [4].

Another factor to be considered is availability of a radionuclide, i.e. whether it is produced by a nuclear reactor, by a cyclotron or obtained *via* generators.

The availability of a cyclotron is in principle the best way, as it allows the radionuclide production internally, "on-demand". Cyclotron is a particle accelerator which, thanks to the presence of an electromagnetic field of adequate strength, is able to generate accelerated particle beams (protons). It is a very convenient method to produce radionuclides: for example, in case of fluorine-18 it is possible to produce up to 500 GBq in a single irradiation run [11].
Thus, radionuclides are one of two "elements" of a radiopharmaceutical, the other being the molecular structure to which they are linked (the "pharmaceutical"), and that may be considered as a "carrier" that brings the radionuclide to the desired target organ/tissue.

1.4 PROSTATE CANCER AND RADIOPHARMACEUTICALS

Prostate Cancer (PCa) is the second most common type of diagnosed malignancy in men worldwide after lungs cancer. More than 1.2 million new cases are diagnosed worldwide every year, and global prostate cancer-related deaths exceed 350,000 annually, making it one of the leading causes of cancer-associated death in men [12].

The most used analysis in routine diagnosis of PCa is the PSA (prostate specific antigen) test, which is detected and quantified via a simple and cost-effective blood sample analysis. Unfortunately, 30% of cases PSA levels can be normal even in presence of malignancy, so every test result must be put in correlation with clinical patient history [13][14].
Generally, after PSA screening, a transrectal ultrasonography (TRUS)-guided systematic biopsy of the gland follows in order to give the most accurate diagnosis possible. Finally, multi-parametric MRI (mpMRI) was introduced to improve detection of underestimated tumors and is indicated after negative TRUS-guided biopsy, where suspicion of PCa presence still remains [15]. However, mpMRI only identifies the location of the lesion, but doesn't give functional information of the biologic "hot spot" within the tumor.

Thus, further information are needed in order to improve diagnosis and subsequent treatment plan, and imaging techniques may be the right choice [8][16].
Many PET radiolabeled tracers for PCa screening were developed in the past 30 years [17].

Probably the most used radiolabeled pharmaceutical for PCa screening have been the radiolabeled choline tracers. Choline can be radiolabeled with Carbon-11 or Fluorine-18 (Figure 1.3).

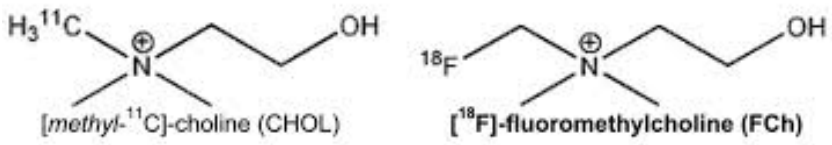

Figure 1.3: *[^{11}C] Methyl-coline and [^{18}F] Fluoromethyl-choline (FCh)*

Choline is an important precursor in the cellular biosynthesis of phospholipids, which are fundamentals molecules in cellular membrane formation [18][19]. Of course, cancerous cells have a

higher proliferation rate compared with healthy ones, and they need more choline for their metabolism [16][18][19].

[^{11}C]Choline is excreted by hepatobiliary system and only a little amount can be found in urinary system and in bladder. Unfortunately carbon-11 half-life is only 20 minutes, which poses some constraints to the number of PET examination/day and can only be prepared if a cyclotron is available; on the other hand, [^{18}F] Fluorocholine is excreted by urinary tract and it can disturb prostate images acquisition, but it is better suited due to the longer half-life of fluorine-18, and the possibility to obtain it from commercial sources [18].
In general, [^{18}F]FCh appears to be useful with high PSA values and repeated negative biopsies. In addition, it is also used to visualize lymph node and bone metastases [20].

Another radiolabeled tracer to detect PCa is [^{18}F]FACBC, also known as Fluciclovine. It is a synthetic isoleucine amino acid analog ("un-natural amino acid") and is brought in cells by amino acid transporters proteins. It has a higher detection rate than [^{11}C]Choline at all PSA values. Moreover, [^{18}F]FACBC is a cell metabolite and shows high sensitivity in primary prostate cancer detection but lack specificity in benign conditions or inflammations [21].

1.5 THE PROSTATIC SPECIFIC MEMBRANE ANTIGEN (PSMA)

In the last decade a very important role in PET imaging and therapy of PCa has been played by PSMA-ligands [22].
PSMA (Prostate Specific Membrane Antigen) is a 750-residue type II transmembrane glycoprotein, also known as glutamate carboxypeptidase II (GPII), N-acetyl-α-linked acidic dipeptidase I or folate hydrolase. It shows a significant expression in prostatic cancerous cells and upregulation in poorly differentiated, metastatic and hormone refractory carcinomas, and it has been identified as a highly attractive target [23]. Moreover, the glycoprotein expression seems to be correlated with disease aggressiveness and presence of metastases [24].
PSMA is a member of zinc-dependent exopeptidase superfamily, which include mononuclear zinc active site carboxypeptidases and carboxy- and aminopeptidases with a binuclear zinc active site. The overall structure is made by a symmetric dimer with each peptide chain containing three domains, analogue to at least four other human proteins: NLDL, NLD2, transferrin receptor (TfR1) and TfR2 [25][26]. Those three residues are divided in: a protease domain (residue 56-116 and 352-591), an apical domain (residues 117-351) and helical domain (residues 592-750).

Protease domain contains eleven α-helices, an eight-stranded β-sheet and insertions which extend a loop joining the sixth and seventh β- strands and include a short α-helix. Moreover, between strands 1 and 2 of protease domain β-sheets is inserted the apical domain, as shown in Figure 1.4. The apical domain is made of two β-sheets, three α-helices and one helical turn. In PSMA it forms half part of the binding cavity.

Finally, the helical domain, consisting of six α-helices and associated connecting regions, forms the other half of binding cavity. Moreover, a very important function of this domain is that involving

three α-helices, which has a role in dimer formation. Only dimeric form of PSMA are expressed on prostate cells surface and has NAALAdase folate hydrolase activity [25].

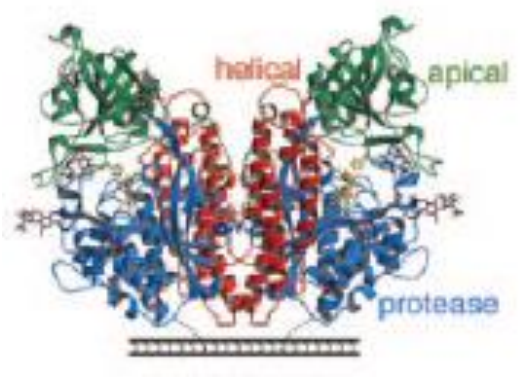

Figure 1.4 – *PSMA receptor domains*

Between apical and helical domain a large cavity is present (≈1,100 Å^2), which includes two nuclei of zinc, separated by ≈3.2 Å, with polar residues, as shown in Figure 1.5. Each zinc atom is coordinated by three endogenous ligands: a histidine (His-553 or His-377), a terminal glutamate (Glu-425) and aspartate (Asp-453) and bridging aspartate (Asp-387). Moreover, a water molecule bridges asymmetrically the two zinc atoms. Water has a crucial role in catalyst activity because a single zinc ion can lower its pK_a from 15.7 to 9.0 and the glutamate adjacent residue (Glu-424) acts as active site base deprotonating the coordinated water, giving to water molecule a hydroxide character. The role of Glu-424 is so crucial that the residue is conserved in all PSMA species and protein family [27][28] (Figure 1.5a).

As shown in Figure 1.5a, substrates containing a glutamate residue take place in S1 and S1' pockets and precisely terminal glutamate substrate residue occupies S1'. Two specific protein residues (Lys-699 and Tyr-700) are the so called "glutamate sensor" in S1' pockets in order to bind selectively a suitable glutamate or glutamate-like moieties residue [28] (Figure 1.5b). As shown, in S1' pocket the hydrolysis of substrate specific peptide bond takes place.
Figure 1.5b shows the presence of another pocket, S1, besides the already explained S1'. S1 pocket contains the so called "arginine patch" comprising Arg-463, Arg-534 and Arg-536 [27]. Moreover, a crystallographic work by Zhang et al. reported the presence of an "arene-binding region" in the S1 site beside the "arginine patch", formed by indole group of Trp-541. Here, the presence of Trp-541 and other amino acid residues like Arg-511 π-interactions with suitable substrates are permitted [26] (Figure 1.5b).

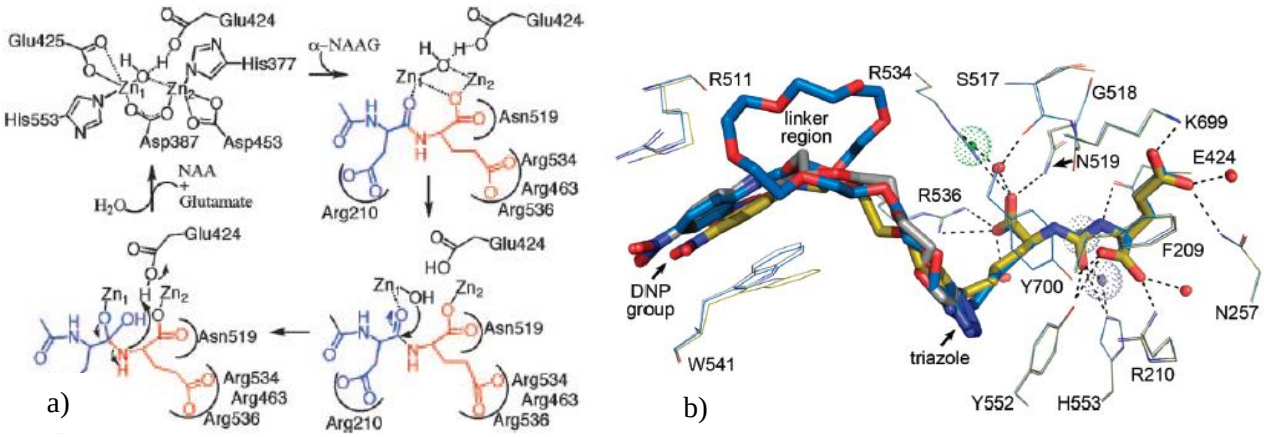

Figure 1.5 – *PSMA receptor binding pockets*

As consequence, in recent years, a new idea of radiotracers for the imaging of PCa took place. The purpose was to synthetize radiolabeled PSMA-ligand, mimetic to the substrate that normally binds the protein [16][29][30]. This approach was extremely relevant because suitable radiolabeled ligands can strongly interact with the binding site outside the cell membrane.

PSMA-ligands demonstrated a great advancement compared to "metabolic" molecules. In fact, PSMA-based radiopharmaceuticals show a higher sensitivity and specificity, especially at low PSA levels [31][32][33]. The above findings brought to a significant growth of PSMA-based ligands for imaging and therapy purposes, and some of them are now commercially available [34][35][36][37][38].
PSMA-based ligands must have a defined structure in order to interact with the antigen. Generally, every ligand can be divided into three parts: i) an "ureido" group, ii) a "specific PSMA linker" and iii) a functional group aimed to link the radionuclide (Figure 1.6).

Ureido group is very important in PSMA-ligand structure because it mimics a planar peptide bond of a GPII substrate but, acting as amide-bioisoster, it resists to enzymatic hydrolysis [27]. The other fundamental structural peculiarity of PSMA-ligands is the specific linker which connects ureido group and functionalization residue. This is the part of molecule which interacts with side chains of "Hydrophobic Pocket" amino acids in S1 site, due to the presence of so-called "arginine patch" and the remote "arene-binding region" (Figure 1.5b). Different linker structures have been tested, showing that they strongly affect a pharmacokinetic [27].

The first specific PSMA-targeting probe was [^{111}In] Capromab pendetide (Prostascint®), whose application was quite limited due to its binding to intracellular domain of PSMA [39]. The most used ligands were initially radiolabeled with gallium-68: [^{68}Ga] PSMA I&T (Imaging and Therapy) and [^{68}Ga] Glu-NH-CO-NH-Lys (Ahx)-HBED-CC ([^{68}Ga] PSMA-HBED-CC or [^{68}Ga] PSMA-11) [33][40][41]. Those two radiotracers showed much higher affinity to PSMA binding motif than Prostascint® and reduced non-specific binding.

First attempt in PSMA-based ligands radiolabeled with fluorine-18 was [^{18}F] DCFBC, developed at Johns Hopkins University which, compared to conventional imaging modalities, detected an overall larger number of lesions in hormone-native and castration resistant PCa patients [24].

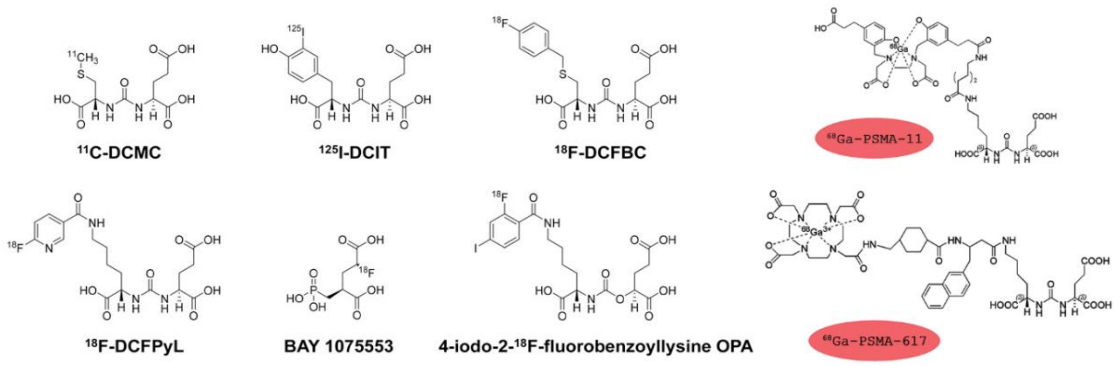

Figure 1.6: *Some PSMA-ligands radiolabelled with different radionuclides*

In 2016, a group from Heidelberg University designed and introduced a new probe called PSMA-617. Here the structural novelty is the presence in the specific linker consisting of 2-naphtylalanine and *trans*-cyclohexane (Figure 1.6 and 1.7). The rigid (cyclohexane) and aromatic amino acids gave the best interaction with protein S1 hydrophobic pocket, especially binding affinity was increased with arene-binding site deep in S1 pocket [42]. The new probe was radiolabeled with gallium-68 and chelated by DOTA. A study showed that [^{68}Ga] PSMA-617 exhibits high binding affinity and is much more internalized in comparison with [^{68}Ga] PSMA-11 [40]. In details, [^{68}Ga] PSMA-617 was much better in terms of renal clearance (20 min vs 24 h), accumulation and retain in tumor. Those studies showed that the presence of specific linker has a significant impact on the tumor-targeting and biological activity as well as on imaging contrast and pharmacokinetics [23].

Since the structural characteristics of [^{68}Ga] PSMA-617 were ascertained to be the best so far, a very interesting challenge was to introduce fluorine-18 on a structurally similar leading candidate. The first PSMA-617 analog was synthetized again by the Heidelberg group, obtaining the new probe [^{18}F] PSMA-1007 [43][44][45] (Figure 1.6). The radiotracer showed interesting binding and internalization properties *in vitro* and high specific uptake *in vivo*.

Based on the above findings, a theranostic approach was proposed, with the aim to translate from imaging to therapy the excellent properties of the above ligands. To this regard, DOTA chelator used in [^{68}Ga] PSMA-617 resulted to permit stable bindings with therapeutic radionuclides like lutetium-177. Studies conducted on castration-resistant PCa patients treated with [^{177}Lu] PSMA-617 showed PSA decline in 64% of patients, including 30% of patients with more than 50% of decline, with an increased overall survival, after two cycles of therapy [46][47].

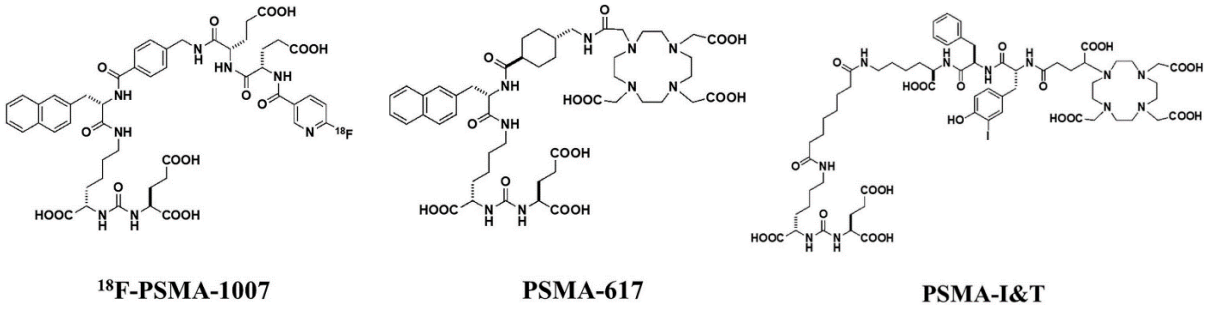

Figure 1.7: *[^{18}F] PSMA-1007, [^{68}Ga] or [^{177}Lu] PSMA-617, [^{68}Ga] or [^{177}Lu] PSMA I&T*

1.6 FLUORINE-18: A CONVENIENT RADIONUCLIDE

Fluorine-18, originally discovered in 1937, is currently the most used PET radionuclide, whose physical properties are summarized in Table 1.1.

It mostly decays by positron emission (β^+= 97%, EC= 3%) with a relatively short half-life time ($t_{1/2}$= 109.8 min) and lower positron energy (maximum 635 keV), that means that it has the shortest positron linear range in tissues, thus giving the highest spatial resolution during PET exam [10][48].

Radionuclide	Half-life time	Decay	Maximal positron energy (MeV)	Theoretical specific activity (Ci/μmol)
Fluorine-18	109.8 min	β^+= 97% EC= 3%	0.635	1712
Carbon-11	20.4 min	β^+= 99.8% EC= 0.2%	0.960	9215
Gallium-68	67.71 min	β^+= 88.9% EC= 11.1%	0.836	2700

Table 1.1: *Fluorine-18, Carbon-11 and Gallium-68 physical properties*

The fluorine-18 half-life is long enough to allow "multi-step" radiosynthetic processes and it is compatible with kinetics and biodistribution of a lot of molecules. The C-F energy bond is 112 kcal/mol compared to C-H bond energy of 98 kcal/mol. It is more thermally stable and oxidation resistant and often yields highly stable products. Moreover, fluorine-18 is produced in large quantities by cyclotron (up to 900 GBq/batch with "dual beam" mode).

All the above properties make it a very advantageous radionuclide for PET imaging [49].
In principle, fluorine-18 can be obtained via different nuclear reactions; however, nowadays it is almost exclusively produced via the nuclear reaction $^{18}O(p,n)^{18}F$, whose threshold energy is 2.3 MeV [48].

1.7 METHODS FOR FLUORINE-18 INTRODUCTION

Fluorine-18 introduction in biologically active molecules has always been a big challenge since the early years, when the first [^{18}F] FDG radiosynthesis was performed.

Fluorine-18 is typically introduced via nucleophilic substitution (S_N2) [50]. [^{18}F]F^-, which is cyclotron produced as an aqueous solution in enriched [^{18}O]H_2O is unsuitable for most transformations due to water solvation [50]. This issue is solved by adsorption of aqueous [^{18}F]fluoride onto an anion-exchange resin column, commonly methylammonium (QMA) cartridges, subsequently eluted with a small volume of a MeCN-water mixture containing a base (K_2CO_3) and a metal-chelating cryptand ligand such as Kryptofix® (K2.2.2.) or tetrabutylammonium salts, serving as phase transfer catalysts (PTC), followed by azeotropic drying [7] [10] [50].
The resulting [^{18}F]F^- is then dissolved in polar aprotic solvents and ready to proceed with the S_N2 reaction [50].

Fluorine-18 may be introduced via both aromatic and aliphatic nucleophilic substitution.

In the last decades a large number of works for fluorination of aryls gave the possibility to obtain a large number of fluoro(hetero)arenes using the most vary types of chemistry.

Fluorine-18 introduction by nucleophilic substitution (S_N2) occurs when the aryl is activated by electron withdrawing groups. Moreover, the electron withdrawing substituent must be a suitable leaving group and should be in *ortho* or *para* aryl position [10][50] (Figure 1.8) and heating (>80°C) is mandatory to success reactions [51]. In Figure 1.8 some possible substituents like diazonium [52] (Figure 1.8 entry a), nitro group , trialkyl ammonium salts (preferentially trimethyl ammonium) [53], halides [50][53] (Figure 1.8 entry b) are shown. These reactions are carried out at high temperatures in polar aprotic solvents.

Moreover, it is important to mention that nowadays new innovative approaches aroused great interest. For example new synthones prepared from anilines as alternative leaving group via SNAr [54] (Figure 1.8 entry c), the use of diaryliodonium salts [55] [56] (Figure 1.8 entry d), fluorine-18-deoxyfluorination of phenols [57][58] (Figure 1.8 entry e) or the use of transition metals like Pd(0) [59], Ni (0) [60], Cu(I) [61] and, more recently, nanoparticles of TiO_2 [62].

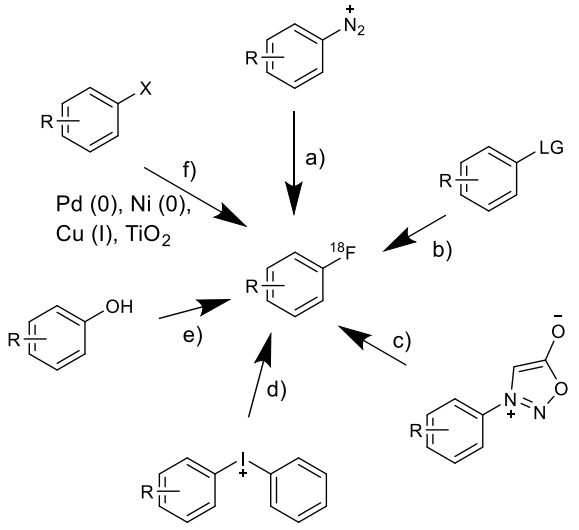

Figure 1.8: *Fluorine-18 introduction on aryles*. a) introduction on diazonium salt, b) introduction on leaving group (-NO_2, -N^+R_3, -Br, -I, …) c) Radiofluorination of sydnones, d) Radiofluorination of aryliodonium salts, e) Deoxyfluorination of phenols via uronium, f) Radiofluorination metal-mediated

The fluorine-18 introduction reaction (S_N2) on aliphatic structures is the other important approach. Formation of Csp^3-F bond is crucial to obtain mimetic of biological molecules (like [^{18}F] FDG) and also it is very interesting to compare metabolic stability with Csp^2-F bond (the case of fluorinated aryls) [63][64]. Generally, this kind of introduction occurs on the nucleophilic displacement of pre-functionalized leaving groups such as halides (Cl, Br), tosylate (OTs), mesylate (OMs) or triflate (OTf) with nucleophilic fluorine. Most of these processes follow a stereospecific bimolecular substitution pathway (S_N2) and are limited to the preparation of primary or secondary alkyl fluoride. Due to the diminished nucleophilicity of fluorine in protic solvents, the S_N2 reactions are generally conducted in aprotic solvents (DMF, DMSO, acetonitrile) heating at high temperatures. Despite of Brønsted basic conditions and the need for high temperatures, and undesired elimination processes can occur, nowadays nucleophilic substitution with [^{18}F]F^- is the most common method for the radiosynthesis of fluorine-18-labelled alkyl-containing radiopharmaceuticals [50][51] (Figure 1.9 entry a).

Again, other very interesting alternative methods are the deoxyfluorination using diethylaminosulfur trifluoride (DAST) or bis(2- methoxyethyl)aminosulfur trifluoride (Deoxo-Fluor) to activate the hydroxyl group [65][66] and, more recently, using PyFluor [67], AlkylFluor [57] and PhenoFluor [68] (Figure 1.9 entry b). In addition, C-F bond can be obtained via reductive elimination from Pd(IV)F complexes on allylic substrates with carefully selected leaving groups [69] (Figure 1.9 entry c).

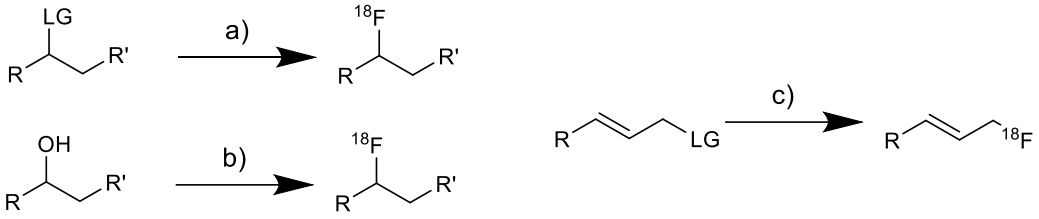

Figure 1.9: *Fluorine-18 introduction on alkyls*. a) introduction on suitable LG, b) introduction by deoxyfluorination c) Pd-mediated reductive elimination on allylic derivatives

In addition, it is interesting to mention about the chemistry of insertion of biologically active -CF_3 group [50] into suitable functionalised substrates. Perfluoroalkylations in radiochemistry still are a challenge but nowadays there is an increasing interest about it. Generally, [^{18}F]CF_3 is obtained by isotopic exchange ^{19}F/^{18}F [70] (Figure 1.10 entry a) but nowadays innovative approaches were studied like [^{18}F]F^- introduction on activated α-bromo-α,α-difluoroalkyls [71] (Figure 1.10 entry b), [^{18}F]F^- exchange on activated α-halogen-α,α-difluoroalkyls (R-CF_2Br) [72], also mediated by 1,8-diazabicyclo[5.4.0]undec-7-ene (DBU) used as nucleophilic activator [73] (Figure 1.10 entry c) and decarboxylation of α,α-difluoro-aryl/alkyl-acetic acids and consequent fluorine-18 introduction by a silver-mediated SET reactions (single electron transfer) [74] (Figure 1.10 entry d).

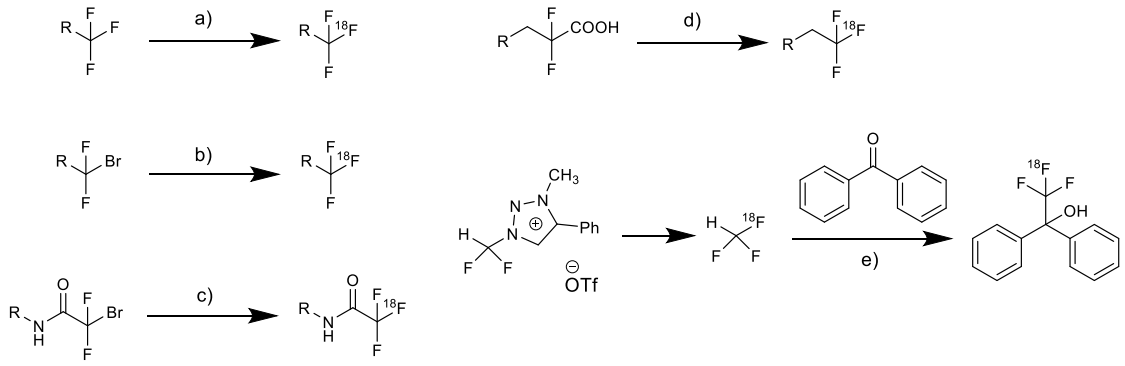

Figure 1.10: *Formation or introduction of CF_3 group:* a) Isotopic ^{19}F/^{18}F exchange, b) α-halogen-α,α-difluoroalkyls exchange, c) Difluorobromo acetamide, d) Fluoro-decarboxylation, e) [^{18}F]HCF_3 formation and introduction [75].

Finally, a very interesting method to introduce [^{18}F]CF_3 is using a reactive intermediate like fluoroform (HCF_3) and subsequent introduction on carbonyl groups (Figure 1.10 entry e). In a paper published by Pees et al. 2021 is indicated the best precursor to obtain [^{18}F]HCF_3 [75] so far.

1.8 CLICK CHEMISTRY – CuAAC REACTION

As shown in the paragraph above, fluorine-18 may be introduced using a large variety of methods and approaches, very different in terms of reaction mechanism, radiochemical yields, specific activity and also reaction conditions.

In general, direct fluorine-18 introduction occurs in polar aprotic solvents and at high reaction temperatures (>80°C). Nowadays macromolecules such as peptides, aptamers, oligonucleotides, antibodies, proteins, and nanobodies such as liposomes, are receiving an increasing attention as potential target for imaging and therapy. Unfortunately, such a "harsh" conditions are not sustainable for macromolecules, whose secondary and tertiary structure may be strongly affected, up to denaturation and complete loss of biological activity.

That's why a variety of indirect methods to introduce fluorine-18 in biologically active macromolecules were developed, to allow reaction in "mild" conditions.
One of the most studied approach is the use of "click-chemistry" reactions, that has recently been recognized as a milestone in the development of new, innovative, synthetic methods by awarding the Nobel prize to the early pioneers Barry Sharpless, Carolyn Bertozzi and Morten Meldal. "Click-chemistry" comprises a set of reactions which are fast, regioselective, easily giving products that can be purified with excellent yields, and often occurs at room temperature in aqueous media [76].

Click chemistry reactions may be divided in four groups:

- cycloadditions of unsaturated species, especially 1,3-dipolar cycloaddition reactions, but also the Diels-Alder family of transformations,

- nucleophilic substitution chemistry, particularly ring opening reactions of strained heterocyclic electrophiles such as epoxides, aziridines, aziridinium ions, and episulfonium ions,

- carbonyl chemistry of the non-aldol type, such as formation of ureas, thioureas, aromatic heterocycles, oxime ethers, hydrazones, and amides,

- additions to carbon-carbon multiple bonds, especially oxidative reactions such as epoxidation, dihydroxylation, aziridination, and sulfenyl halide addition, but also Michael additions of Nu-H reactants [76].

The most investigated "click-reaction" is probably the Cu(I)-catalyzed Huisgen [3+2] cycloaddition between an azide and a terminal alkyne (CuAAC). Fluorine-18 may be introduced in harsh condition, usually via "classic" nucleophilic substitution, on an azide-functionalized prosthetic group and the resulting [^{18}F]fluorine-azide is then conjugated with terminal alkyne-functionalized biomolecule, yielding a stable 1,4-disubstitued 1,2,3-triazole [77][78][79] (Figure 1.11).

The use of Cu(I) is essential to catalyse CuAAC reaction (Figure 1.11). Cu(I) is the less stable oxidation state and it can easily disproportionate in Cu(II) or Cu(0). So, Cu(I) salts need to be used under inert atmosphere (e.g. under nitrogen). That's why the method proposed by Fokin et al. is nowadays the most used: it consists in the reduction *in situ* of Cu(II) salts. In order to apply those

conditions, copper is generally added to the reaction as copper(II) sulfate pentahydrate together with ascorbic acid or sodium ascorbate reductant [80]. Copper (I) formed *in situ* is very reactive especially in aqueous media and catalyse the reaction in an order of magnitude of 10^7 more than Huisgen cycloaddition without copper. Moreover, Cu(II) salts are cheaper and more pure than Cu(I) salts and only 1,4-disubstitued 1,2,3-triazole is often observed as the unique regioisomer [81].

The alkyne deprotonation (Figure 1.11) is very easy and occurs rapidly even in aqueous media. Basic additives like amines should be used only if the reaction is carried out in aprotic organic solvents.
As shown in Figure 1.11 the most reliable mechanism was demonstrated by Fokin and co-workers (based on a DFT calculation) and indicates that the reaction starts when two Cu(I) ions cooperate to form the first C-N bond. The formation of the copper-metallacycle is the rate-limiting step. At first the first Cu(I) centre π-coordinates the alkyne, which is easily deprotonated, then another Cu(I) centre attracts the acetylide complex. In the following step the negatively charged nitrogen on the azide is attracted by σ-bonded copper on acetylide and, when both azide and acetylide are σ-bonded together with copper, C-N formation can occur [82][83].

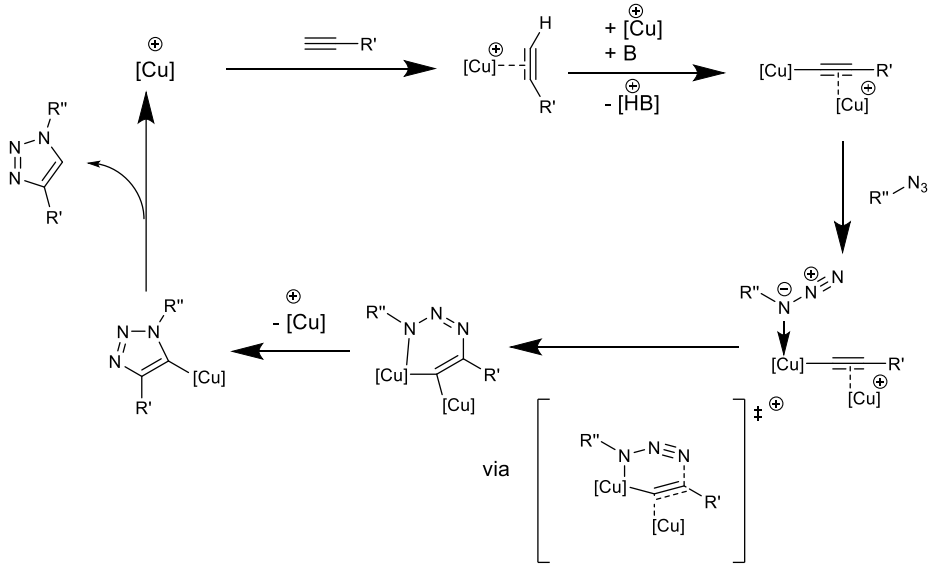

Figure 1.11: *Cu(I)-catalyzed Huisgen [3+2] cycloaddition between an azide and a terminal alkyne (CuAAC).* R' and R" indicate organic residues. In this thesis R" is the residue which contains fluorine-18 (Chapter II).

Direct Cu(I) salts, like CuBr, CuI, $CuOTf{\cdot}C_6H_6$ and others, are used without a reducing base and require acetonitrile as co-solvent and one equivalent of nitrogen base like triethylamine (TEA), diisopropylethylamine (DIPEA) and others. Unfortunately, it often brings to formation of various by-products such as bis-triazoles, 5-hydroxytriaoles, diacetylenes.
Finally, CuAAC reaction was empirically found to be a kinetically second order in concentration of Cu(I) under catalytic conditions. But, at higher metal concentration, due to aggregates formation, the reaction was found to be between first and second order in the concentration of the alkyne. Moreover, it seems that azide concentration doesn't influence reaction kinetics [84].
A potential drawback of this class of reaction, especially in case they are aimed to prepare compounds to be administered to patients, is that copper in the form of Cu(I) ions is cytotoxic, leading to

oxidative degradation of DNA [85] and proteins [86] via hydroxyl radicals formations. For this reason, it is mandatory to oxidise to Cu (II) or reduce to Cu (0) the cytotoxic Cu (I) specie. In any case, Cu(I) may also be quantitatively remove following a suitable purification step.

In addition, due to copper ions cytotoxicity, catalyst-free alternatives "click" reaction methods were developed. For example a strained version of Huisgen [3+2] dipolar cycloaddition [87] (Figure 1.12). The driving force to conduct cyclization is given by releasing the energy contained in the strained cyclooctine when the azide adds to the triple bond (Figure 1.12 entry a).

Alternatives to the Huisgen [3+2] dipolar cycloaddition are represented by inverse electron demand Diels-Alder, for example between a *trans*-cyclooctene and a tetrazine derivative to give a cyclooctapyridazine (Figure 1.12 entry b). Moreover, Staudinger ligation can be employed too: it occurs between an organic azide and a phosphine activated compound. The result is the formation of amidic bond (Figure 1.12 entry c).
Those reaction are advantageous in terms of no-catalytic system and can be carried out in physiological systems.

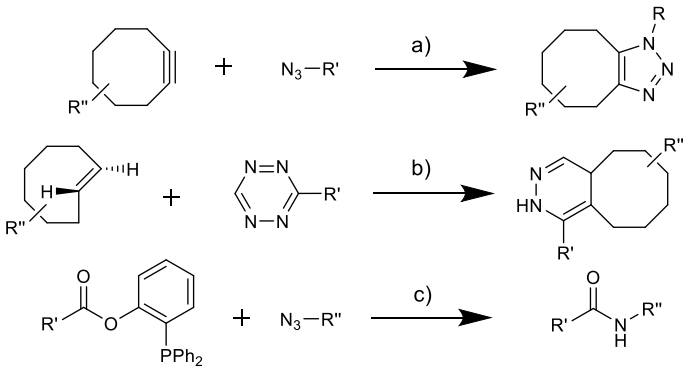

Figure 1.12: *Copper-free "click" reactions*

Recently, other metals have been investigated in order to substitute copper and accelerate the reaction. In particular, zinc and ruthenium complex were found to catalyse the formation of 1,5-disubstitued triazoles from azides and terminal alkynes [88][89].

Anyway, even if copper ion can be cytotoxic, CuAAC offers a very large choice in the design of new molecules and "building blocks". It is a very simple procedure and no by-products are formed. Moreover another advantage is the use in physiologic environment [90].
Thanks to the large use of CuAAC in radiolabelling biologically active molecules, a wide variety of "prosthetic" azido groups were developed. Generally, fluorine-18 is introduced on a suitable azide with a S_N2 nucleophilic substitution heating at high temperature. Then, after the fluorine-18 azide is obtained, the CuAAC reaction is performed at room temperature in conditions showed above.

In Figure 1.13 are shown some examples of the most used and investigates type of fluorine-18 azides and alkynes. One of the most used is for sure the [^{18}F]fluoroethylazide (FEA), which is produced starting from the correspondent tosyl-ethyl azide. It is produced with a high RCY and even reaction

with several alkynes brought good results in terms of reaction rate and yields [91]. Unfortunately, [^{18}F]FEA is volatile and difficult to handle. In addition, the smaller is the azide, the less is table.
So, in order to reduce volatility and increase stability, a [^{18}F]Fluoro-PEG derivative was synthetized and conjugated with several terminal alkyne functionalized biomolecules [92].
Maschauer and Prante developed fluorine-18 azide glycoderivates, which were reacted with propargylglycine [93] and they published the first evaluation in vivo of a terminal alkyne functionalized RGD peptide radiolabelled with a [^{18}F]FDG-β-Az. Results showed an increased blood clearance and stability [94].
Finally, as shown in Figure 1.13, in literature there are also a lot of examples of fluorine-18 radiolabelled terminal alkyne. One example is [^{18}F]serine which was produced in good yields and CuAAC was tested on protected azido-functionalized cRGD [95].

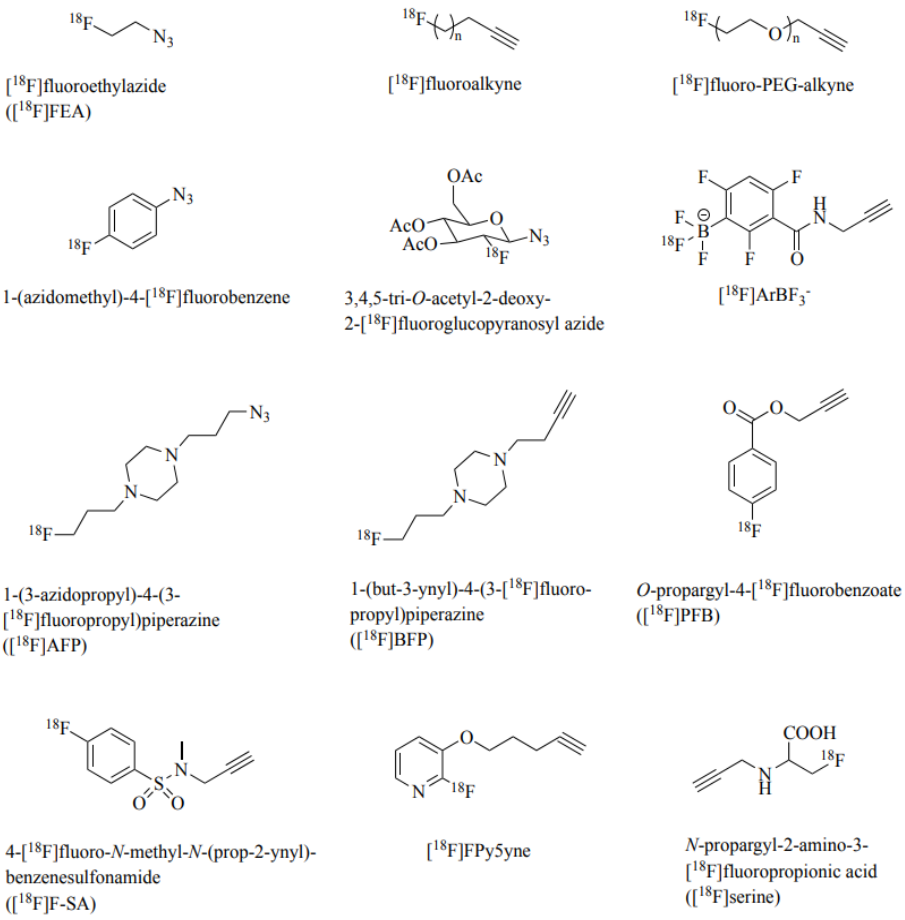

Figure 1.13: *[^{18}F] fluoro-azide examples*

1.9 ALUMINUM-FLUORIDE AND CHELATION CHEMISTRY

In the previous paragraphs, the fluorine-18 introduction with formation of a covalent bond was described. As mentioned, C-F bond is suitable for radiopharmaceuticals due to high *in vivo* stability. Anyway, in the last decade a new, very interesting approach for fluorine-18 introduction in

biologically active molecules was developed. It is a method based on the formation of aluminium-fluoride complexation into a molecule functionalized with suitable chelator, as demonstrated with the pioneering work of McBride et al., who first reported the $[^{18}F]AlF^{2+}$ radiolabelling of IMP449 protein [96].

This method is based on the strength of the bond between fluoride anion $[^{18}F]F^-$ and aluminum cation (Al^{3+}), which is ca. 670 kJ/mol. The resulting salt tends to form thermodynamically stable and kinetically inert metal chelates with polyaminocarboxylate ligands [97]. In addition Al-F bond is stable *in vivo* [98][99].
In practice, fluorine-18 transferred from the cyclotron is converted in its anionic specie, and then allowed to react with $AlCl_3$ salt. In the $[^{18}F]AlF^{2+}$ salt formation, tight control of pH is mandatory. The value must be ~4: a more acidic pH brings to back-formation of $[^{18}F]HF$, while more basic pH lead to insoluble aluminium hydroxide species [100]. Moreover, the use of organic co-solvent is essential for complex stabilization in solution [101]. Al^{3+} ion has a maximum coordination number of 6. So, it can be complexed by suitable pentadentate chelators which occupy 5 positions, the last being occupied by fluorine-18, giving place to a preferential octahedral geometry [102].
Chelator nature is crucial for this kind of chemistry. As shown in Figure 1.14 entry 1, the first chelator studied was an acyclic pentadentate N_3O_4 chelator, with N_3O_2 donor set, the diethylenetriaminepentaacetic acid (DTPA). Unfortunately, often acyclic chelators show poor stability *in vitro* and *in vivo*, [96] thus prompting for testing cyclic chelators, and the use of macrocyclic appeared to be the most suitable for $[^{18}F]AlF^{2+}$ chelation. For example, 2,2′,2″-(1,4,7-triazacyclono- nane-1,4,7-triyl)-triacetic acid (NOTA) and 1,4,7-triazacyclononane-1,4-diacetate (NODA) both showed in Figure 1.14 entry 3 and 4, were very well studied. Both chelators bind with N_3O_2 donor set and forms complexes very stable in solution and *in vivo* with $[^{18}F]AlF^{2+}$ [96][101][103]. NODA and NOTA chelators have been widely used in radiopharmaceutical applications [104][105][106]. Unfortunately, like with all macrocyclic chelators, heating at high temperatures (> 80°C) is mandatory, and those conditions may be too harsh for many biologically active macromolecules.

In order to overcome this problem, Cleeren et al. developed new polydentate ligands that allow chelation of aluminium monofluoride at moderate temperatures (<40 °C), due to a more flexible and non-cyclic structure, which allows to reduce activation energy in $[^{18}F]AlF^{2+}$ ion chelation. Several chelators were synthetized and tested, and the most promising, which were synthetized with an ethylenediamine-N,N′-diacetic acid scaffold in common and different substituent on tertiary amines, (H_3L_{1-4}), showed a very good $[^{18}F]AlF^{2+}$ chelation and good yields at room temperatures [107]. Unfortunately, most of them resulted to be unstable *in vitro* and *in vivo*, except for chelator H_3L_3 (Figure 1.14 entry 6) [107]. In addition, the new chelator was conjugated with the urea-based PSMA inhibitor Glu-NH-CO-NH-Lys to form Glu-NH-CO-NH-Lys(Ahx)L3 (Figure 1.15), and a biodistribution study in healthy mice was performed with the $[^{18}F]AlF$-labeled construct.

Later, the same authors reported about a new chelator, namely (±)-H_3RESCA (Figure 1.14 entry 7), an acyclic pentadentate chelator with a N_2O_3 coordinative set of donor atoms, with increased rigidity and capable to bind $[^{18}F]AlF^{2+}$ complex at room temperature, while at the same time having suitable stability for at least 4 h in rat plasma and phosphate-buffered saline [108]. Moreover, in order to test

its stability *in vivo*, (±)-H_3RESCA was conjugated to human serum albumin with excellent radiochemical yields, and high stability. In addition, an affibody targeting HER2 (PEP04314) and the nanobody NbV4m119 were efficiently conjugated with (±)-H_3RESCA [109].

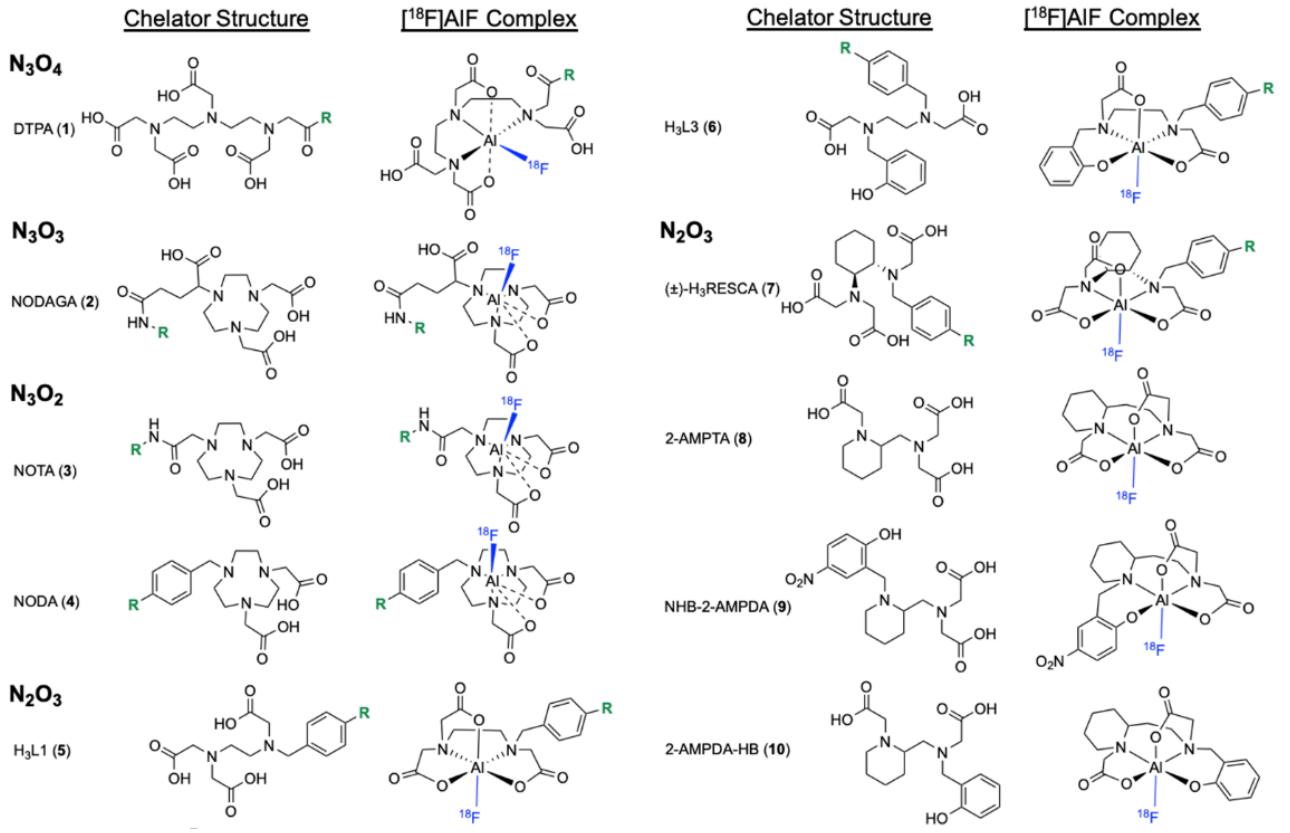

Figure 1.14: *[^{18}F]AlF^{2+}chelators* [102]

As above described, [^{18}F]AlF^{2+} complexation in suitable chelators is a very interesting approach to radiolabel biologically active molecules. Due to good radiochemical yields and sufficient specific activity, many radiolabelled biomolecules were tested in rodents and also brought to clinic for evaluation in patients. In addition, chelators can complex many other metallic radionuclides which can be useful for PET or SPECT imaging, such as gallium-68 and technetium-99m which are used for clinical routine.

An important mention is for PSMA-ligand radiopharmaceuticals conjugated with suitable chelators for radiolabelling by [^{18}F]AlF^{2+} or radiometals complexation. A lot of radiopharmaceuticals were obtained having in common the Lys-Urea-Glu motif, like PSMA-HBED and PSMA-11 (Figure 1.15), which nowadays is perhaps the most widely used agent for prostate cancer PET/CT imaging. Radiolabelling occurs with aluminium-fluoride and gallium-68 [110][111][112] [113][114][115].

In addition, NODA and NOTA chelator are very useful in PSMA-ligand functionalization. The synthesis of [^{18}F] AlF-NOTA(5)-DUPA-Pep (Figure 1.15), [^{18}F]AlF-PSMA-BCH (Figure 1.15) were published showing higher yields and higher stability *in vivo* [116][117]. In details, experimentation in patients [^{18}F]AlF-PSMA-BCH showed a high uptake in PSMA-expressing organs like kidneys,

salivary glands, lacrimal glands, and parotid glands. It is a very interesting compound, which was obtained functionalizing with DOTA chelator the promising PSMA-617 ligand. PSMA-617 was studied by Benesova et al. and was at first conjugated by DOTA for gallium-68 radiolabelling (Figure 1.15) [42] and nowadays is used for therapy after radiolabelling with Lutetium-177 [118][119].

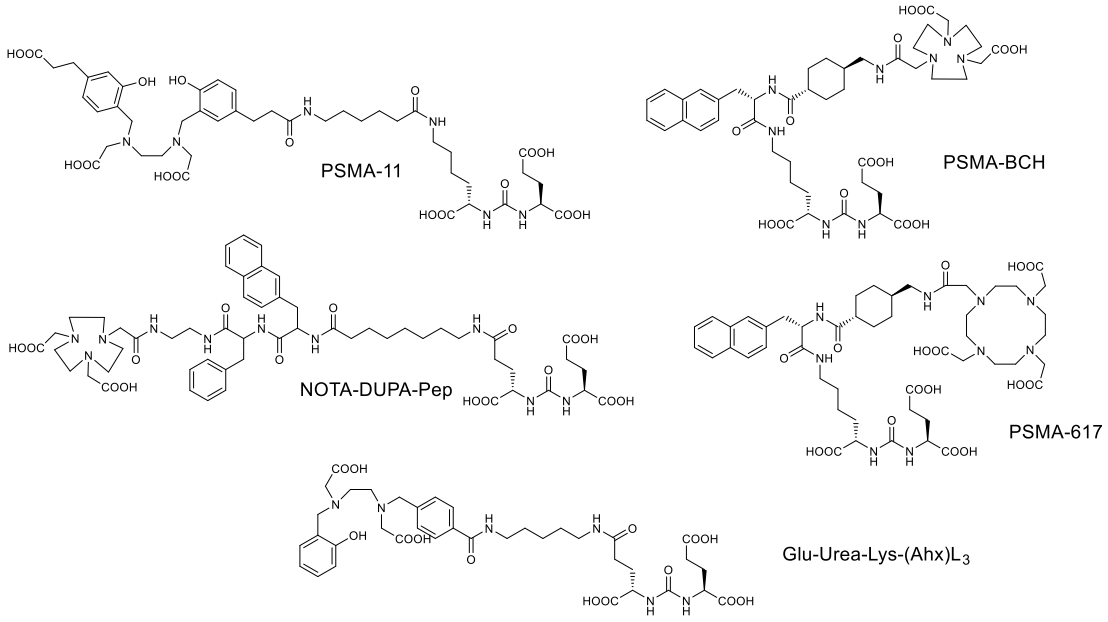

Figure 1.15: *Examples of PSMA-ligands for [^{18}F]AlF^{2+} and [^{68}Ga]Ga^{3+} radiolabelling*

1.10 AIM OF THE THESIS

The present work has been focused on the radiosynthesis and characterization of a series of PSMA-617 derivatives functionalized in different ways, aimed to implement general purpose method for the introduction of fluorine-18, in *mild* conditions, in macromolecules of potential interest as PET radiopharmaceuticals. Indeed, as above reported, there is a growing interest in the radiolabelling of large sized molecules capable of binding with high specificity and selectivity to biological targets involved in the pathophysiology of many important diseases. Three different approaches have been considered, choosing PSMA-617 as a suitable model, due to its well established and suitable *in vivo* behaviour; fluorine-18 was introduced: i) via "click chemistry", ii) by coordination of suitable chelators with [^{18}F]AlF^{2+}, and iii) nucleophilic substitution of potentially new leaving groups. The latter may seem to be contradictory with the stated goal to develop "*mild*" methods, but the idea was to explore the possibility to replace classic leaving groups (e.g. p-toluensulphonyl derivatives) with new ones capable to react with a more favourable thermodynamic. As the precursor for radiolabelling were not commercially available, they have been fully synthesized in the course of the present work. The aim was also to develop automated radiosynthetic routines for the three considered approaches. Finally, depending on the advancement of the various sub-projects, the radiolabelled compounds will be tested *in vivo*, using small animal PET camera, to at least evaluate their pharmacokinetic and biodistribution properties, *in vivo*.

CHAPTER II

Synthesis of new PSMA-617 derivatives and radiolabeling with fluorine-18 with a CuAAC radiosynthetic approach

Publication: Iannone MN, Stucchi S, Turolla EA, et al. Synthesis and automated fluorine-18 radiolabeling of new PSMA-617 derivatives with a CuAAC radiosynthetic approach. *J Label Compd Radiopharm*. **2022**;65(3): 48-62.

2.1 ABSTRACT

This Chapter focuses on the radiolabeling with fluorine-18 of a PSMA-617 derivative via "click chemistry". The copper-catalyzed azide-alkyne cycloaddition (CuAAC) is considered one of the best ways to introduce fluorine-18 on macromolecules in *mild* condition and resulted to be very useful. Chemical synthesis of precursors **2.1** (Figure 2.1) was conducted with an overall yield of ~19%. Then, a two steps radiosynthesis was implemented and automated. Fluorine-18 radiolabeled product was obtained with high purity (radiochemical purity >99%, radiosynthesis time 112 min, ~6% of not-corrected RCY, ~30 GBq/μmol). Moreover, it resulted to be stable *in vitro* and in human plasma.

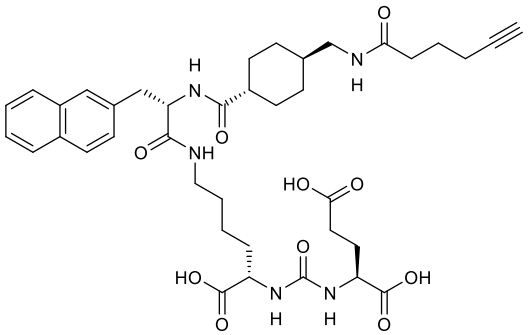

Figure 2.1: *Precursor **2.1***

Thus, a "general purpose" method for the radiolabeling of macromolecules via CuAAC chemistry was developed [120].

2.2 RESULTS AND DISCUSSION

Preparation of "cold" products, as well as NMR characterizations, were implemented in the laboratories of Medical Biotechnology and Translational Medicine Department of Università degli Studi di Milano, under the supervision of prof. Patrizia Ferraboschi and Diego Colombo. Radiolabeled products, RP-HPLC analysis and RP-HPLC purifications were performed in the laboratories of Tecnomed, Foundation of the Università degli Studi di Milano-Bicocca. MS characterizations were performed at Department of Medicine and Surgery of Università degli Studi di Milano Bicocca.

2.2.1 Chemistry

The synthesis of Precursor **2.1** was realized through the obtainment of the following building blocks: Glu-urea-Lys residue, PSMA-617 specific linker, and terminal alkyne, which were separately synthetized and conjugated. Finally, functionalization with terminal alkyne was carried out and the synthesis accomplished by the final deprotection step. After RP-HPLC semipreparative purification the overall yields were 18.8%.

2.2.1.1 Synthesis of Glu-urea-Lys residue

The first building block to be synthetized was Glu-urea-Lys. Protecting groups choice was very important because amino acidic carboxylic groups had to remain protected until the last step of the synthesis. In fact, a basic-resistant protecting group was chosen because basic media were commonly used in this synthetic pathway in order to conduct coupling reactions. Choice felt on tert-butyl ester protection.
As shown in Scheme 2.1, following a procedure described in literature [121], a pure compound **2.4** was obtained with overall yields of 73%.

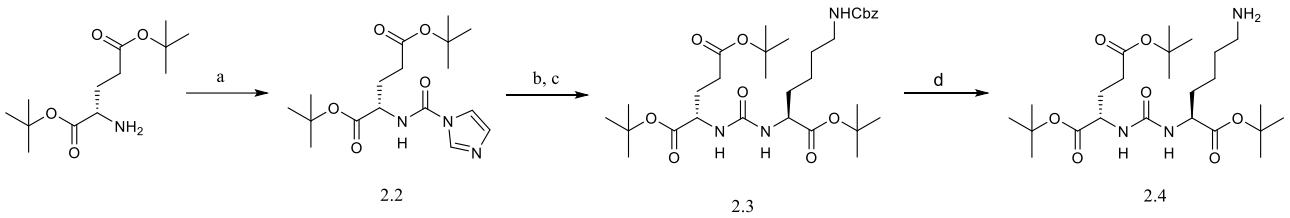

Scheme 2.1: *synthesis of Glu-urea-Lys residue*. Reagent and conditions: (a) CDI, TEA, DMAP, DCM, rt, overnight (92%); (b) MeOTf, TEA, DCE, 0 °C; (c) Cbz-Lys-Ot-Bu, 40°C, 2h (80%); (d) $HCOO^-NH_4^+$, 5% Pd-C, EtOH, rt, 5h (99 %).

Starting from commercial L-di-*tert*-butyl glutamate, carbonylic group was introduced under anhydrous conditions with carbonyldiimidazole (CDI), obtaining the activated acylimidazole derivative (intermediate **2.2**), with the presence of triethylamine and DMAP.
Without conducting reaction under anhydrous conditions, a large quantity of byproducts was formed, probably due to the strong reactivity of acylimidazole derivative with air humidity.
Subsequently, the crude intermediate **2.2** was activated with methyl triflate (MeOTf) in presence of triethyl amine as shown in Scheme 2.2.

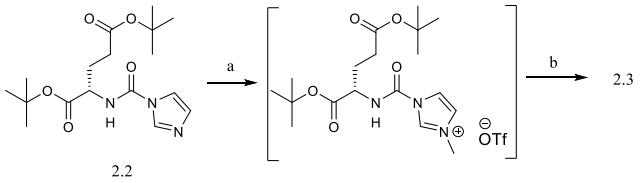

Scheme 2.2: *Activation imidazole mechanism*. Reagent and conditions: (a) MeOTf, TEA, DCE, 0 °C; (b) Cbz-Lys-Ot-Bu, 40°C, 2h (80%).

The activated intermediate was reacted with commercial Lysine, protected as tert-butyl ester on the carboxylic group and as carboxybenzyl derivative on the amino group at the ε position (Cbz-Lys-Ot-Bu), in order to obtain the heterodimer **2.3**.
Yields were satisfactory (80%) and only a few side products were detected.
Anyway, a column chromatography purification was necessary to separate two reaction's byproducts and unreacted Cbz-Lys-OtBu.
After purification with column chromatography, Cbz protecting group on Lys ε position was removed by hydrogenolysis to give intermediate **2.4** (Scheme 2.1).

In this reaction, hydrogen was generated *in situ,* using ammonium formate catalyzed by 5% palladium on carbon.
The reaction progress was monitored by TLC, by detection with ninhydrin: a vivid red spot appears, due to the presence of the reaction product. Yield was >99% and crude **2.4** intermediate was not purified by chromatography because byproducts such as benzylic alcohol and ammonia were separated during the workup and the obtained purity grade was suitable.

2.2.1.2 Specific PSMA-617 linker synthesis

The second retrosynthetic pathway was aimed to synthetize the PSMA-617 specific linker.
In order to minimize byproducts formation, a suitable protection strategy was established, as all possible combinations of dimers can potentially be obtained, with special emphasis for peptide bonds, that can be formed between acid and amine functional groups of two different residue or the same, forming random dimers, trimers and so on.
For this reasons, specific functional groups protection is fundamental to obtain the desired dimer, and to obtain amidic bond between the intended functional groups.
In particular, commercial L-naphthyl alanine was protected on carboxylic group as an ester. At first, a Fischer esterification in acidic media with methanol, in order to obtain methyl ester, was attempted, but no product was formed. Since it is an equilibrium reaction, conditions and substrates were not able to "push" reaction toward product formation: in particular, the water generated during the reaction couldn't be selectively removed by distillation due to methanol evaporation. Thus, a "classical" esterification using thionyl chloride and refluxing ethanol was tested. The compound **2.5** was obtained in very good yields and without the need for further purification (97%) because ethyl ester also resists in basic coupling conditions of the next step.
Moreover, *trans*-4-(aminoethyl) cyclohexane carboxylic acid was protected selectively on amine residue with benzyl chloroformate and after column chromatography intermediate **2.6** was obtained in good yield (96%).
After the two amino acids were protected on selective functional groups, a coupling reaction between intermediate **2.5** and **2.6** was performed. By means of a retrosynthetic approach, the protecting groups were chosen evaluating their stability in subsequent reaction steps (mostly coupling reactions). Ethyl and carboxy benzyl esters are among the most used functionalities resistant to weakly basic conditions of coupling reaction.

Coupling reaction was conducted with (1-[Bis(dimethylamino)methylene]-1H-1,2,3-triazole[4,5-b] pyridinium 3-oxide hexafluorophosphate (HATU) as condensing agent in presence of triethylamine. HATU is a widely used coupling agent in peptide synthesis, especially in solid phase. Although there are many other coupling agents that could be used for the same purpose [122], in our hands HATU gave immediately satisfactory results in terms of coupling reaction yields, and no other agents were tested. During reaction, carboxylic group of intermediate **2.6** is activated by HATU giving a very reactive ester and allowing formation of peptide bond with intermediate **2.5** amine residue. Dimer **2.7** was obtained in good yield and purified by column chromatography. As shown in Scheme 2.3, a selective peptide bond between specific functional groups was achieved.

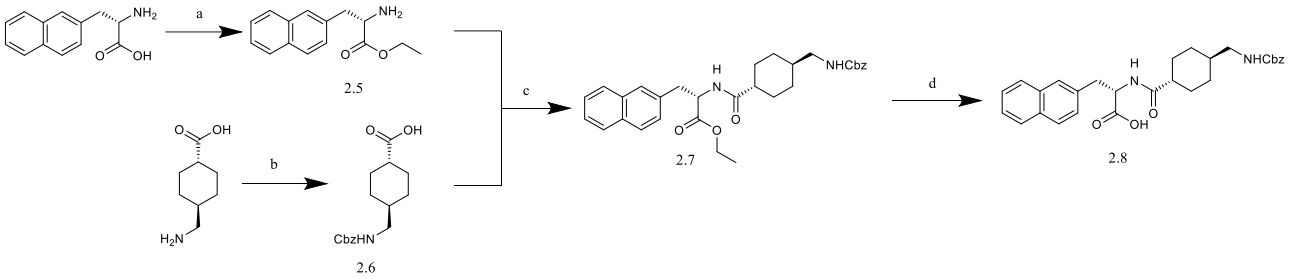

Scheme 2.3: *Synthesis of PSMA-617 specific linker*. Reagent and conditions: (a) $SOCl_2$, EtOH, 0°C-reflux, 3h (97 %); (b) Cbz-Cl, 2M NaOH, THF/H_2O, rt, overnight, (96 %); (c) HATU, TEA, DMF, 0°C-rt, 5h, (90 %); (d) 1M LiOH·H_2O, MeOH/H_2O, 0°C, 2h, (95 %)

Finally, ethyl ester was removed by hydroxylation under basic conditions achieving intermediate **2.8**, which was obtained suitably pure without subsequent purification and with an overall yield of 82%.

2.2.1.3 Coupling and Terminal Alkyne Functionalization

After the two dimers **2.4** and **2.8** were obtained, they were coupled together and final alkyne functionalization was performed.
As shown in Scheme 2.4 the two dimers were coupled through HATU, forming a specific peptide bond through the same mechanism explained above. Intermediate **2.9** was formed in good yields (94%) and purified by column chromatography. The ligand PSMA-617 "core" was finally completed and ready to be functionalized.
The Cbz protection on amine residue was removed by hydrogenolysis and intermediate **2.10** was obtained in good yield (91%) and suitable purity. In this reaction, more equivalents of 5% palladium carbon were necessary, compared with the previous hydrogenolysis step to give intermediate **2.4**, probably due to presence of more amidic nitrogen, which saturated palladium. Under these conditions, the reaction was successfully completed.

Functionalization was achieved coupling intermediate **2.10** with 5-hexynoic acid in order to obtain terminal alkyne - ligand PSMA-617 (intermediate **2.11**). Amide bond was obtained as in the previous reaction steps using HATU, with good yield (89%) after purification through column chromatography.

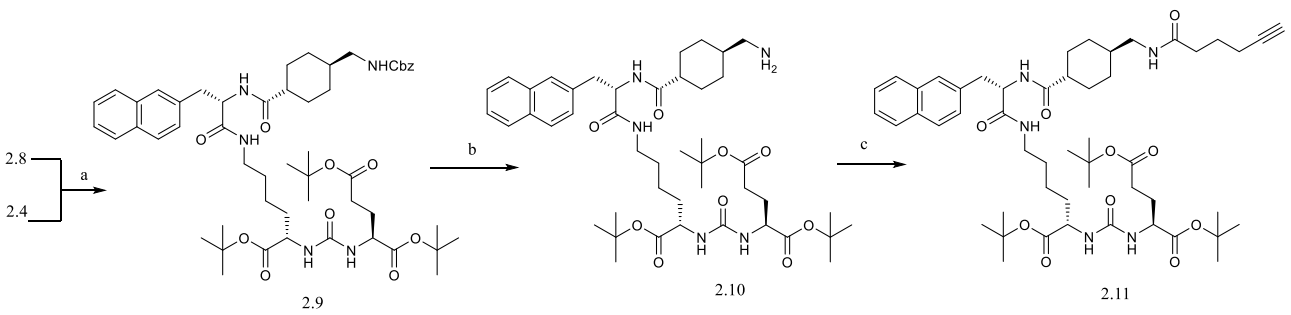

Scheme 2.4: *Preparation of precursor*. Reagent and conditions: (a) HATU, TEA, DMF, 0°C-rt, overnight, (94 %); (b) $HCOO^-NH_4^+$, 5% Pd-C, THF/MeOH, rt, overnight (91 %); (c) 5-hexynoic acid, HATU, TEA, DMF, 0°C-rt, 3h, (89 %).

Finally, the deprotection of Glu-urea-Lys moiety was performed.

Tert-butyl protecting groups were removed in acidic pattern. As shown in Scheme 2.5, two different paths were tested. Best results were obtained dissolving the substrate in dichloromethane, followed

by trifluoroacetic acid (TFA) addition dropwise under anhydrous conditions. Here, anhydrous conditions are essential to avoid large quantity of byproducts, potentially generated by the very acidic conditions, which can degrade the entire oligomer structure.
In the alternative pathway, intermediate **2.11** was dissolved in dioxane and a 4M HCl solution was added. After three days heating at 30°C the crude product was obtained, but for the reasons above mentioned, a larger amount of byproducts was observed. Purity and byproduct formation were monitored by analytical HPLC.

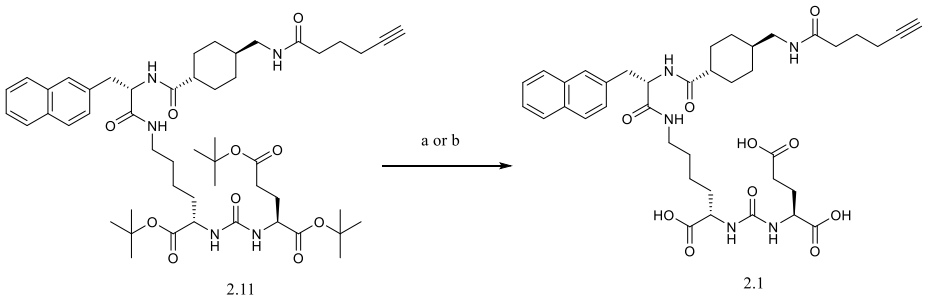

Scheme 2.5: *Precursor deprotection*. Reagent and conditions: (a) TFA, DCM, rt, 2 days, (34 %); (b) 4M HCl, dioxane, 30°C, 3 days, (22%).

Crude product **2.1** had to be purified by semipreparative RP-HPLC in order to remove byproducts and give the requested purity. The most abundant side product, as shown in Figure 2.2, is derived by the complete removal of glutamic acid residue which occurs during deprotection step (13.8 min retention time, with respect to 10.8 min of Precursor **2.1** retention time). It must be removed completely because the by-product also carries terminal alkyne, which can compete in the subsequent CuAAC reaction.

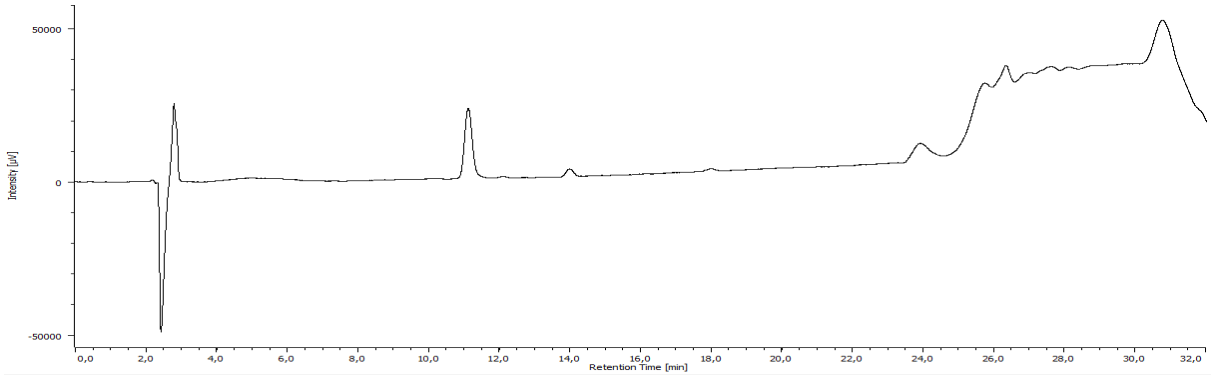

Figure 2.2: *Crude analytical RP-HPLC deprotection profile*. t_R of **2.1** product: 10.8 min, t_R of Glu residue removal: 13.8 min

Finally, the pure product was successfully obtained in ~34% yield after purification.
Moreover, although protecting groups removal was satisfactory, another attempt was executed using a sulfonic acid resin Dowex, in order to remove *tert*-butyl protecting groups and avoiding RP-HPLC purification. Compound **2.11** should enter into resin pores and be deprotected by acidic resin's functionalities, but no suitable results were observed, probably because compound **2.11** was too large to enter resin pores.

2.2.1.4 CuAAC reaction

After product **2.1** was successfully obtained, the development of [3+2] Huisgen dipolar cycloaddition between azide and terminal alkyne was performed. As previously mentioned, CuAAC reaction is the most investigated "click reaction" used to conjugate radiolabeled prosthetic groups on suitably functionalized large biomolecules in *mild* conditions. Reaction was performed using Cu(II)$SO_4 \cdot 5H_2O$ *in situ* reduced by a sodium ascorbate excess, obtaining Cu(I) specie.
As our previous work [120] suggested, the used amounts of copper(II) and ascorbate were quite low compared with those reported by other authors [91] and five-fold diluted catalyst was used, offering a modification which, considered the copper toxicity, is important in view of possible *in vivo* future studies.
In the mentioned previous work, a new azide was synthetized, and its reliability was proved studying CuAAC reaction on commercial non-protected L-propargylglicine. As shown in Figure 2.3 azide **2.12** was functionalized with iodine leaving group, in order to obtain better yields of fluorinated azide (compound **2.13**) during the S_N2 fluorine-18 radiolabeling reaction. Despite other leaving groups like mesylate or tosylate are more frequently used for this kind of purposes, iodine gave higher yields and less hydrolysis and elimination byproducts during fluorination [120].

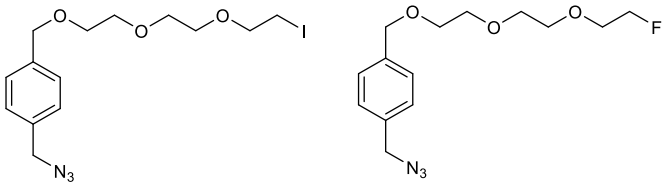

2.12 2.13

Figure 2.3: *Iodine and "cold" Fluorine azide*

The design of the iodinated azide **2.12** was selected for the following reasons: i) the arene ring provide high UV absorbance to the molecule, thus allowing HPLC monitoring of radiolabeling reactions and implementation of efficient purification procedures, ii) the azido group in benzylic position instead of directly bound to the arene ring is more accessible, and thus more reactive during the subsequent click reaction, iii) triethylene glycol residue may potentially improve metabolic stability of the whole molecular structure, *in vivo*.

Precursors **2.13** and **2.1** were reacted together with copper(II)$SO_4 \cdot 5H_2O$ and sodium ascorbate. The resulting triazole **2.14** was used as "cold" reference standard for identification of the desired radiolabeled compound using radio-HPLC.

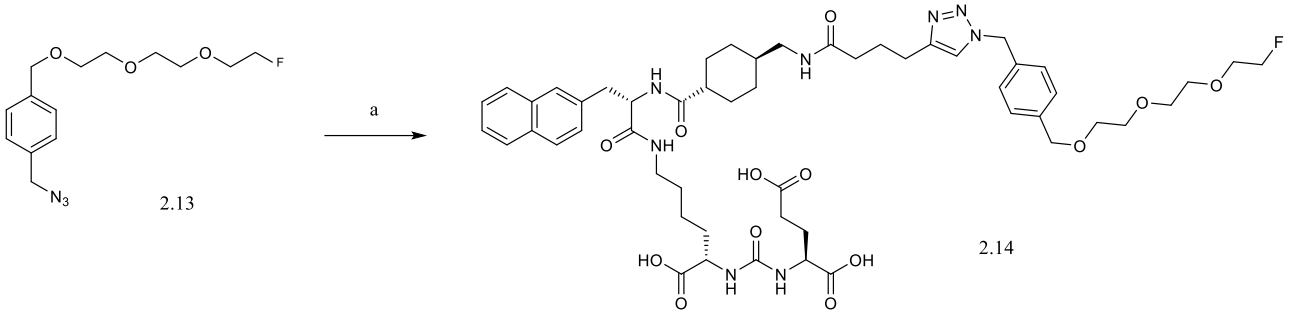

Scheme 2.6: *CuAAC reaction*. Reagent and conditions: (a) Precursor **2.1**, Cu(II)$SO_4 \cdot 5H_2O$, sodium ascorbate, EtOH/H_2O/ACN, rt (45 %).

Reagent	Equivalents	Dilution
Precursor **2.13**	1	In 100 µl ACN
Precursor **2.1**	1.1	In 200 µl MeOH
Cu(II)$SO_4 \cdot 5H_2O$	1.8	In 100 µl H_2O
sodium ascorbate	5.4	In 100 µl H_2O

Table 2.1: *CuAAC Reaction conditions*

The major hurdle to be overcome was caused by the different solubility of the various involved chemical species. Indeed, $CuSO_4$ is soluble only in water and methanol, while sodium ascorbate is soluble in water and poorly in alcohols. On the other hand, fluorinated azide **2.13** can be dissolved in any organic solvent, while precursor **2.1** is not soluble in water and acetonitrile, and it can be diluted in ethanol or methanol only after sonication but tends to precipitate after a little time. The same behavior was observed using dimethyl sulfoxide. The better compromise was conducting the reaction in a mixture of methanol, water and acetonitrile as solvents.

In order to obtain cold product **2.14**, freshly diluted reagents had to be added and the reaction was stirred vigorously and sometimes sonicated. In this case, only a negligible quantity of precipitate was noticed. Those conditions resulted suitable for a "cold" CuAAC reaction, and the step next was to verify whether the above conditions could be adapted to the case of reaction with radioactive [^{18}F]fluoro azide using the peculiar automated radiosynthesis system.

Reaction was monitored by analytical RP-HPLC at time 0, after 5, 10 and 20 min.

As shown in Figure 2.4, reaction could be considered completed after 10 min.

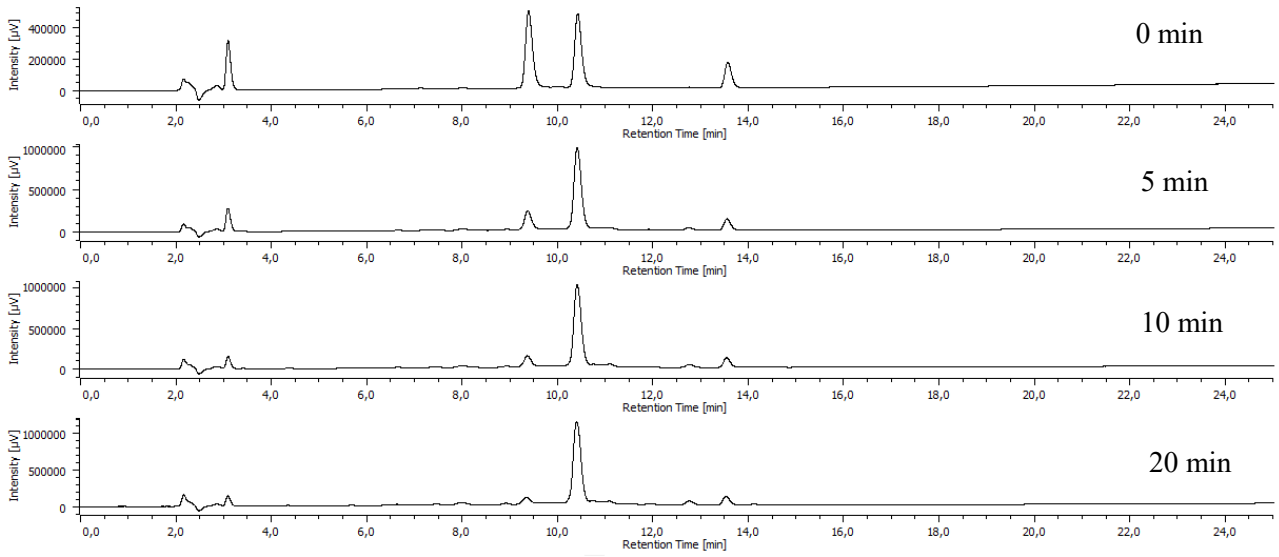

Figure 2.4: *CuAAC monitoring*. Rt Precursor **2.1**: 9.2 min; Rt Product **2.14**: 10.4 min; Rt Precursor **2.13**: 13.5 min.

Once completed, the reaction was quenched dropping 1M HCl and precipitate was solubilized with 400µl acetonitrile. Addition of HCl is important because it permits Cu(I) specie oxidation, obtaining a Cu(II) $CuCl_2$ soluble salt, present in non-catalytic amount. Finally, pure product was obtained after semi-preparative RP-HPLC.
After lyophilization, pure triazole **2.14** was obtained in 45% yield and excellent purity, as confirmed by NMR and ESI-MS mass spectrometry characterization.

2.2.2 Radiochemistry

Macromolecules like proteins, oligomers, ribonucleotides but even large peptides are very sensitive to strong reaction conditions. Temperature is a very important parameter to consider because at high temperatures those macromolecules can denature. $[^{18}F]F^-$ is typically introduced in the desired molecular target via nucleophilic substitution reactions, whose conditions (> 70°C, organic solvents) are not compatible with the need to maintain structural integrity of macromolecules [123].
Thus, radiochemical synthesis was divided in two parts. At first the precursor **2.12** was radiolabeled with fluorine-18, and then the resulting intermediate **[^{18}F] 2.13** was allowed to react with terminal alkyne functionalized product **2.1** in order to obtain product **[^{18}F] 2.14** under *mild* conditions through CuAAC reaction.
The reactions were performed on a Trasis-All in One radiosynthesis module and the entire procedure was automated.

2.2.2.1 Fluorine-18 radiolabeling

In order to afford the desired labelled azide **[^{18}F] 2.13**, various experiments were performed.
Fluorine-18 was produced on-site following standard protocols for an 18 MeV proton beam cyclotron. At the end of bombardment (EOB), fluorine-18 was transferred to the radiosynthesis module in form of $[^{18}F]$hydrofluoric acid solution in water and trapped onto an anionic exchange cartridge (QMA), which was then eluted with a potassium carbonate solution, carrying fluorine-18 in potassium salt form into the automated system reactor. Then, a cryptand (Kryptofix 2.2.2) dissolved in acetonitrile

was added and the mixture was azeotropically distilled to provide anhydrous $K^+[^{18}F]F^-$/K.2.2.2 salt. Fluorine-18 in this form was ready for the S_N2 reaction.

As shown in Scheme 2.7, precursor **2.12** was reacted with fluorine-18 in "harsh" conditions (100°C for 20 min) [123]. The chosen solvent was acetonitrile (1 ml) and the solution was placed into the reactor.

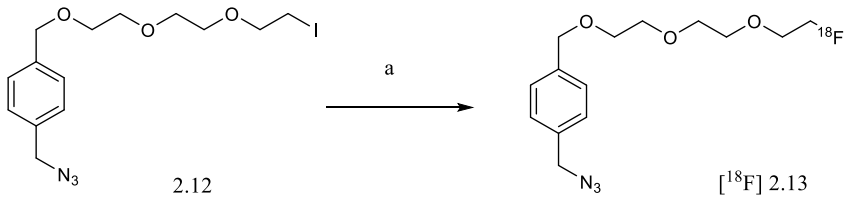

Scheme 2.7: *Fluorination reaction*. Reagents and conditions: (a) $K^+[^{18}F]F^-$/Kryptofix 2.2.2, dry CH_3CN, 100°C, 20 min, (25-36%).

After 20 minutes of reaction, temperature was decreased to 50°C and the crude mixture was diluted with water obtaining a solution water/acetonitrile 90:10. It was then passed through a tC18 Sep-Pak cartridge previously conditioned with 10 ml of ethanol and 10 ml of water, resulting in **[^{18}F] 2.13** trapping. After elution on Sep-Pak the trapped crude mixture was separated from unreacted fluorine-18.
This nucleophilic substitution yields significant amounts of byproducts, due to the particularly strong reaction conditions; moreover, due to the large molar excess of precursor **2.12**, unreacted precursor is also of concern.

As shown in previous studies carried out in our laboratory [120], main byproducts were generated both by hydrolysis and elimination reactions. Both by-products still carry the azide group because hydroxyl or double bond are formed in place of CH_2-I bond. Those two byproducts resulted to be very abundant and had to be removed because they could interfere in the next CuAAC reaction (figure 2.5).
Considered that semi-preparative HPLC had to be used for product **[^{18}F] 2.14** final purification, and that with the automated system only one HPLC purification in the same radiosynthetic procedure was practically feasible, a method for the SPE purification of the crude mixture of **[^{18}F] 2.13** had to be developed.
Hydrolysis byproduct is more polar than product **[^{18}F] 2.13**, as shown in figure 2.5, so it could be eluted washing cartridge with suitable water/acetonitrile mixture.

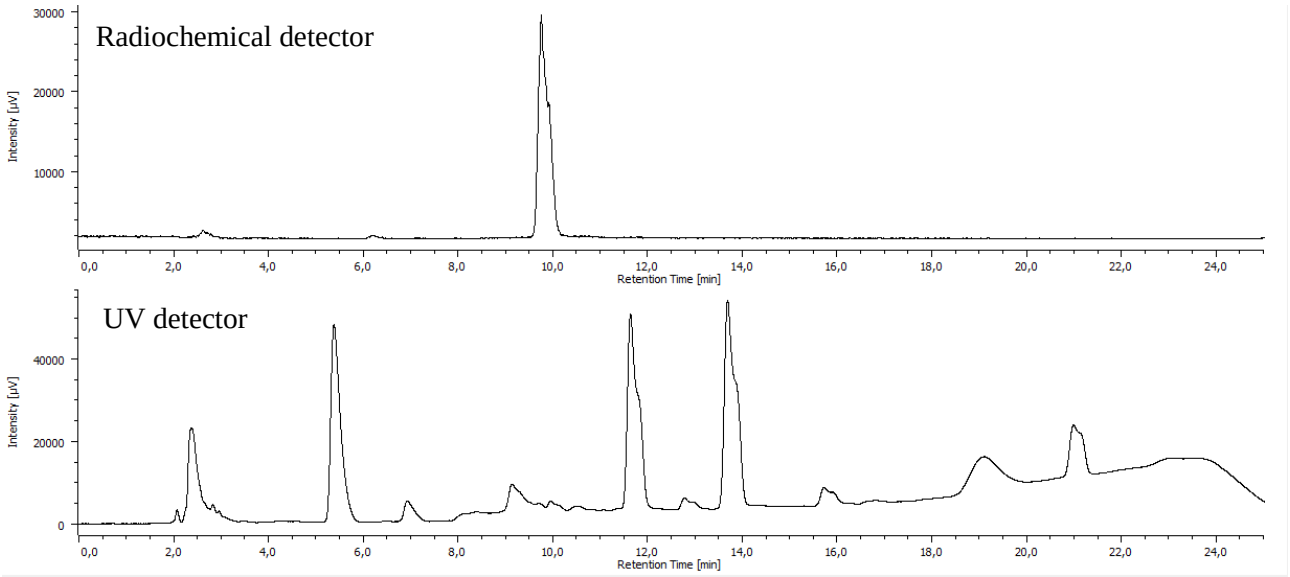

Figure 2.5: *Chromatogram of crude reaction mixture of* ***[^{18}F]2.13***. Crude mixture: Rt **[^{18}F]2.13**: 9.6 min; Rt hydrolysis byproduct: 5.2 min; Rt elimination byproduct: 11.4 min; Rt compound **2.12**: 13.5 min.

At first attempt the tC18 Sep-Pak was eluted with a solution of water/acetonitrile 80:20. Results showed a good UV chromatogram due to the removal of hydrolysis byproduct, but some of the desired product co-eluted (around 30% of product **[^{18}F]2.13** was desorbed by 80:20 elution, Figure 2.6 entry "a" and "b").

Finally, after purification, the mixture was desorbed by Sep-Pak cartridge eluting with 1 ml of acetonitrile. As shown in Figure 2.6 entry "c" and "d", around 70% of [^{18}F] fluorine-azide was collected into the vial and no hydrolysis by-product was collected.

As a loss of activity of ~30% is significant, various attempts by changing eluent ratio or also using a different C18 Sep-Pak cartridge were performed, but purification efficiency did not improve. However, at least the predominant hydrolysis by-product could be removed.

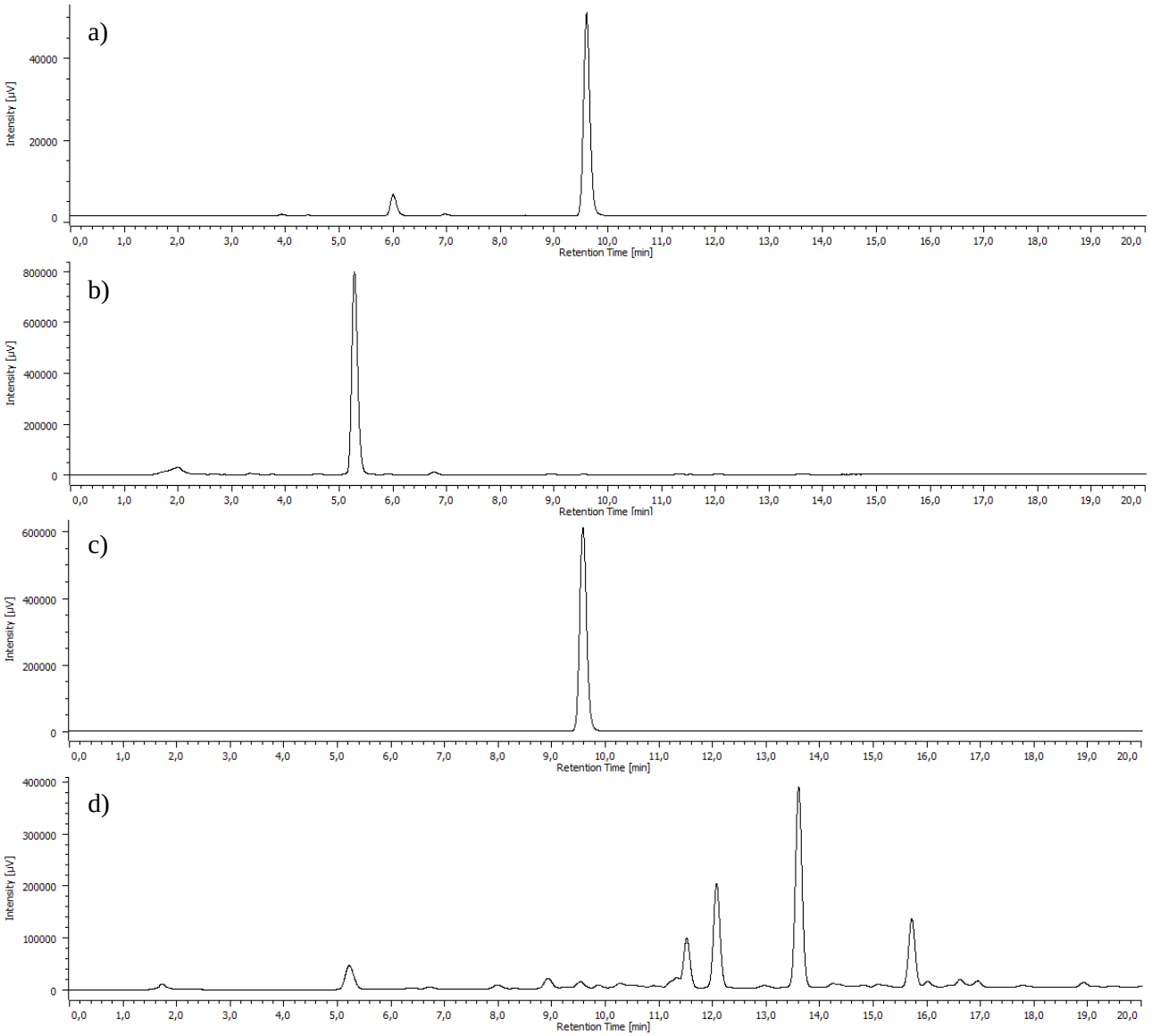

Figure 2.6: *Purification of [^{18}F]2.13*. a) Radiochemical detector: eluted 80:20 water/ethanol solution chromatogram. b) UV detector: eluted 80:20 water/ethanol solution chromatogram. c) Radiochemical detector: 1 ml acetonitrile elution chromatogram. d) UV detector: 1 ml acetonitrile elution chromatogram. Rt **[^{18}F]2.13**: 9.6 min; Rt hydrolysis byproduct: 5.2 min; Rt elimination byproduct: 11.4 min; Rt compound **2.12**: 13.5 min.

Due to the above findings, several studies were conducted in order to improve purity and attempt to remove unreacted iodine-azide **2.12**.

After washing with 80:20 water/acetonitrile solution, the tC18 Sep-Pak was eluted by different ratio of water/acetonitrile solution. 70:30, 60:40 and 50:50 solutions were used but results showed not only the product **[^{18}F]2.13** removal from cartridge, but also large amount of elimination byproduct and unreacted **2.12** precursor, as expected.

So, results showed the impossibility of improving purity by eluting the cartridge with water/acetonitrile solutions.

In order to proceed with CuAAC reaction and in order to evaporate the eluting solvent more easily, it was decided to proceed under conditions showed in Figure 2.6: washing cartridge with water/acetonitrile 80:20 solution and desorbing **[^{18}F]2.13** product mixture with acetonitrile.

Finally, after fluorine-18 nucleophilic substitution reaction occurred under condition showed above and after the mentioned conditions to purification, yield in range of 25-36% was obtained. Then, product **[^{18}F]2.13** was reacted directly with alkyne in order to study CuAAC reaction and to introduce fluorine-18 with a biological macromolecule under *mild* conditions.

2.2.2.2 CuAAC reaction

The radiolabeling [3+2] Huisgen dipolar cycloaddition between azide and terminal alkyne reaction was carried out using the fluorine-18 radiolabeled azide purified by the previously reported Sep-Pak method. Compound **[^{18}F] 2.13** in 1 ml acetonitrile was brought to the second reactor of the automated system, and solvent was evaporated. Then, temperature was decreased to 30°C (room temperature). Unfortunately, due to technical constraints, reactor can be cooled only by a stream of compressed air and the cooling step was slow, taking an overall time of 8 min.
Reaction is shown in Scheme 2.8.

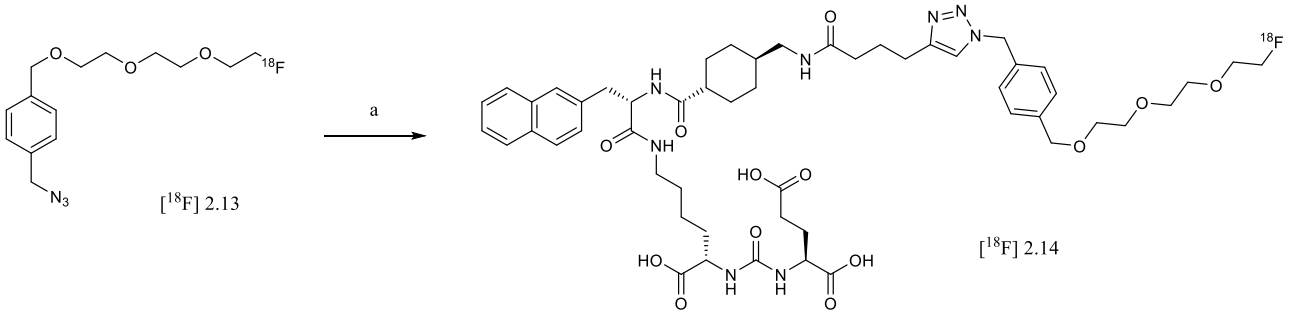

Scheme 2.8: *CuAAC reaction*. Reagent and conditions: (a) Precursor **2.1**, sodium ascorbate, $Cu(SO_4)\cdot 5\ H_2O$, 0.5 M NH_3 in H_2O, rt.

As previously described, ascorbate reduces copper (II) to copper (I) *in situ* and this specie catalyzes the cycloaddition between alkyne and azide. The resulting product is a regioselective 1,4 di-substituted 1,2,3 triazole (Chapter I).
CuAAC efficiency depends on concentration of the interested reagents, and solvents and co-solvents must be carefully chosen in order to avoid precipitation during reaction.
In Table 2.2 are summarized the different tested reaction conditions and related results.

	Solvent for solubilization of precursor 2.1 (Solution 1)	Solvent for solubilization of sodium ascorbate (Solution 2)	Solvent for solubilization for copper (II) sulfate pentahydrate (Solution 3)	Reaction time	Conversion
1	400µl DMSO	100µl H_2O	100µl H_2O	20 min	32%
2	200µl DMSO	100µl H_2O	200µl H_2O	20 min	40%
3	300µl MeOH	100µl H_2O	100µl H_2O	20 min	42%
4	200µl MeOH	100µl H_2O	100µl H_2O	20 min	13%
5	200µl MeOH	70µl MeOH + 30µl H_2O	100µl MeOH	20 min	1%
6	200µl 0.5M NH_3 in H_2O	100µl 0.5M NH_3 in H_2O	100µl H_2O	20 min	92%
7	200µl 0.5M NH_3 in H_2O	100µl 0.5M NH_3 in H_2O	100µl H_2O	10 min	80%

Table 2.2: *Solvent mixture for CuAAC reaction and triazole conversion percentage. Results refers to single tests.*

The general reaction procedure was as follows: Solution 1 and Solution 2, containing precursor **2.1** and sodium ascorbate, respectively, were put together in the same automated system reservoir, while solution containing copper (Solution 3) was placed into another reservoir. After compound **[^{18}F] 2.13** was collected into the reactor and acetonitrile was evaporated, solutions 1+2 were added, followed by Solution 3. In this way reaction started when copper was dropped into reactor.
The most critical factor of the "click" reaction step was the different solubility of the various involved components, which made it difficult to find the proper solvent mixture that allowed a fast and efficient reaction, while at the same time minimizing precipitations, that might also affect reagents/solvent transfer through the tubing/valves assembly of the automated system; for this reason, different solvents were tested.

First attempts were conducted using dimethyl sulfoxide; precursor **2.1** proved to be soluble, giving a clear, colorless solution, but addition of Solution 2, caused the mixture to immediately turn to opaque. Indeed, the two tests performed using dimethyl sulfoxide as the solvent for Solution 1 showed conversion rate not fully satisfactory, and the formation of a precipitate was noticed at the bottom of reactor. As shown in Table 2.2 entry 1-2, a larger amount of water gave better conversion rate, but precipitation increased as well (Figure 2.7).

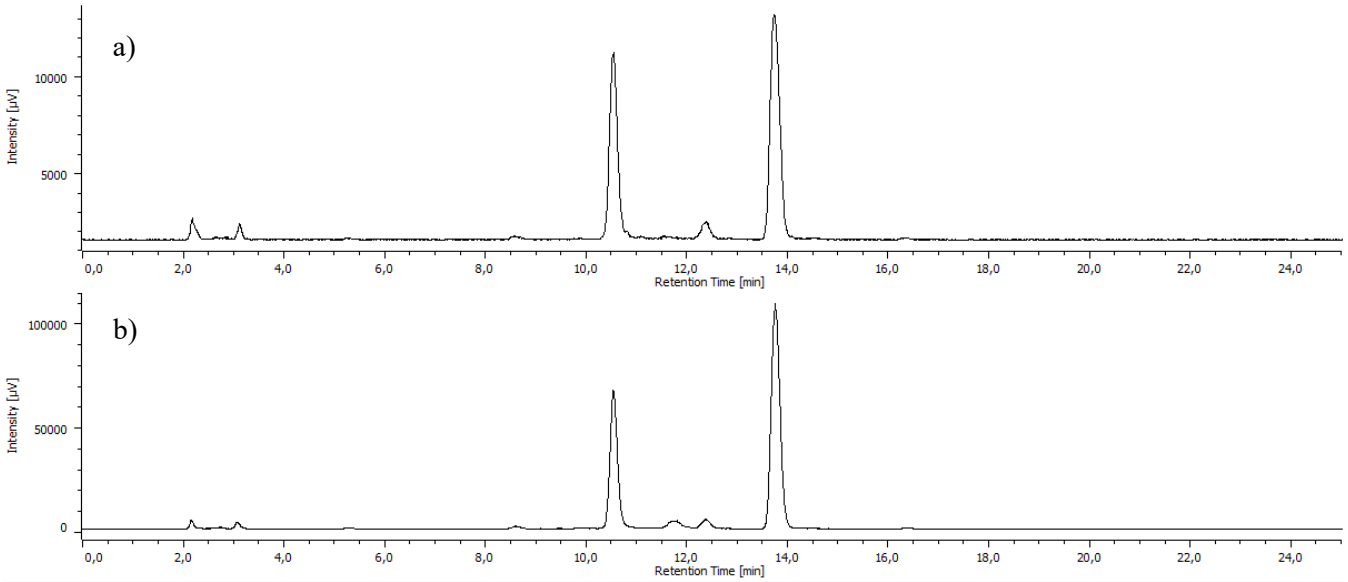

Figure 2.7: *[18]F-CuAAC in DMSO/water monitoring. Radiochemical detector*. Image a): DMSO/H_2O 200µl:300µl (Table 2.2 entry 2), b) DMSO/H_2O 400µl:200µl (Table 2.2 entry 1). Rt Product **[^{18}F] 2.14**: 10.2 min; Rt Precursor **[^{18}F] 2.13**: 13.5 min.

Diluting precursor **2.1** in methanol gave better results in terms of solubility. After sonication, it was possible to mix Solution 1 and Solution 2 without any immediate precipitation in the solvent reservoir, but unfortunately precipitation still occurred after their transfer in the reactor and addition of Solution 3. Moreover, decreasing methanol amount in Solution 1, decreased radiochemical yields (Figure 2.8); thus, with the aim to reduce water content to a minimum extent, one test using precursor **2.1** dissolved in pure methanol and ascorbate solubilized in a 30% water solution in methanol was performed (Table 2.2, entry 5).

In these conditions, no precipitation in reservoir and no precipitation in reactor were noticed, but unfortunately conversion rate was very low (Figure 2.8).

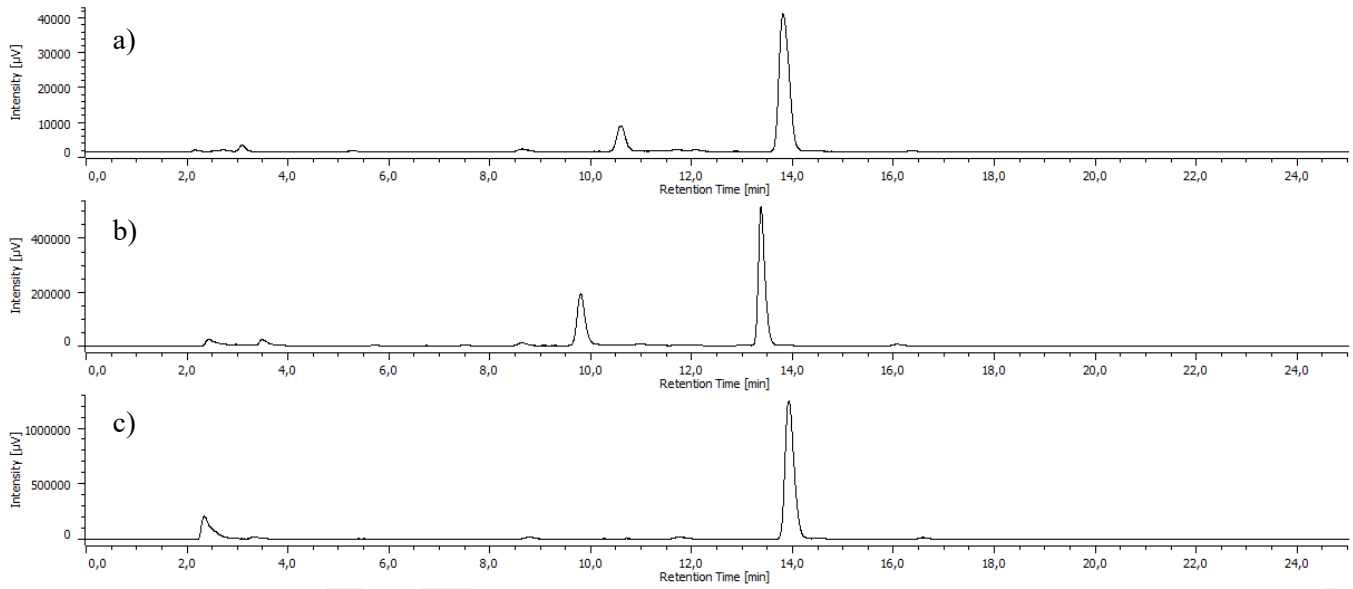

Figure 2.8: *[18]F-CuAAC in MeOH/water monitoring. Radiochemical detector*. Image a): MeOH/H_2O 200µl:200µl (Table 2.2 entry 4); b) MeOH/H_2O 300µl:200µl (Table 2.2 entry 3); c) MeOH/H_2O 330µl:70µl (Table 2.2 entry 5). Rt Product **[^{18}F] 2.14**: 11 min; Rt Precursor **[^{18}F] 2.13**: 13.5 min.

Based on the above results, a change of strategy was necessary. Ji and Atheron [124] studied CuAAC behavior in liquid ammonia. Indeed, ammonia is able to form tri-coordinated coplanar species $[Cu(NH_3)_3]^+$ with reduced copper (I), acting as Lewis acid and increasing the acidity and rates of alkynes ionization (Figure 2.9).

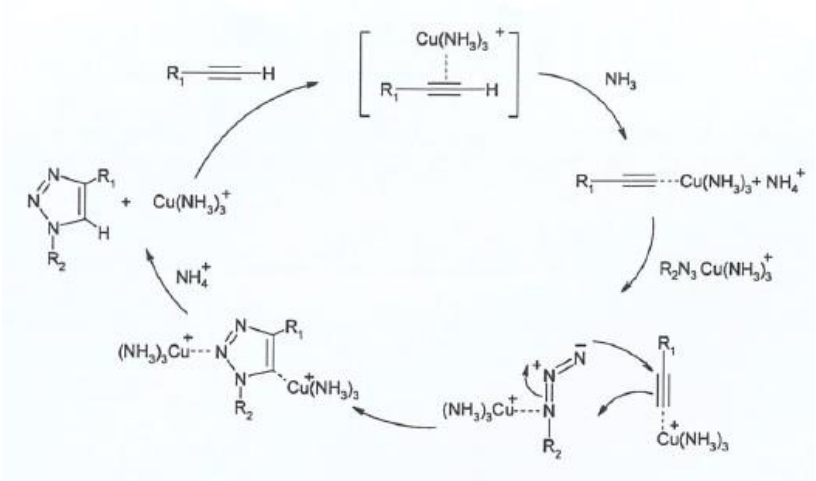

Figure 2.9: *CuAAC cycle in aqueous ammonia*

Thus, as shown in Table 2.2 entry 6-7, a test dissolving precursor **2.1** and sodium ascorbate in 0.5 M NH_4OH solution in water was conducted. No particular problems of reactivity and solubility were observed even after addition of $Cu(II)SO_4 \cdot 5H_2O$ diluted in water (Solution 3). Solubility of terminal alkyne in 0.5 M NH_3 aqueous solution was much better without precipitation. In fact, in basic pH the three carboxylic groups of Glu-urea-Lys residue are in carboxylate form, making precursor **2.1** much more soluble in water.

So, Solution 1+2 of precursor **2.1** and sodium ascorbate diluted in 0.5M NH_3 aqueous solution were added to the reactor containing fluorine-azide **[^{18}F] 2.13**, and then copper sulfate diluted in water was added. Reaction took place in aqueous ammonia media and no precipitation was observed.
As shown in Figure 2.10, the first test at 20 min gave the best results in terms of conversion from **[^{18}F] 2.13** to **[^{18}F] 2.14**, with a percentage of ~92% (Table 2.2 entry 6).

With the aim to further improve the radiochemical yield, and considering that in radiochemistry time factor is always of concern, attempts to reduce reaction time were performed.
However, as shown in Figure 2.10, results were no completely satisfactory. Indeed, slowing down reaction time to 10 minutes, a reduction of conversion percentage from 92% to 80% was observed, and for this reason no further reaction time reductions were tested. It has to be noted that [3+2] Huisgen dipolar cycloaddition between azide and terminal alkyne reactions (CuAAC) are usually faster than 20 minutes; a possible explanation for this discrepancy may be due to the very different reaction molarity ratio between the various reagents that is typical of radiochemistry reactions, compared with "standard" organic chemistry reactions; furthermore, the reaction "environment" of the automated system reactor is quite different from that of typical "laboratory" conditions (with standard glassware, stirring, etc.) .

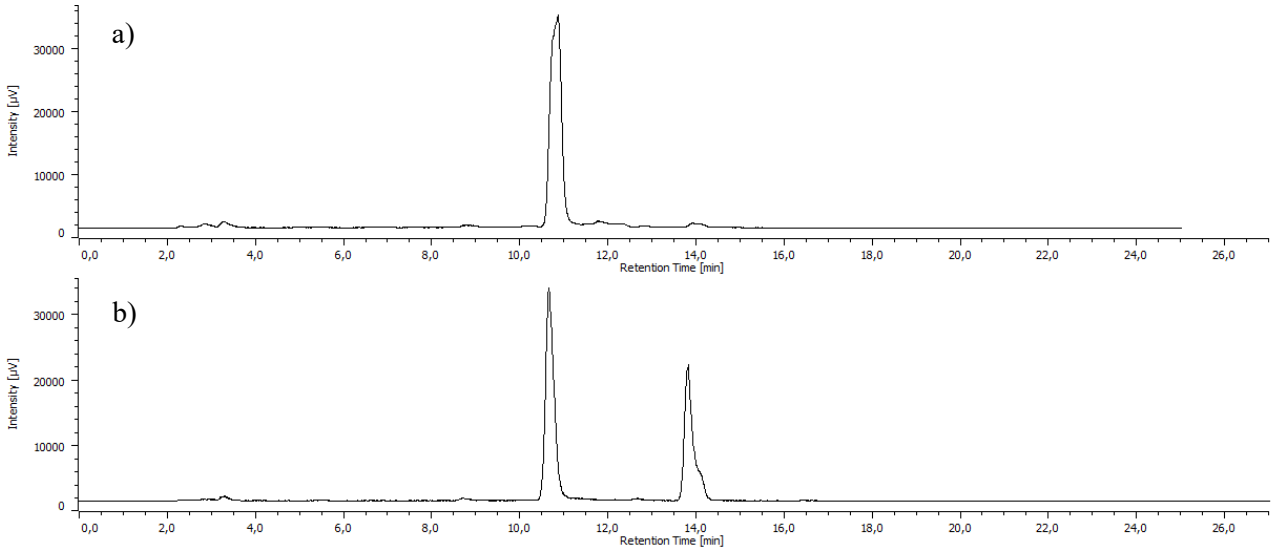

Figure 2.10: *[^{18}F]- CuAAC in 0.5 M NH_3 aqueous solution monitoring. Radiochemical detector*. a) CuAAC in 20 minutes (Table 2.2 entry 6); b) CuAAC in 10 minutes (Table 2.2 entry 7). Rt Product **[^{18}F] 2.14**: 11 min; Rt Precursor **[^{18}F] 2.13**: 13.5 min

On the other hand, CuAAC reaction occurred at room temperature, and so the most important initial objective (to allow radiofluorination of macromolecules in *mild* conditions) was finally achieved successfully.

After suitable formation of product **[^{18}F] 2.14**, product was quenched with 1 ml of 1M HCl, with oxidation of Cu(I) to Cu(II)Cl_2. Then the solution was diluted in mobile phase in order to purify with a semi-preparative RP-HPLC, achieving final 1,4-substituited 1,2,3-triazole with higher "cold" chemical purity (Figure 2.11). To this regard, the mixture was diluted in 70:30 water + 0.1% TFA/ acetonitrile + 0.1% TFA solution, and injected into the column. Gradient from 70:30 to 60:40 in 20 minutes was set, and after 17 min pure product **[^{18}F] 2.14** was eluted.

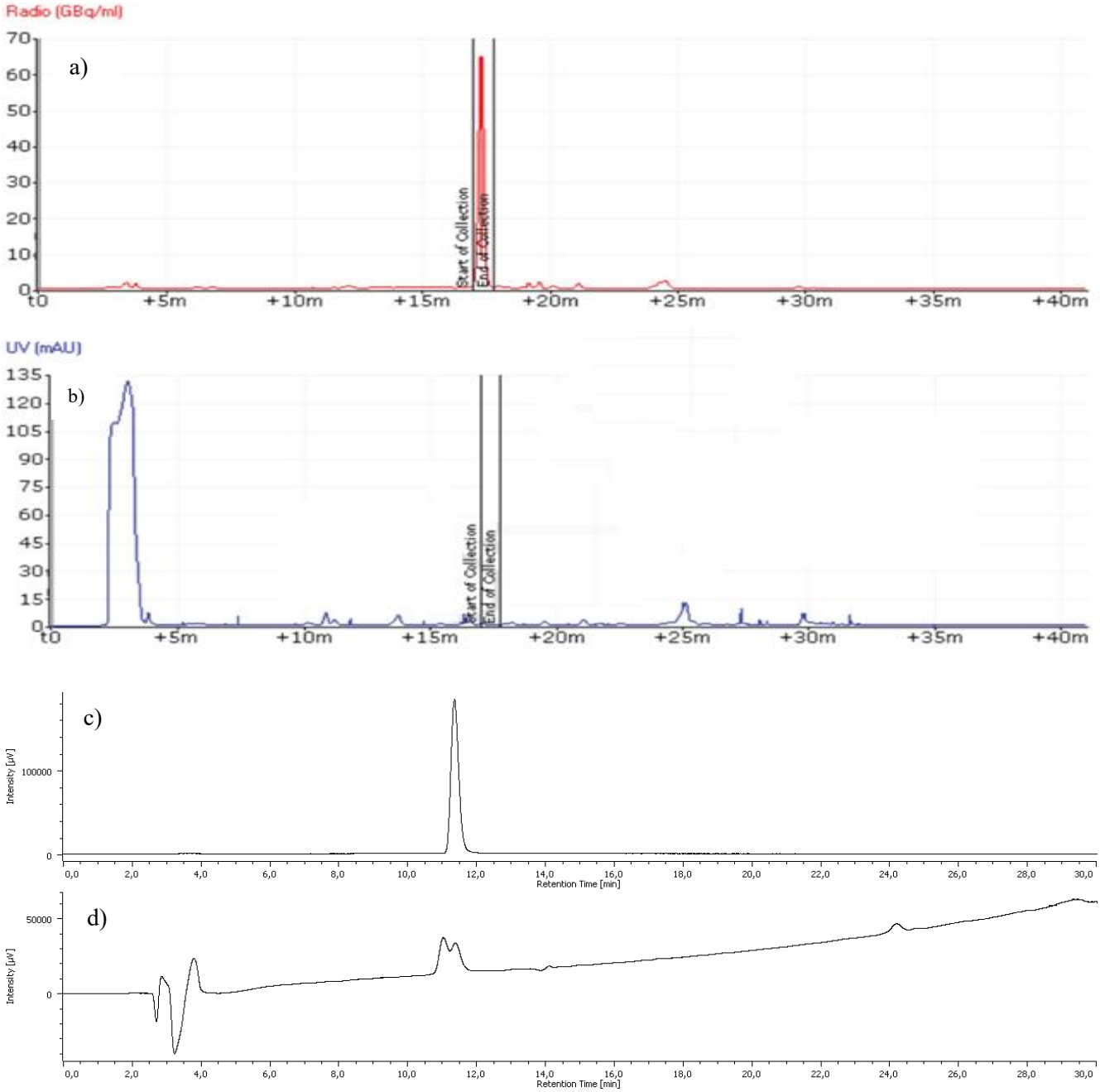

Figure 2.11: *Semi-preparative and analytical chromatogram of product [^{18}F] 2.14 purification*. a) Semi preparative radiochemical detector; b) Semi preparative UV detector; c) Analytical radiochemical detector; d) Analytical UV detector. Semi preparative Rt Product **[^{18}F] 2.14**: 17 min, Analytical Rt Product **[^{18}F] 2.14**: 11 min.

Finally, 1,4-substituited 1,2,3-triazole **[^{18}F] 2.14** was formulated in order to make it available for *in vivo* preclinical testing.

The solution recovered by elution from the column was diluted with 50% of water and passed through tC18 Sep-Pak cartridge. The cartridge was washed with 20 ml of water in order to wash out TFA residues. Final product was collected eluting the cartridge with 1 ml of ethanol. Then, 20 ml of saline physiological solution was added to the final container.

With an overall radiosynthesis time of 112 min, ~6% of not decay corrected yield was obtained. As shown in Figure 2.11 (d), a significant peak very close in retention time to the peak of the desired product was UV detected. Unfortunately, attempts to remove it failed, to date. MS analyses revealed the presence of by-products which couldn't be associated to an adduct or product **[^{18}F] 2.14**

degradation. The nature of these by-product has not been elucidated, so far, and it makes impossible to properly calculate the molar activity because UV peak of product **[^{18}F] 2.14** is almost merged with that of the by-product. However, even in the worst case, with molar activity calculated considering the sum of the two UV peaks, it resulted to be ~ 30 GBq/μmol.

As already mentioned previously, the radiolabeling procedure was automated using a Trasis AllinOne radiosynthesis platform (Figure 2.12). Automation is essential in the preparation of fluorine-18 labeled radiopharmaceuticals, as it allows radiosynthesis reproducibility with minimal radiation exposure to the personnel. The radiosynthesis "cassette" is a pre-assembled network of lines, syringe, manifold valves and reactors where the radiosynthesis takes place (Figure 2.12). The method was optimized starting with an empty cassette, which was adapted to the desired process, performing both the nucleophilic substitution reaction that lead to the formation of the fluorine-18 labeled azide, and the subsequent coupling with the alkyne functionalized PSMA precursor, and included two purifications steps, using SPE and semi-preparative HPLC, respectively.

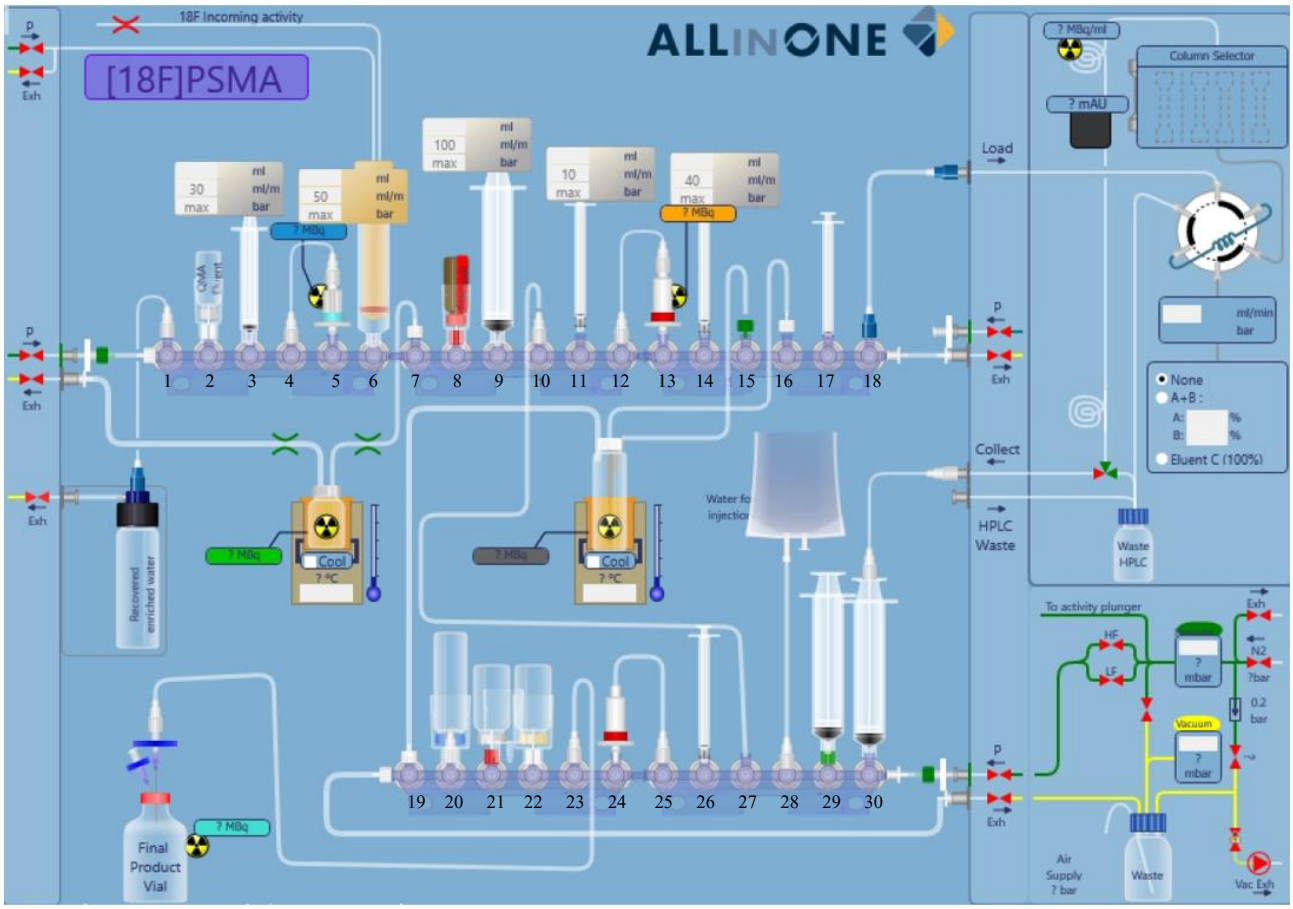

Figure 2.12: *Configuration of Trasis All-in-One automated system.* Main reagent positions are indicated:
P2: Kryptofyx 2.2.2 solution, P3: potassium carbonate solution, P5: QMA Sep-Pak cartridge (0.4 ml hold up volume), P8: compound **12** in acetonitrile solution, P11: Precursor **11** + sodium ascorbate in 0.5M NH_3 solution, P13: tC18 Sep-Pak cartridge (0.8 ml hold up volume), P14: Copper sulfate in water solution, P17: 1M HCl, P24: tC18 Sep-Pak cartridge (0.8 ml hold up volume), P26: EtOH, P29: saline physiological solution.

Chemical and radiochemical stability were tested by HPLC analysis of samples of the purified product up to eight hours after the end of radiosynthesis, at time intervals of two hours and storing the vial at room temperature.
Product **[^{18}F] 2.14** was stable in those conditions and no loss of radioactivity due to radiolytic degradation was detected.
Moreover, a study to evaluate the product degradation in human plasma was conducted. Plasma was obtained by blood centrifugation at 2800 rpm for 15 min. Then, to the obtained plasma just few microliters (20µl) of the final solution were injected and the mixture was incubated at 37°C for 2 and 4 hours. Then, at the end of incubation acetonitrile was added to the mixture precipitating the plasma proteins. The resulting mixture was monitored in HPLC. Finally, even in this case no degradation of the product **[^{18}F] 2.14** was observed.

2.3 CHAPTER CONCLUSION

In conclusion, a novel ligand PSMA-617 functionalized with terminal alkyne was synthetized. Synthetic pathway started from cost effective reagents and good final yield and purity grade were achieved. A new automated method to radiolabel the new PSMA-617 ligand with fluorine-18 via CuAAC in *mild* conditions was developed, obtaining satisfactory radiochemical yields, excellent radiochemical purity (>99%) but low chemical purity, due to an unknown impurity that also lead to a reduction of molar activity. Moreover, the stability of the final product **[^{18}F] 2.14** was confirmed *in vitro* and in human plasma. Overall, automated fluorine-18 radiolabeling procedure via "click-chemistry" was satisfactory, allowing its use for new potentially interesting biomolecules.

CHAPTER III

Synthesis of new PSMA-617 NODA and RESCA derivatives and radiolabeling with fluorine-18 by [^{18}F]AlF^{2+} complexation approach.

3.1 ABSTRACT

This Chapter focuses on the radiolabeling with $[^{18}F]AlF^{2+}$ of two derivatives of PSMA-617 functionalized with chelators NODA and RESCA (Figure 3.1). At first, chemical synthesis of precursors was conducted with ~31% overall yields for precursor **3.1** and ~25% for precursor **3.2**. Then, radiosynthesis was implemented and automated. Radiolabeling conditions, *in vitro* and *in vivo* stability were compared for the two derivatives: in case of PSMA-617-NODA, $[^{18}F]AlF^{2+}$ complex introduction occurred by heating at 110°C, but the final product resulted to be stable both in solution and in human plasma (radiochemical purity >99%, radiosynthesis time 59 min, ~23% of not-corrected RCY, molar activity >170 GBq/μmol). On the other hand, in case of PSMA-617-RESCA, $[^{18}F]AlF^{2+}$ complex introduction occurred at room temperature, but the final product resulted to be less stable both in solution and in human plasma (radiochemical purity >99%, radiosynthesis time 42 min, ~40% of not-corrected RCY, molar activity >90 GBq/μmol). Finally, the two radiopharmaceuticals were tested *in vivo* on human prostate tumor and human glioblastoma tumor inoculated mice.

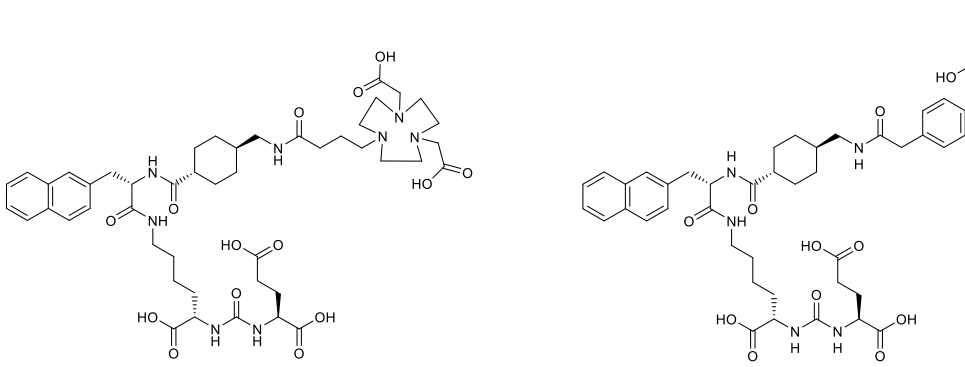

PSMA-617-NODA derivative (**3.1**) PSMA-617-RESCA derivative (**3.2**)

Figure 3.1: *Precursor **3.1** and **3.2***

3.2 RESULTS AND DISCUSSION

Preparation of "cold" precursors, as well as NMR characterizations, were performed at the laboratories of Medical Biotechnology and Translational Medicine Department of Università degli Studi di Milano, under the supervision of prof. Patrizia Ferraboschi and Diego Colombo. Radiolabeled products, RP-HPLC analysis and RP-HPLC purifications were implemented in the laboratories of the Tecnomed Foundation- Università degli Studi di Milano-Bicocca. MS characterizations were made at Departement of Medicine and Surgery of Università degli Studi di Milano Bicocca. Moreover, elemental analysis, final products MS characterization and LC-MS were subcontracted to COSPECT, Università degli Studi di Milano. Preclinical studies on mice were conducted by group of prof. Rosa Maria Moresco, Department of Medicine and Surgery, Università degli Studi di Milano-Bicocca.

3.2.1 Chemistry

The synthesis of precursor **3.1** and **3.2** was designed adding specific linkers and chelators to PSMA-617 "core" (Compound **2.10**), whose synthetic strategy has previously been described (see Chapter II).
In a work of Shetty et al. [103], a study aimed to determine the relationship between NODA chelating agent, linker and radiolabelling efficiency was reported, that took advantage of X-ray crystallography techniques on the structure of [^{19}F]AlF-chelators complexes. One of their major finding was that, in terms of radiolabelling yield and stability, ideal spacer between the chelator and the biomolecule, should include a propyl group. The above findings were confirmed by the work of Wang *et al*., where it was noticed that a propyl chain in the structure allows to reduce potential steric NODA hindrance during the AlF^{2+} chelating process [125].
For this reason, the synthesis of three-carbon atoms linker was designed, starting from commercial bromo-butyric acid and di-tert-butyl 2,2′-(1,4,7-triazacyclononane-1,4-diyl)diacetate (NO_2AtBu).

3.2.1.1 Synthesis of PSMA-617-NODA derivative

3.2.1.1.1 PSMA-617 "core" functionalization for NO_2AtBu introduction by S_N2 nucleophilic substitution

The first attempts to synthetize PSMA-617-NODA derivative (product **3.1**) were focused on the functionalization of PSMA-617 "core" (compound **2.10**) with suitable leaving group, in order to perform the subsequent nucleophilic substitution reaction S_N2 with the free amine residue of commercial NO_2AtBu. NO_2AtBu (Scheme 3.5) was chosen to be used in this synthetic strategy because it is merely the tert-butyl protected NODA chelator and, due to free secondary amine, it is possible to functionalize it in different ways (in this case with a propyl linker).
Thus, as shown in Scheme 3.1, compound **2.10** was suitably transformed to be functionalized by bromine or iodine leaving groups. Those halogens can be substituted easily in subsequent NO_2AtBu introduction.

Starting from 4-bromo-butyric acid and 4-iodine-butyric acid, a coupling reaction was set with PSMA-617 "core" biomolecule.
Exploiting free amine residue of the biomolecule and acidic residue of the δ-halogen butyric acids, coupling reactions in DMF were performed, in presence of HATU as condensing agent and triethylamine (TEA) to activate the reaction.

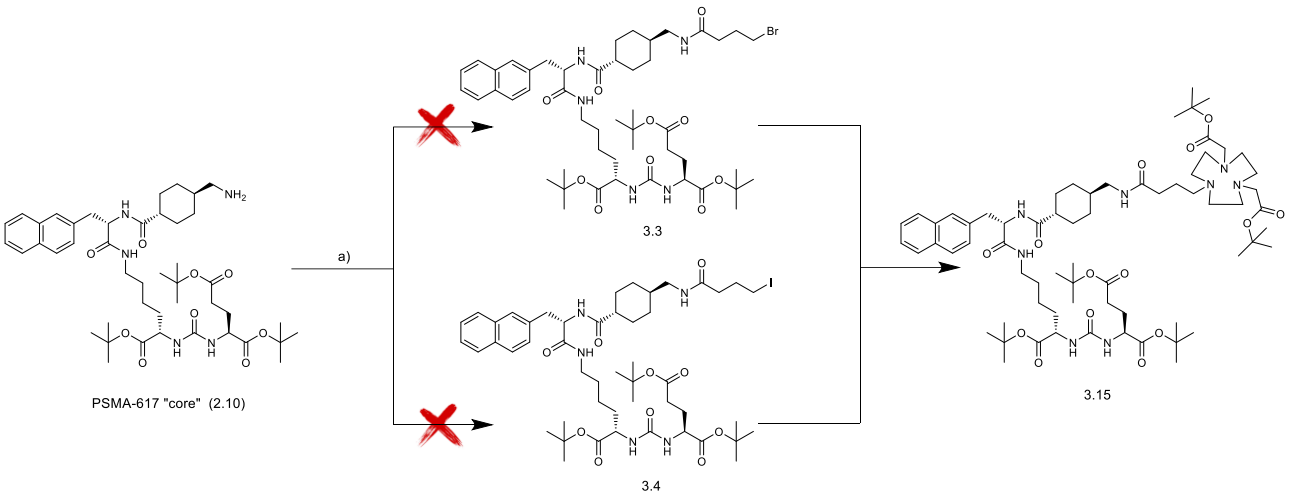

Scheme 3.1: *Coupling between PSMA-617 biomolecule and δ-halogen acid*. Reagent and conditions: (a) 4-bromine butyric acid or 4-iodine butyric acid, HATU, TEA, DMF, 0°C-rt, overnight.

Unfortunately, results were not satisfactory. In case of bromine-derivative (compound **3.3**), crude mixture was very difficult to purify by chromatography, due to the large number of by-products. Most likely, in the considered reaction conditions, bromine is too weak and the CH_2-Br bond is not sufficiently stable. This hypothesis was confirmed by finding hydrolyzed by-product (CH_2-OH, compound **3.5** in Scheme 3.3) and internal cyclization by-products in column fractions.
In addition, competition can occur also with free primary amine residue of the biomolecule which, instead forming an amidic bond in the coupling reaction, can directly interact with bromine giving place to a competitive S_N2 substitution reaction.
NMR and MS characterization confirmed that expected compound **3.3** was not formed.
The same reaction pattern was observed using iodine instead of bromine, and that can be explained because CH_2-I is even weaker than bromine, and by-products of internal cyclization and hydrolyzed were easily formed.

Then, another attempt was made, reacting compound **2.10** with the 4-bromine butyric acid activated in alkanoyl chloride form (Scheme 3.2). The idea was to use a very reactive derivative of bromine-acid, avoiding the use of a condensing agent as mentioned before. In this case the free amine residue was attracted to the very reactive Cl-CO bond, instead of competing with a S_N2 on bromine. Moreover, the reaction was conducted in dry dichloromethane, giving a very easy work-up: in this case DCM was evaporated at the end of the reaction, while using dimethyl formamide (DMF) as shown in Scheme 3.1 a work-up in aqueous media was needed, a fact that further promoted the formation of by-products.

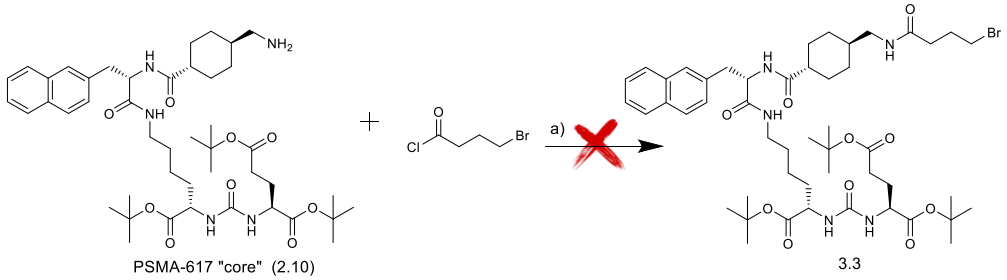

Scheme 3.2: *Formation of amide bond reacting alkanoyl chloride*. Reagent and conditions: a) TEA, dry DCM, from 0°C to rt, overnight.

Unfortunately, even in this case the product **3.3** was not formed and only by-products were detected.

The next attempted strategy is shown in Scheme 3.3.

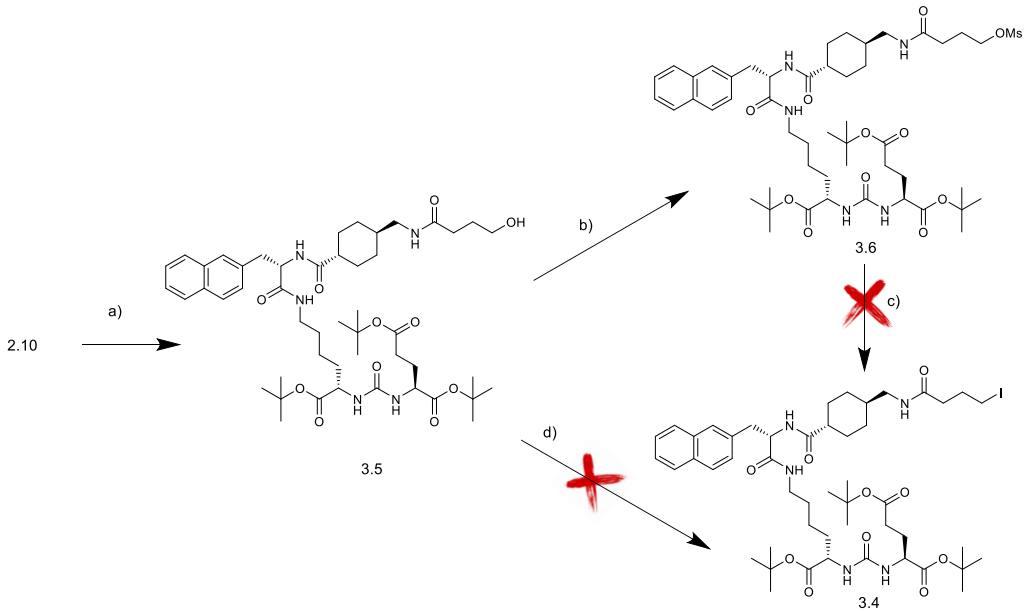

Scheme 3.3: *Formation of PSMA-617 hydroxyl derivate and iodine introduction*. Reagent and conditions: a) δ-butyric lactone, toluene, reflux (130°C), 3 days, 72%; b) Ms-Cl, TEA, dry DCM, 0°C, 3h, 99%; c) LiI, THF dry, rt, overnight; d) Ph_3P, I_2, imidazole, DCM, from 0°C to rt, overnight.

Compound **3.5** was obtained in high yields (72%) by a δ-butyric lactone opening in condition of aminolysis reaction. As shown in Scheme 3.3 the PSMA-617 "core" was reacted with a δ-butyric lactone in toluene heating at 130°C for three days, and the mixture was then purified by column chromatography. The purity grade of compound **3.5** was satisfactory and it was characterized by NMR and MS spectrometry.

After the hydroxyl derivate was obtained, two ways to introduce iodine leaving group (and so obtaining compound **3.4**) were attempted. In the first case, a "classical" activation of the hydroxyl group with a very reactive mesylate leaving group was performed. The reaction, as shown in Scheme 3.3 took place in dry dichloromethane in presence of little amount of TEA in order to activate the compound **3.5**.
The mesylate-derivative **3.6** was obtained but could not be purified, because of the acidity of the column SiO_2 that promote reverting reaction to compound **3.5**, so the crude mixture was used for the subsequent reaction iodide as such. In addition, the presence of the product was demonstrated by NMR but also a large presence of by-products which, without purification, certainly competed in subsequent reaction steps. Anyway, it was decided to proceed on crude **3.6** mixture.

Lithium iodide was added to the crude **3.6** compound in dry THF and it was stirred overnight (Scheme 3.3, entry c). Unfortunately, even in this case, the iodine PSMA-617 derivative **3.4** was not obtained. NMR results showed that mesylate in those conditions was unstable giving evidence of competing reactions such as elimination, internal cyclization and/or mesylate hydrolyzation with subsequent reverting to compound **3.5**. Moreover, given the low level of purity obtained of compound **3.6**, it was

also decided not to try the direct introduction of chelator NODA (from S_N2 reaction with NO_2AtBu) on mesylate product, as we can expect that the results would not have been satisfactory, due to by-products.

At last, a quite new method to directly insert iodine group on hydroxyl was attempted. As shown in Scheme 3.3 entry d, the reaction occurred in Mitsunobu-like conditions.
The hydroxyl derivative **3.5** was reacted with iodine in presence of triphenylphosphine and imidazole. Reacting with iodine, triphenyl phosphine forms an iodine-phosphonium salt with positive charge on phosphorous, which is the specie that interacts with hydroxyl group oxygen. Finally, iodine substitutes hydroxyl with a configuration change, and oxygen reacts with phosphine, forming triphenylphosphine oxide.
Unfortunately, even in this case the formation of many byproducts was observed, and no presence of compound **3.4** was found. Probably iodine and also bromine groups form a too weak CH_2-LG bond, which is easily spoiled on high functionalized biological macromolecule like PSMA-617.
So, the strategy of introducing suitable leaving groups directly into the whole PSMA-617 "core" molecule was abandoned.

3.2.1.1.2 Functionalization of a PSMA-617 "core" fragment for NO_2AtBu introduction by S_N2 nucleophilic substitution

Considering the failed attempts to directly functionalize the whole "core" of PSMA-617, a different approach, based on the introduction of suitable leaving group on a fragment of the biomolecule PSMA-617, followed by the coupling of the functionalized fragment with the rest of the "core" structure, was attempted. Based on the fact that too many functionalities could compete in LG introduction and make the molecule prone to internal cyclization, the introduction was focused on *trans*-4-(aminoethyl) cyclohexane carboxylic acid residue.
The ratio was to functionalize the residue and then introduce NODA chelator by a S_N2 nucleophilic substitution with NO_2AtBu.

As shown in Scheme 3.4, *trans*-4-(aminoethyl) cyclohexane carboxylic acid had to be protected selectively on the acidic residue.
A "classical" approach using thionyl chloride in ethanol was used and compound **3.7** was obtained in quantitative yield without purification.

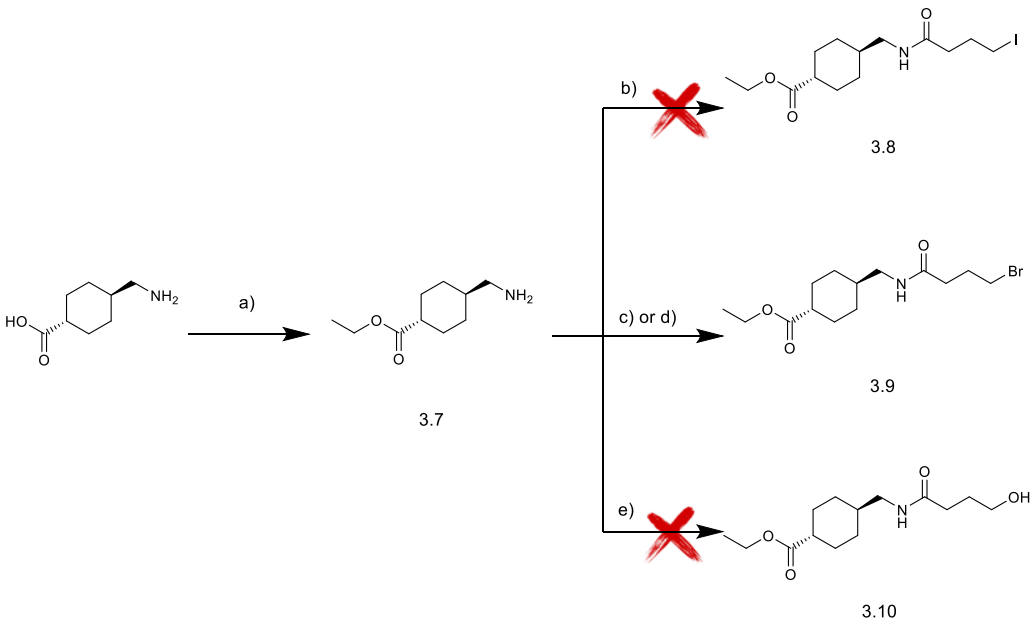

Scheme 3.4: *Functionalization of small PSMA-617 residue*. Reagent and conditions: a) $SOCl_2$, EtOH, from 0°C to reflux, overnight, >99%; b) 4-iodine butyric acid, HATU, TEA, DMF, from 0°C to rt, overnight c) 4-bromine butyric acid, HATU, TEA, DMF, from 0°C to rt, overnight, 25%; d) 4-bromine butyric acid, DCC, DMAP, dry DCM, from 0°C to rt, 3 days, 40%; e) δ-butyric lactone, toluene, reflux (130°C), 3 days.

Once compound **3.7** was obtained, it was possible to set different strategies to functionalize the amine residue.

As first attempt, an iodine functionalization was attempted and performed by a coupling reaction. Unfortunately compound **3.8** was not obtained, due to the formation of many by-products and internal lactonization took place. Again, iodine-carbon bond seemed to be too weak and not stable even in small aminoacidic residues.

Due to those results a bromine functionalization took place. In this case compound **3.9** was successfully obtained and characterized.

As shown in the Scheme 3.4 (entry c and d), compound **3.7** was reacted with 4-bromine butyric acid testing two different coupling reaction conditions.

At first a classical method with HATU, triethylamine and DMF was performed (scheme 3.4, entry c) and a crude mixture which included many by-products was obtained. Crude mixture was purified twice by column chromatography, and product **3.9** was obtained in low yields.

Probably the presence of triethyl amine and aqueous work-up can bring to by-products formation.

In the second case, 4-bromine butyric acid was reacted with amino acidic residue in presence of catalytical amount of DMAP and dicyclohexyl carbodiimide (DCC) as condensing agent in dry dichloromethane. In this case crude mixture was worked-up by dichloromethane evaporation, and so no aqueous work-up was necessary. The crude mixture was purified by column chromatography and product **3.9** was obtained.

Finally, the last attempt of 4-butyric lactone opening was performed, but even heating to reflux for many days no product **3.10** was formed. Instead, reaction mixture in toluene was clear during heating mixture but immediately turn to a gel once to room temperature. Anyway, as already mentioned, product **3.10** was not obtained.

Once product **3.9** was obtained, it was finally reacted with NO_2AtBu, via a S_N2 reaction (Scheme 3.5 entry a). Potassium carbonate was used to push equilibrium and cleave formed HBr in the reaction.

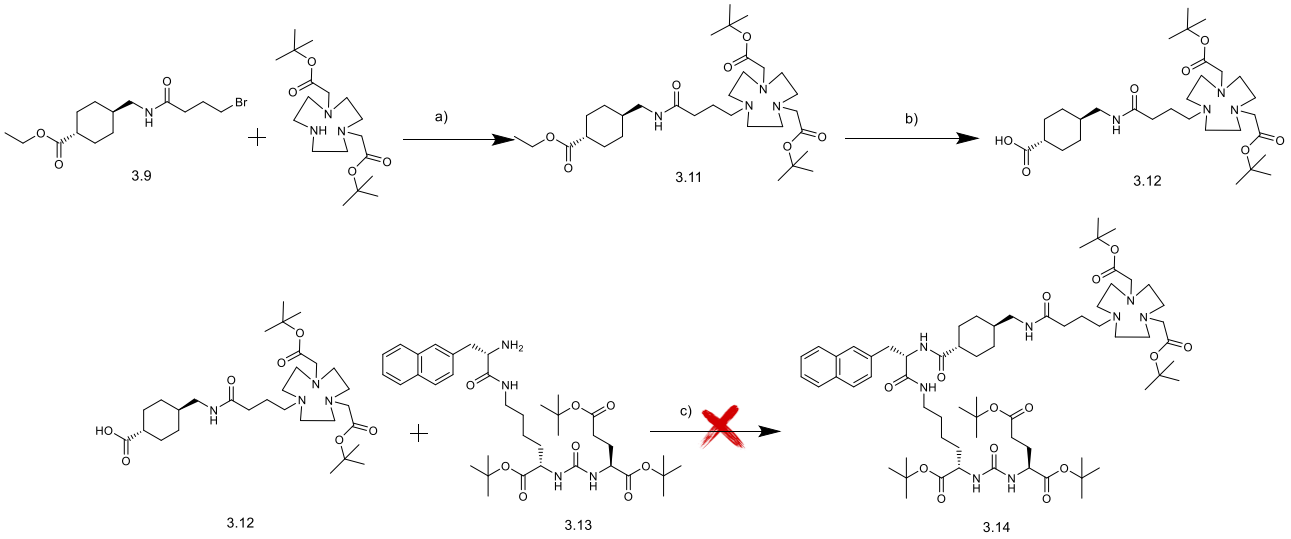

Scheme 3.5: *Introduction of NO_2AtBu by nucleophilic substitution*. Reagent and conditions: a) K_2CO_3, dry ACN, rt, overnight, (>99%); b) 1M $LiOH{\cdot}H_2O$, MeOH/THF, 0°C, 3h, (>99%); c) HATU, TEA, DMF, from 0°C to rt, overnight.

Compound **3.11** was obtained in quantitative yields but no purification on silica-gel was made due to the degradation of NODA chelator, and reaction mixture was used as such in the subsequent synthesis step. Anyway, conjugation of NODA chelator derivative was finally obtained and so the hydrolysis of ethyl ester was performed in basic aqueous media. Compound **3.12** formation was monitored by TLC, observing the disappearance of starting material and the appearance of a spot at Rf=0. Then, crude mixture was worked-up by extraction in organic solvent (ethyl acetate). In this case, the compound **3.12** resulted to be extracted successfully due to the large lipophilic part of the molecule. From TLC analysis the crude mixture contained many by-products which couldn't be separated due to **3.12** degradation in chromatographic column.
So, it was decided to react the crude mixture with previously synthetized PSMA-617 derivative **3.13** (Scheme 3.5) in a coupling reaction in DMF and using HATU as condensing agent.
Unfortunately, due to due to the lack of purification of crude **3.12**, reaction mixture presented a significant number of by-products, which made interpretation of TLC pattern quite difficult, and desired product **3.14** couldn't be found.

For this reason, also this strategy was not explored further, and we proceeded with the direct NODA-propyl linker introduction on PSMA-617 "core", with the purpose of finally obtain compound **3.14** in higher yield and purity grade.

3.2.1.1.3 Direct introduction of NO_2AtBu in the linker and subsequent conjugation with PSMA-617 "core"

Due to failures of the strategies shown above, it was decided to functionalize NO_2AtBu with a propyl linker. Then, the functionalized chelator had to be conjugated to the biologically active PSMA-617. Different attempts were performed in order to introduce 4-bromine butyric acid or derivatives directly on NO_2AtBu in nucleophilic substitution reaction conditions. In this case, bromine resulted to be a

good leaving group. Moreover, performing the reaction on small molecules, without many competing functionalities like PSMA-617 "core" **2.10**, no byproducts of internal cyclization occurred.

At first, as shown in Scheme 3.6 (entry a), NO_2AtBu was reacted with 4-bromine butyric acid in dry acetonitrile and potassium carbonate to push reaction equilibrium toward product **3.16**.
However, results were unsatisfactory and no product was obtained, possibly due to the deactivation of secondary amine by free acidic moiety, giving a salt.

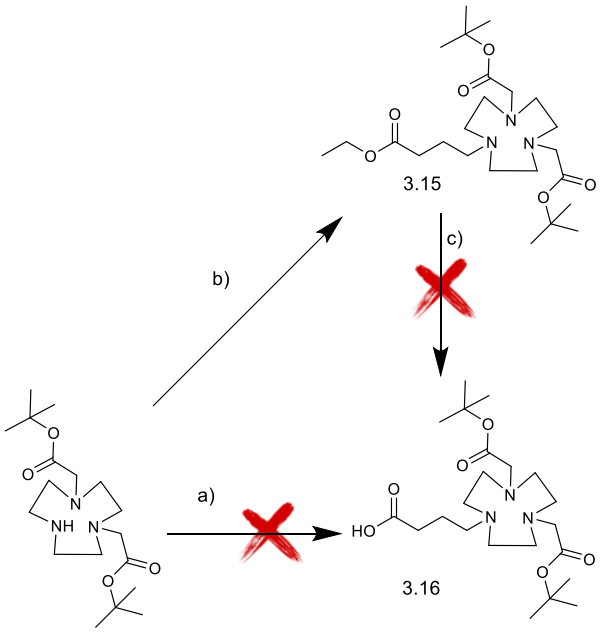

Scheme 3.6: *NO_2AtBu functionalization*. Reagent and conditions: a) 4-bromine butyric acid, K_2CO_3, dry ACN, rt, overnight; b) 4-bromine butyric acid ethyl ester, K_2CO_3, dry ACN, rt, overnight, 76%; c)1M $LiOH \cdot H_2O$, EtOH, 0°C, 4h.

A new attempt was then performed in the same conditions as above, but using the ethyl ester of the acid (Scheme 3.6 entry b).
In this case nucleophilic introduction was satisfactory and the desired product **3.15** was obtained in good yields (76%). The obtained product, as already mentioned, couldn't be purified by column chromatography and ester hydrolysis was conducted on crude **3.15** in basic media; although product **3.16** seemed to be formed, based on TLC monitoring, its zwitterionic nature did not allow to extract the product from aqueous phase in a pure form. Considering that, it was decided to don't proceed further with purification optimization (e.g. via a reverse phase purification) on compound **3.16**, but rather to change the type of protecting ester. In this case, we obtained better results. So, another way to protect 4-bromine butyric acid had to be found. The choice fell on Cbz protecting group, which is removed by hydrogenolysis, avoiding aqueous work-up.

As shown in Scheme 3.7, NO_2AtBu was reacted with benzyl 4-bromo butanoate via a S_N2 nucleophilic substitution. In this case the obtained product **3.17** was not purified by chromatography due to high degradation in column, and it was used as such for the next step.

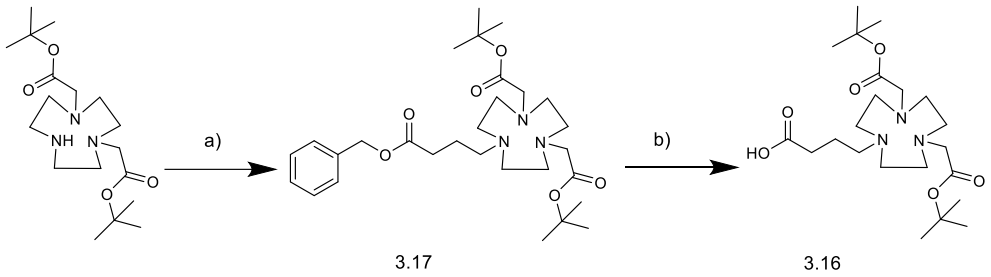

Scheme 3.7: *NO_2AtBu functionalization*. Reagent and conditions: a) benzyl 4-bromo butanoate, K_2CO_3, dry ACN, rt, overnight, 79%; (b) H_2, Pd/C 10%, EtOH, rt, overnight, 94%.

Compound **3.17** was obtained in high yields (79%) and carboxy benzyl group was removed by hydrogen flow catalyzed by 10% palladium on activated charcoal; the deprotection occurred overnight in ethanol and it was the key to obtain product **3.16**. Once the product was obtained and Cbz completely removed, ethanol was evaporated and final product was obtained avoiding aqueous work-up.
Yields were very high and also the crude mixture showed a satisfactory level of purity.

The coupling reaction between chelator and compound **2.10** occurred under the same conditions shown before. Free carboxylic functionality of compound **3.16** was reacted with free amine residue of PSMA-617 "core" biomolecule (Scheme 3.8). Finally, a PSMA-617-NODA derivative biomolecule was obtained (**3.14**) and only the last step of *tert*-butyl deprotection still had to be performed.

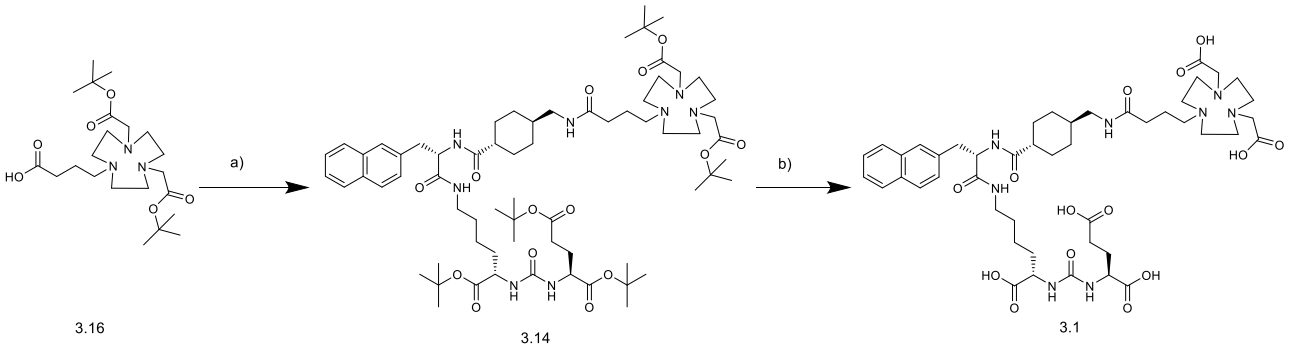

Scheme 3.8: *PSMA-617 functionalization with NODA*. Reagent and conditions: a) Compound **2.10**, HATU, TEA, DMF, 0°C-rt, 3h, (>99%); (b) 4M HCl, dioxane, rt, 4h, (45%).

Deprotection occurred at room temperature, monitoring the reaction progression by RP-HPLC.
As shown in Figure 3.2 a not negligible amounts of by-products were formed, and the correct UV peak of product **3.1** was selected following LC-MS analysis.

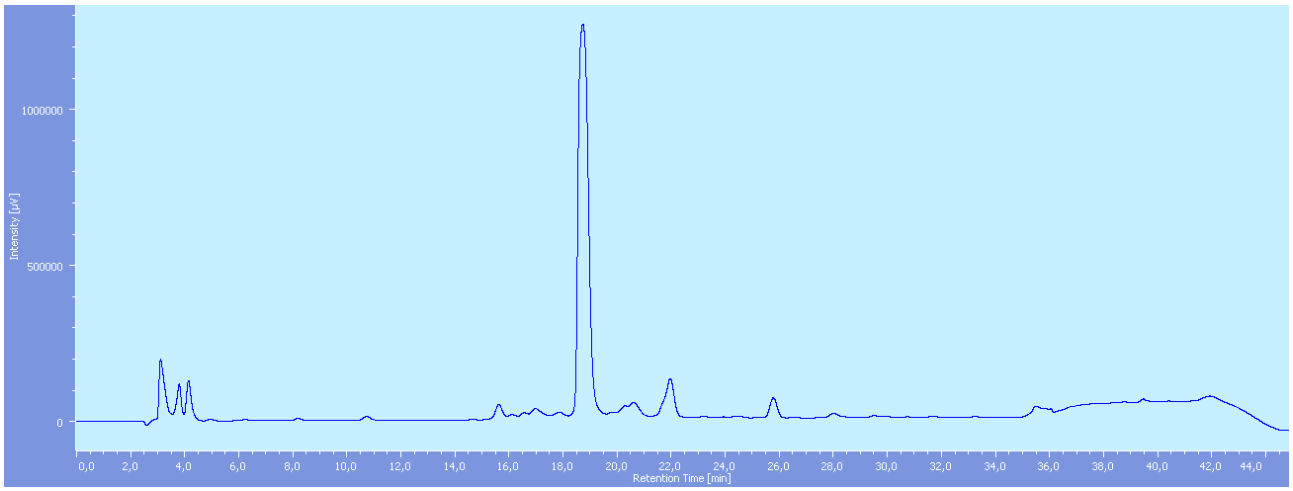

Figure 3.2: *HPLC chromatogram of deprotection reaction*. t_R of **3.1** product: 19 min.

Product **3.1** was purified by semipreparative RP-HPLC and lyophilized. The purity grade (>99%) was satisfactory and the synthesis overall yield was ~31% calculated on benzyl 4-bromo butanoate initial amount. The obtained PSMA-617-NODA derivative was then used for the radiolabelling via $[^{18}F]AlF^{2+}$ chelation chemistry.

3.2.1.2 Synthesis of PSMA-617-RESCA derivative

As said above, the biologically active PSMA-617 molecule was also functionalized with RESCA chelator.

The chemical synthesis of compound **3.2** is shown in Scheme 3.9.
The commercial RESCA-chelator derivative is the so called (±)-H_3RESCA-TFP, which is the chelator without protection on carboxylic groups and activated for a coupling reaction with tetrafluoro phenol.

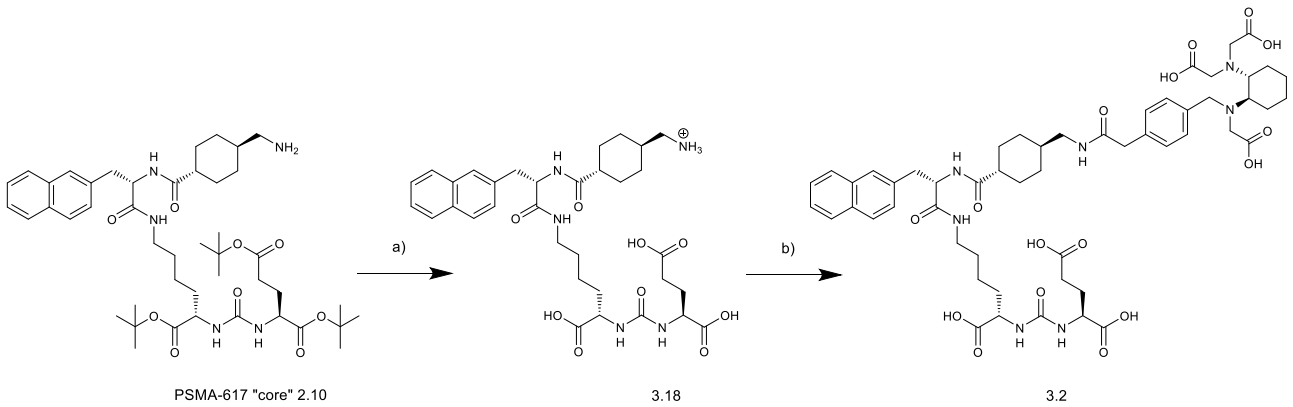

Scheme 3.9: *Synthesis of PSMA-617-RESCA derivative (**3.2**)*. Reagent and conditions: (a) TFA, DCM, rt, overnight, (59%); (b) (±)-H_3RESCA-TFP, DMSO, 0.05M buffer sodium acetate, rt, 4h, (42%).

As shown in the Scheme, PSMA-617 “core” was deprotected from *tert*-butyl on carboxylic functionality. It was obtained in acidic media and reaction progress were monitored by RP-HPLC. As already explained, this kind of deprotection gives a not negligible number of by-products like Glu-residue removal, which must be removed.

Thus, at the end of the reaction, compound **3.18** was purified by semi-preparative RP-HPLC (Figure 3.3), lyophilized and obtained in good yield and high purity (>99%).

Once biomolecule "core" was obtained, coupling reaction with (±)-H_3RESCA-TFP was performed (Scheme 3.9, entry b).
As shown, the reaction occurred in controlled basic media, using a sodium acetate buffer. Indeed, at acidic pH the reaction can't proceed because compound **3.18** free amine is not activated, while at too basic pH the hydrolysis of the active RESCA ester may take place.

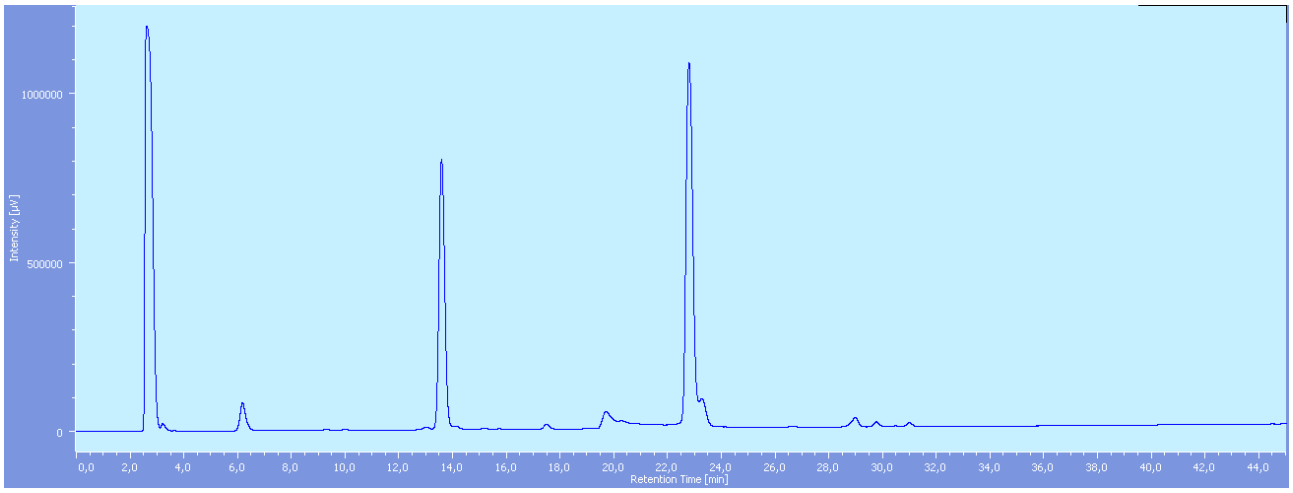

Figure 3.3: *HPLC chromatogram PSMA-617-RESCA precursor formation*. t_R of **3.18**: 13.5 min t_R of **3.2** product: 23.5 min. HPLC method: water+0.1%TFA / acetonitrile+0.1%TFA 80:20, Isocratic 1 min, then gradient to 50:50 in 40 min.

Finally, precursor **3.2** was purified by semi-preparative RP-HPLC chromatography, was lyophilized and obtained with excellent grade of purity (>99%).
The overall yield of this synthesis was ~25%.

3.2.2 Radiochemistry

3.2.2.1 Radiosynthesis with $[^{18}F]AlF^{2+}$ of PSMA-617-NODA derivative

In order to find the best radiolabeling condition to coordinate $[^{18}F]AlF^{2+}$ with PSMA-617-NODA derivative (precursor **3.1**), several attempts using the commercially available NODA-derivative NODA-MPAA-NH_2 (Scheme 3.10) were made.

Fluorine-18 was produced and purified as already described in Chapter II. In this case, QMA cartridge was washed several times with ultra-pure water, because removal of all metal impurities coming from the target is crucial in $[^{18}F]AlF^{2+}$ radiochemistry, as they could compete in aluminum-fluorine complexation.

After the cartridge was washed, fluorine-18 was desorbed as $[^{18}F]NaF$ by passing a solution of sodium acetate buffer.

Reactive $[^{18}F]NaF$ then reacts with $AlCl_3$ with formation of $[^{18}F]AlF^{2+}$.

The reaction proceeds smoothly, but pH must be strictly controlled in a short range around pH = 4. Indeed, at pH < 4 a fully ionized Al^{3+} specie is formed, while at pH > 4 aluminum hydroxide species such as $Al(OH)^{2+}$, $Al(OH)_2^{+}$, $Al(OH)_3$, and $Al(OH)_4^{-}$ are formed [126].

In order to find the best stoichiometric and reaction conditions, a preliminary study using the chelator NODA-MPAA-NH_2 alone were performed, as shown in Scheme 3.10.

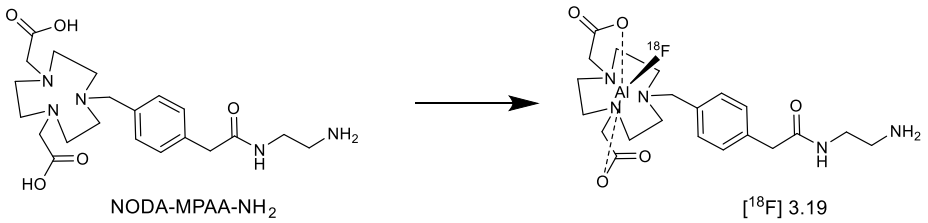

Scheme 3.10: *Introduction of [^{18}F]AlF^{2+} into NODA-MPAA-NH_2 chelator*. Reagent and conditions: a) [^{18}F] AlF^{2+}, 0.1M sodium acetate buffer pH=4, ethanol; 110°C, 15 min.

Best results were obtained using an equivalent ratio of 1:2 $AlCl_3$: chelator. Moreover, the reaction took place in 15 minutes heating at 110°C, using 0.1M sodium acetate buffer.

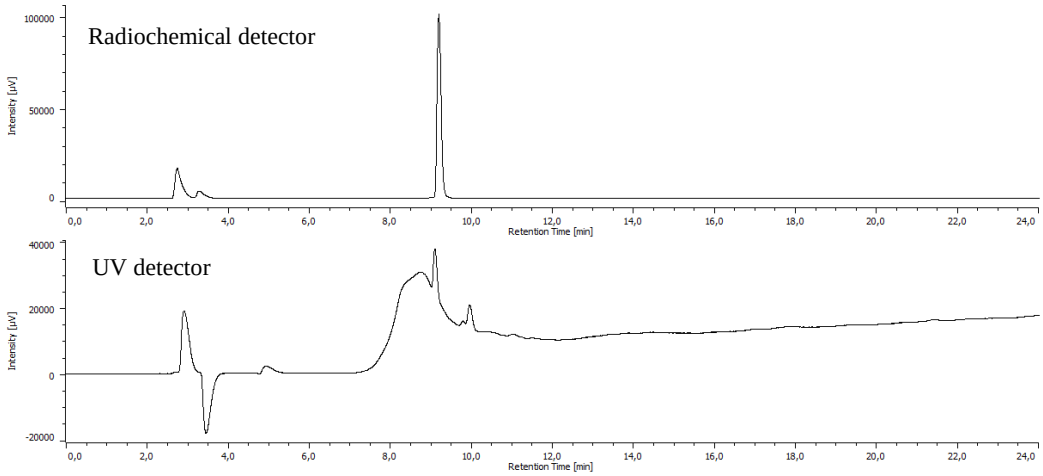

Figure 3.4: *Introduction of [^{18}F]AlF^{2+} into NODA-MPAA-NH_2 chelator.* t_R of **[^{18}F]3.19**: 9.4 min, t_R of NODA-MPAA-NH_2: 10 min.

As shown in Figure 3.4, compound **[^{18}F] 3.19** was obtained with a conversion rate of 75% of [^{18}F]AlF^{2+} into the chelator. The radiochemical detector shows a high radioactive peak in correspondence to product retention time, moreover free aluminum-fluoride in solution is not retained in RP-HPLC and comes out close to the solvent front, as shown by the radioactive peak at retention time of 3 min.

The reaction conditions implemented with NODA-MPAA-NH_2 were then considered for the conjugation of [^{18}F]AlF^{2+} with PSMA-617-NODA derivative.
For radiolabeling studies on PSMA-617-NODA derivative, the radiolabeling procedure was automated using a Trasis AllinOne radiosynthesis platform (Figure 3.5).

As already mentioned previously, automation is essential in the preparation of fluorine-18 labeled radiopharmaceuticals, as it allows radiosynthesis reproducibility with minimal radiation exposure to the personnel. The cassette was adapted to our purposes and the radiosynthesis was automated.

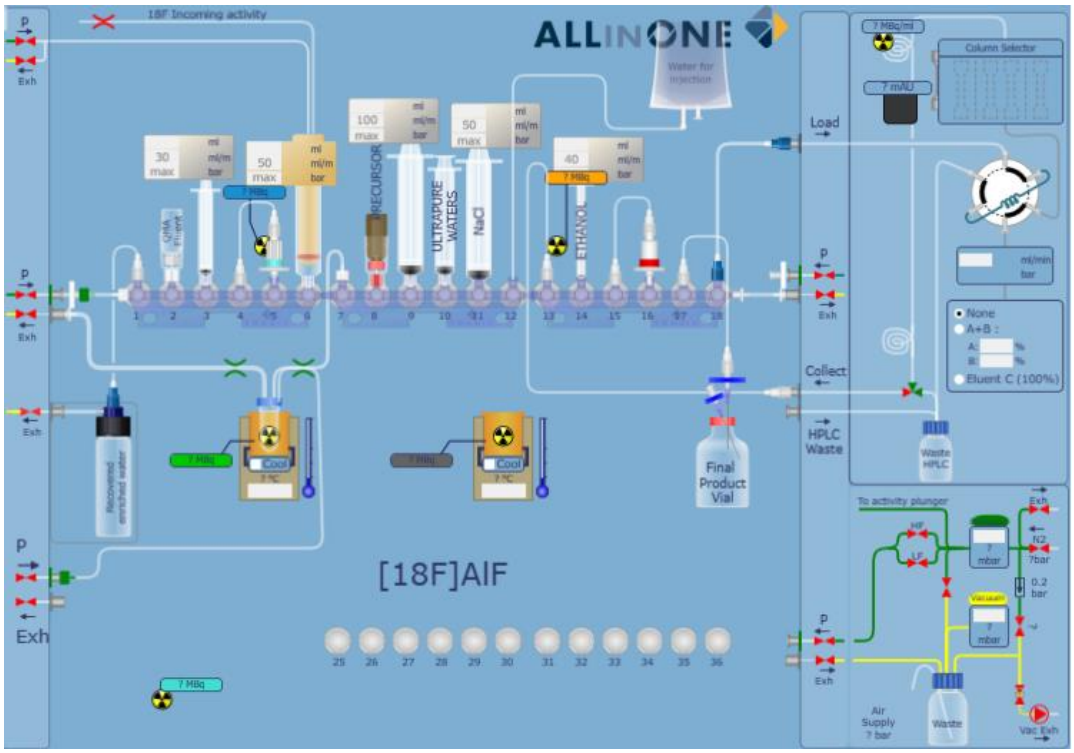

Figure 3.5: *Configuration of Trasis All-in-One automated system. Main reagent positions are indicated:* P2: 0.1M sodium acetate buffer pH=4; P5: QMA Sep-Pak cartridge (0.4 ml hold up volume); P8: precursor in 2mM solution; P10: ultrapure water; P11: Saline physiologic solution; P14: Ethanol; P16: C_{18} Sep-Pak cartridge (0.8 ml hold up volume); Reactor: $AlCl_3$ 0.2 mM solution.

Radiolabeling reaction is depicted in Scheme 3.11. After the formation of aluminum-fluoride, a solution of sodium acetate buffer pH=4, ethanol and precursor **3.1** was added.
After heating 15 min at 110°C compound **[^{18}F]3.20** was obtained. As shown in Figure 3.6, a high [^{18}F]AlF^{2+} complexation with NODA chelator occurred, and only ~5% of free aluminum-fluoride still remained in solution.

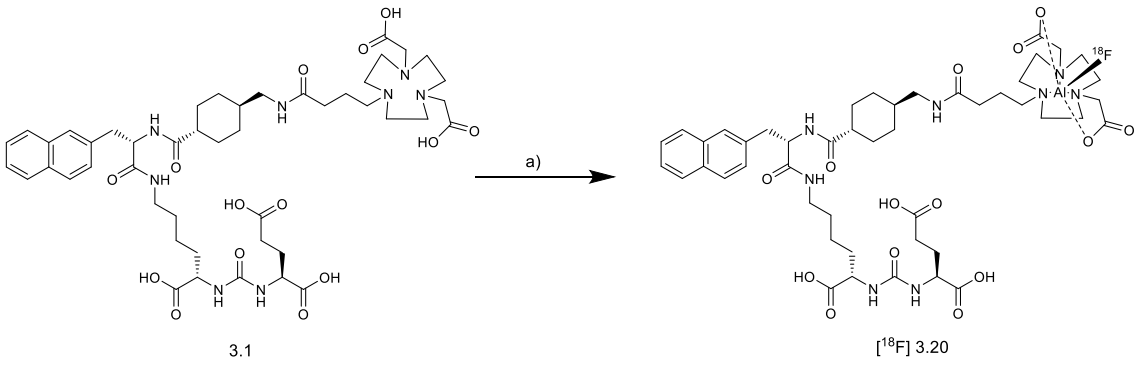

Scheme 3.11: *Introduction of [^{18}F]AlF^{2+} into PSMA-617-NODA derivative precursor **3.1**:* Reagent and conditions: a) [^{18}F] AlF^{2+}, 0.1M sodium acetate buffer pH=4, ethanol; 110°C, 15 min.

Three radioactive by-products were also displayed in the chromatogram. In order to purify the final product, the mixture was adsorbed on a C_{18} Sep-Pak cartridge. Then, the cartridge was washed with water and the radioactive product was eluted with ethanol.

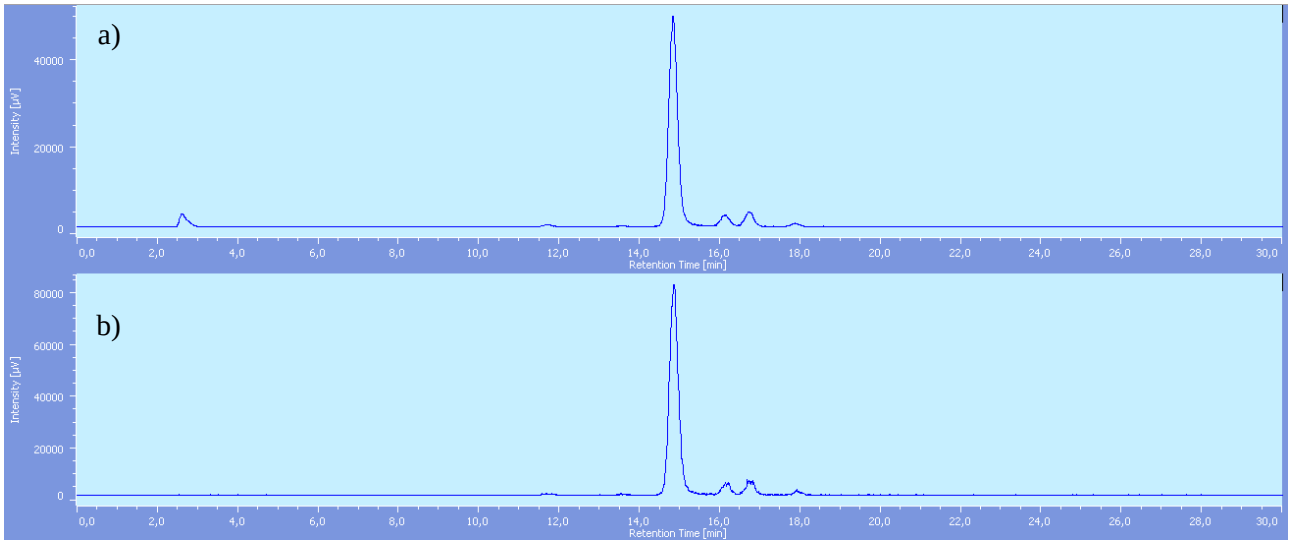

Figure 3.6: *PSMA-617-NODA mix and C_{18} purification chromatogram:* Radiochemical detector: a) [^{18}F] AlF^{2+}+ Product **[^{18}F] 3.20** mix. b) Product **[^{18}F] 3.20** after C_{18} purification. Rt [^{18}F] AlF^{2+}: 2.5 min, Rt Product **[^{18}F] 3.20**: 14.9 min, Rt Precursor **3.1**: 19 min.

Unfortunately, as shown in Figure 3.6 (entry b), the purification by C_{18} cartridge only removed free [^{18}F]AlF^{2+} and a semi-preparative RP-HPLC was required to obtain **[^{18}F]3.20** with a suitable purity.

To this regard, crude reaction mixture was diluted in 80:20 water + 0.1% TFA/ acetonitrile + 0.1% TFA solution, and injected into the column. Gradient conditions were from 80:20 to 60:40 in 30 minutes; the desired product **[^{18}F] 3.20** eluted at 18 minutes (Figure 3.7).

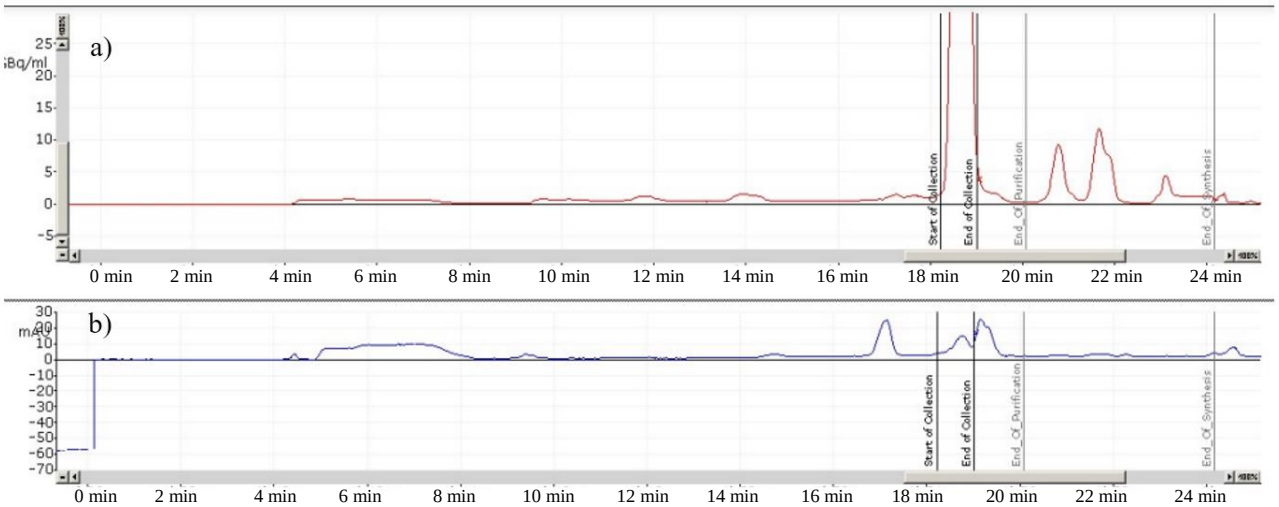

Figure 3.7: *PSMA-617-NODA (***[^{18}F] 3.20)** *semi preparative RP-HPLC chromatogram:* a) Radiochemical detector. b) UV detector. Rt **[^{18}F] 3.1**: 18 min.

HPLC fraction was collected and diluted with water, adsorbed on C_{18} Sep-Pak cartridge, and then washed several times with water. Pure **[^{18}F]3.20** was collected into the final vial eluting the cartridge with 1 ml of ethanol, and formulated with 20 ml of saline physiological solution.

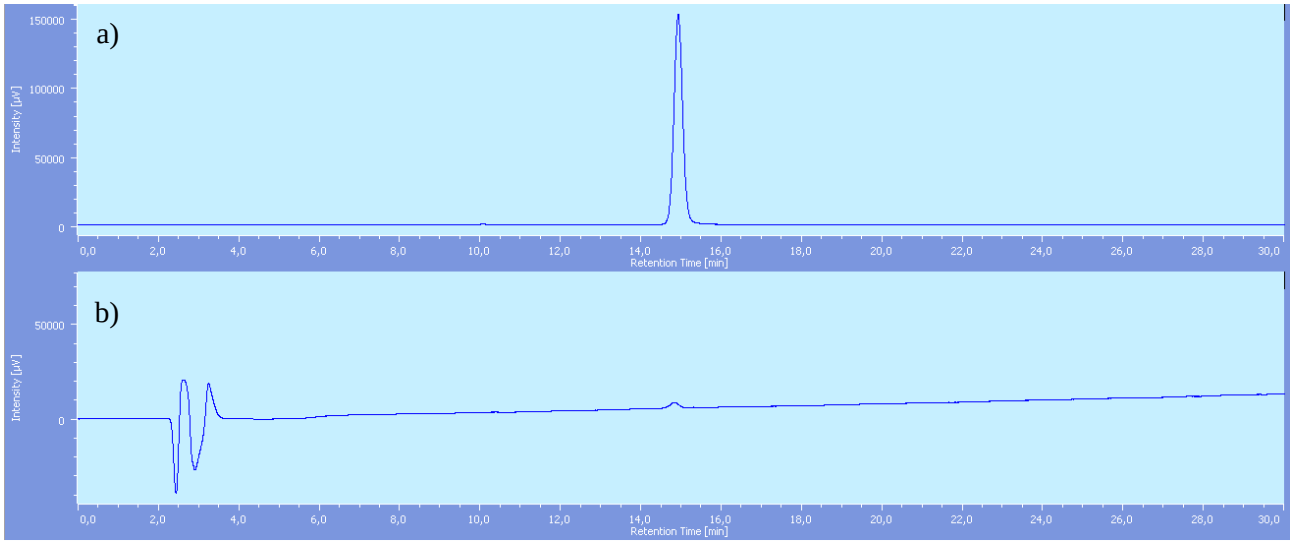

Figure 3.8: *PSMA-617-NODA* **[^{18}F] 3.20** *after RP-HPLC purification:* a) Radiochemical detector. b) UV detector. Rt **[^{18}F] 3.20**: 14.9 min.

The radiosynthetic procedure took an overall time of 59 min, with a final RCY of ~23 %, not decay correct and radiochemical purity was >99%. In addition, it was noticed that the by-product consisting of PSMA-617-NODA complexed with $AlCl^{2+}$ had the same retention time of product **[^{18}F] 3.20** and it was not possible to purify even by semi-preparative HPLC. However, considering the worst case, namely that the totality of the "cold" mass detected at UV corresponds to that of the product, the molar activity resulted to be >170 GBq/µmol.
Chemical and radiochemical stability were tested by analytical HPLC analysis of samples of the purified product up to four hours after the end of radiosynthesis, at time intervals of two hours and storing the vial at room temperature. Product **[^{18}F] 3.20** was stable under these conditions and no loss of radioactivity due to radiolytic degradation was detected.

Moreover, a study to evaluate the product degradation in human plasma was conducted. Plasma was obtained by blood centrifugation at 2800 rpm for 15 min. Then, 20 µl of the final solution were added to the plasma, and the mixture was incubated at 37°C for 2 and 4 hours. At the end of incubation, acetonitrile was added to the mixture precipitating the plasma proteins. The resulting mixture was monitored in HPLC, and it also proved to be stable.

3.2.2.2 Radiosynthesis with [^{18}F]AlF^{2+} of PSMA-617-RESCA derivative

PSMA-617-RESCA-derivative (**[^{18}F]3.21)** was radiolabelled following the same procedure described in the previous paragraph, except for reaction temperature, which was set a room temperature.
Indeed, this is the advantage expected from using RESCA chelator [108], because in principle this procedure can be used even for radiolabeling of large macromolecule preventing denaturation.

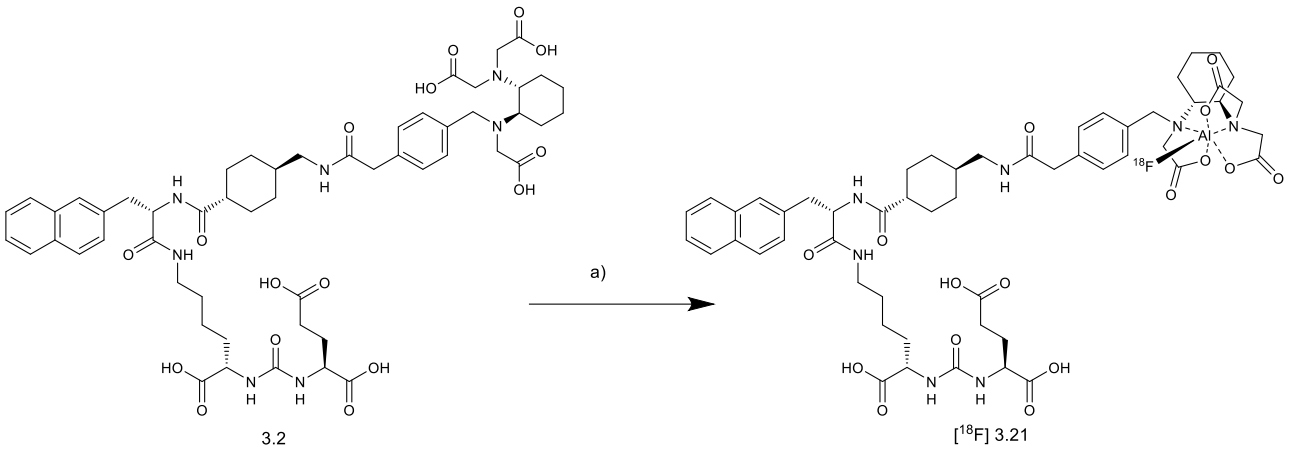

Scheme 3.12: *Radiosynthesis of [^{18}F]3.21*. Reagent and conditions: a) [^{18}F]AlF^{2+}, acetate buffer 0.1M pH=4, ethanol; rt, 15 min.

Product **[^{18}F]3.21** was obtained after 15 min of reaction.

As shown in Figure 3.8 entry a) and b), [^{18}F]AlF^{2+} complexation with RESCA chelator was ~84%, and no radioactive by-products were formed.

Purification was performed loading the reaction mixture on a C_{18} Sep-Pak cartridge, washing with water and eluting the desired product **[^{18}F]3.21** with ethanol.

As shown in Figure 3.8 entry c) and d), after purification the product was obtained with a radiochemical purity of >95%.

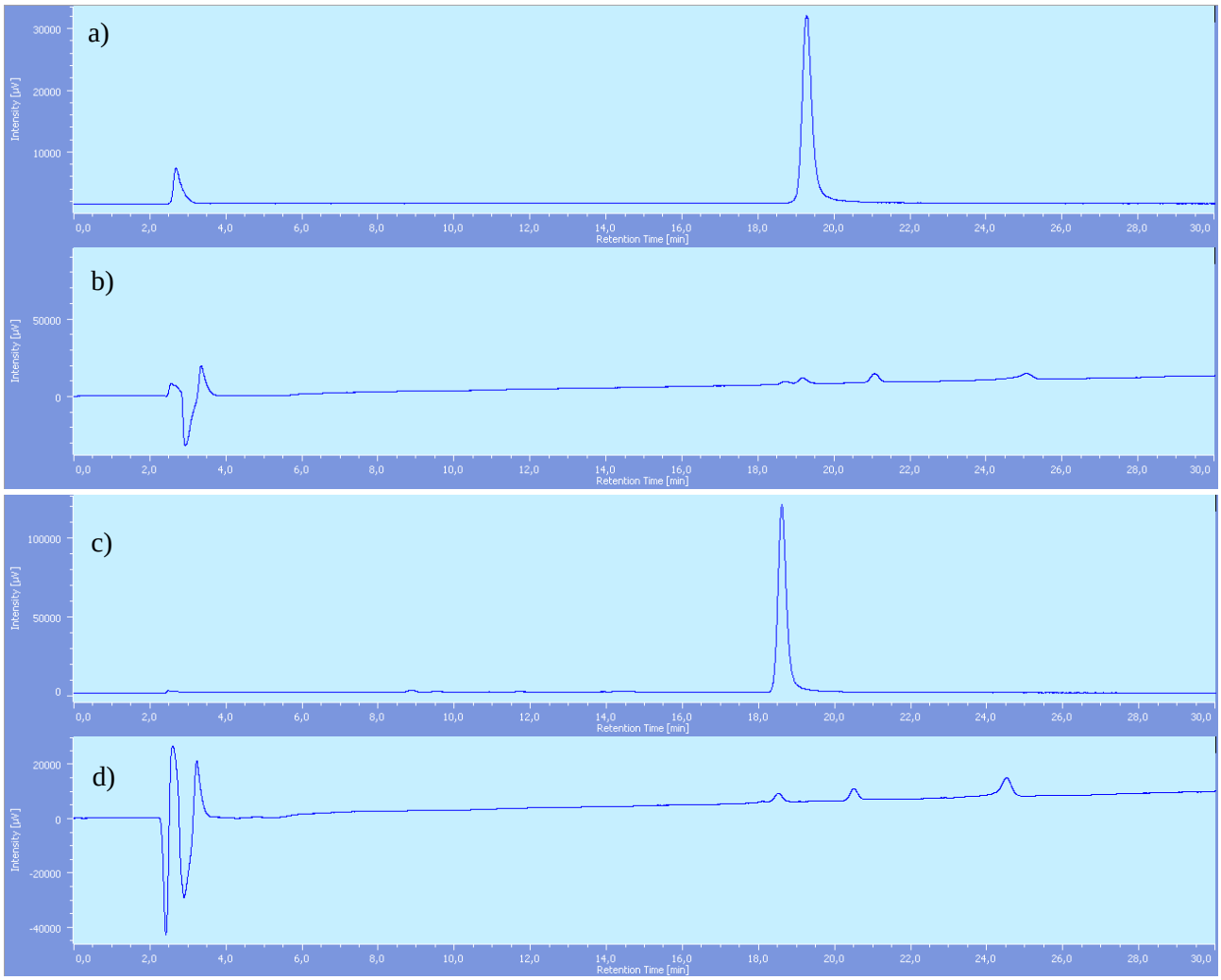

Figure 3.8: *PSMA-617-RESCA (***[^{18}F] 3.21)** *reaction mixture and after C_{18} purification chromatograms:* a) Radiochemical detector: [^{18}F] AlF^{2+}+ Product **[^{18}F] 3.21** mix. b) UV detector: [^{18}F] AlF^{2+}+ Product **[^{18}F] 3.21** mix. c) Radiochemical detector: Product **[^{18}F] 3.21** after C_{18} purification and formulation. d) UV detector: Product **[^{18}F] 3.21** after C_{18} purification and formulation. Rt Product **[^{18}F] 3.21**: 18.6 min, Rt PSMA-617-RESCA with $AlCl^{2+}$: 21.5 min, Rt Precursor **3.2**: 24.7 min.

Finally, after elution formulation with saline physiological solution took place to make it available for *in vivo* preclinical testing. Radiosynthetic procedure took an overall time of 42 min with a RCY of ~40 %, not decay correct. Molar activity was very high (>900 GBq/µmol) calculated on **[^{18}F] 3.21** "cold" mass. In addition, it was noticed that in final formulation there was the presence of the competitors PSMA-617-RESCA complexed with $AlCl^{2+}$ and Precursor **3.2**, identified injecting the respective reference standards. So, considering the total amount of "cold" masses, molar activity decreased to >90 GB/µmol.
The above by-products cannot be removed by purification with C_{18} Sep-Pak cartridge only, probably due to similar structural characteristics.
Both molar activity and purity were considered to be satisfactory for further *in vitro* and *in vivo* stability tests.

As expected, results showed that coordination of [^{18}F]AlF^{2+} with RESCA is kinetically favored, compared with NODA, but the complex is less stable, and labeled aluminum fluoride is gradually released from the desired product, reaching a peak of ~10% at five hours after end of synthesis (EOS) (Table 3.1).

Time	[^{18}F] 3.21 percentage	Free [^{18}F] AlF^{2+} percentage
T=0	96.95%	1.2%
After 1h	96.3%	2.8%
After 2h	94.36%	4.7%
After 3h	92.1%	6.9%
After 4h	90.2%	8.9%
After 5h	90%	9%

Table 3.1: *[^{18}F]AlF^{2+} release in PSMA-617-RESCA final formulation.*

However, purity after 2 hours was of ca 94-95%, still suitable for *in vivo* preclinical studies. In addition, stability test in human plasma gave the same *in vitro* results. $Al^{18}F$ specie is known to accumulate in bone and it is an interesting parameter to determine PSMA-617-RESCA derivative stability in *vivo* [102].

3.2.3 Preclinical studies

The two PSMA-617 derivatives were tested *in vivo* on a set of mice. Studies were conducted on inoculated subcutaneous prostate tumor model. In addition, the uptake of the products **[^{18}F]3.20** and **[^{18}F]3.21** was studied also on a model of glioblastoma, the most aggressive primary brain tumor in adults. Indeed, recent findings revealed that PSMA may be expressed not only in PCa, but also in other types of cancer, including glioblastoma.

In detail, human prostate tumor model was subcutaneously injected in female nu/nu mice, and when the tumor was visible a PET/CT biodistribution at different times study was performed. The same animals in subsequent days were injected with standard PSMA-1007 (the fluorine-18 radiolabeled PSMA ligand used for human PCa routine imaging, see Chapter I) and PSMA-617-NODA functionalized **[^{18}F]3.20**. Mice were injected into a tail vein with ~4 MBq and PET images were acquired after 10, 60 and 120 min.
As shown in Figure 3.9, compared with PSMA-1007, our derivative PSMA-617-NODA showed higher uptake in tumor lesions, better tumor/background ratio and better specificity, with poor or no uptake in in salivary glands, which further improve clarity of imaging and reduce unwanted irradiation of the above healthy organs.

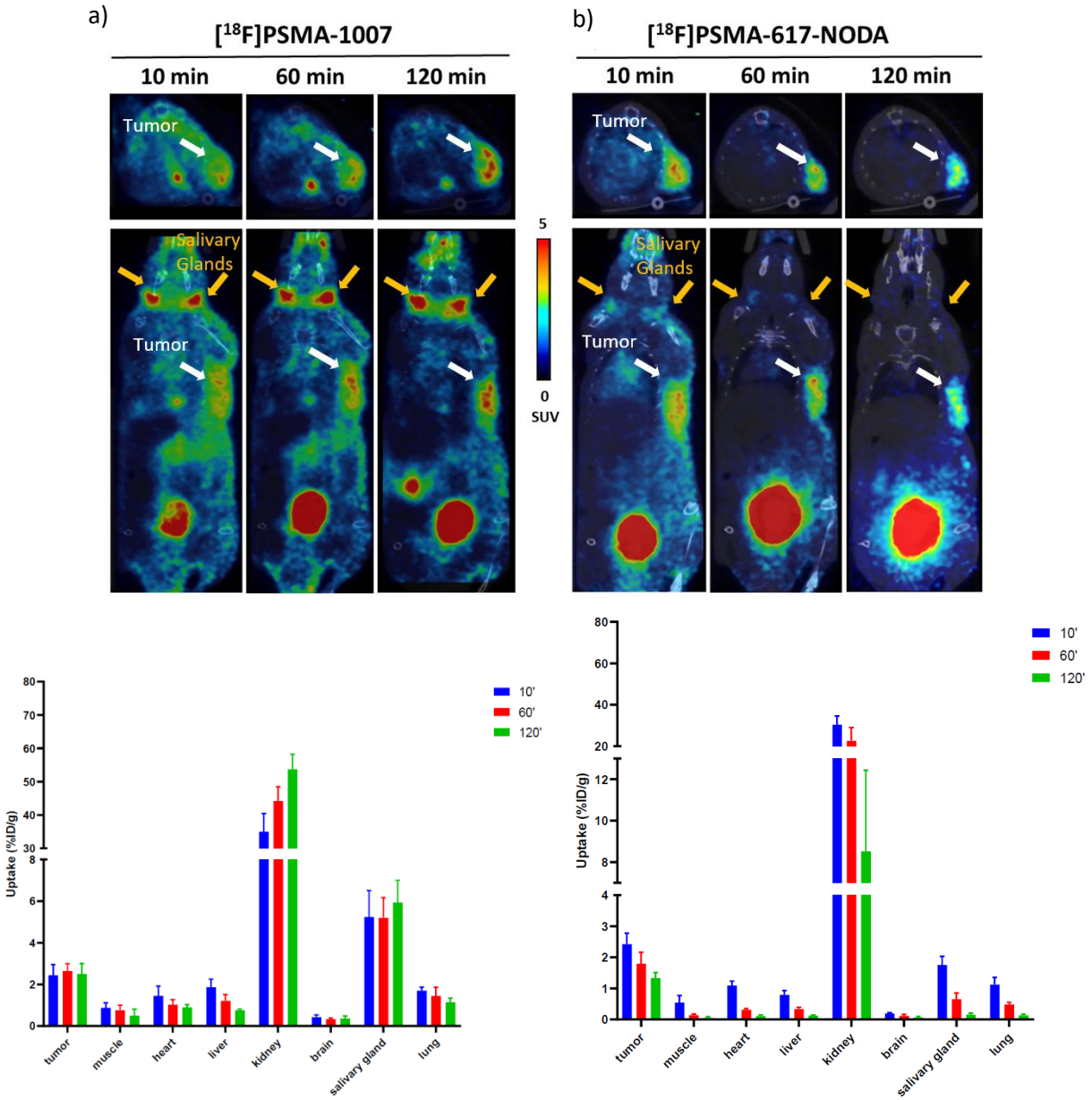

Figure 3.9: *Comparison between PSMA-1007 and product* ***[18F]3.20*** *on human prostate tumor inoculated mice*. a) PSMA-1007 PET/TC at different time of acquisition b) Product **[18F]3.20** PET/TC at different time of acquisition c) PSMA-1007 uptake in different tissues d) Product **[18F]3.20** uptake in different tissues.

In a second study, a comparison between products **[18F]3.20** and **[18F]3.21** was conducted on a glioblastoma model. Human glioma cells Gli36dEGFR were injected into the brain. Before PET acquisition, MRI was conducted to evaluate the volume of the tumor and for cerebral quantification the MRI was co-registered with the PET/CT at different temporal intervals. The quantification at the brain level was done by placing a ROI (region of interest) at the tumor level and one on the healthy counterpart of the brain.

Results showed that tumor uptake of PSMA-617-NODA was higher than that of PSMA-617-RESCA (Figure 3.10). Moreover, in the case of product **[18F]3.21** at the peripheral level it was observed a higher uptake in the liver and intestine, which was not noticed in the case of product **[18F]3.20** images.

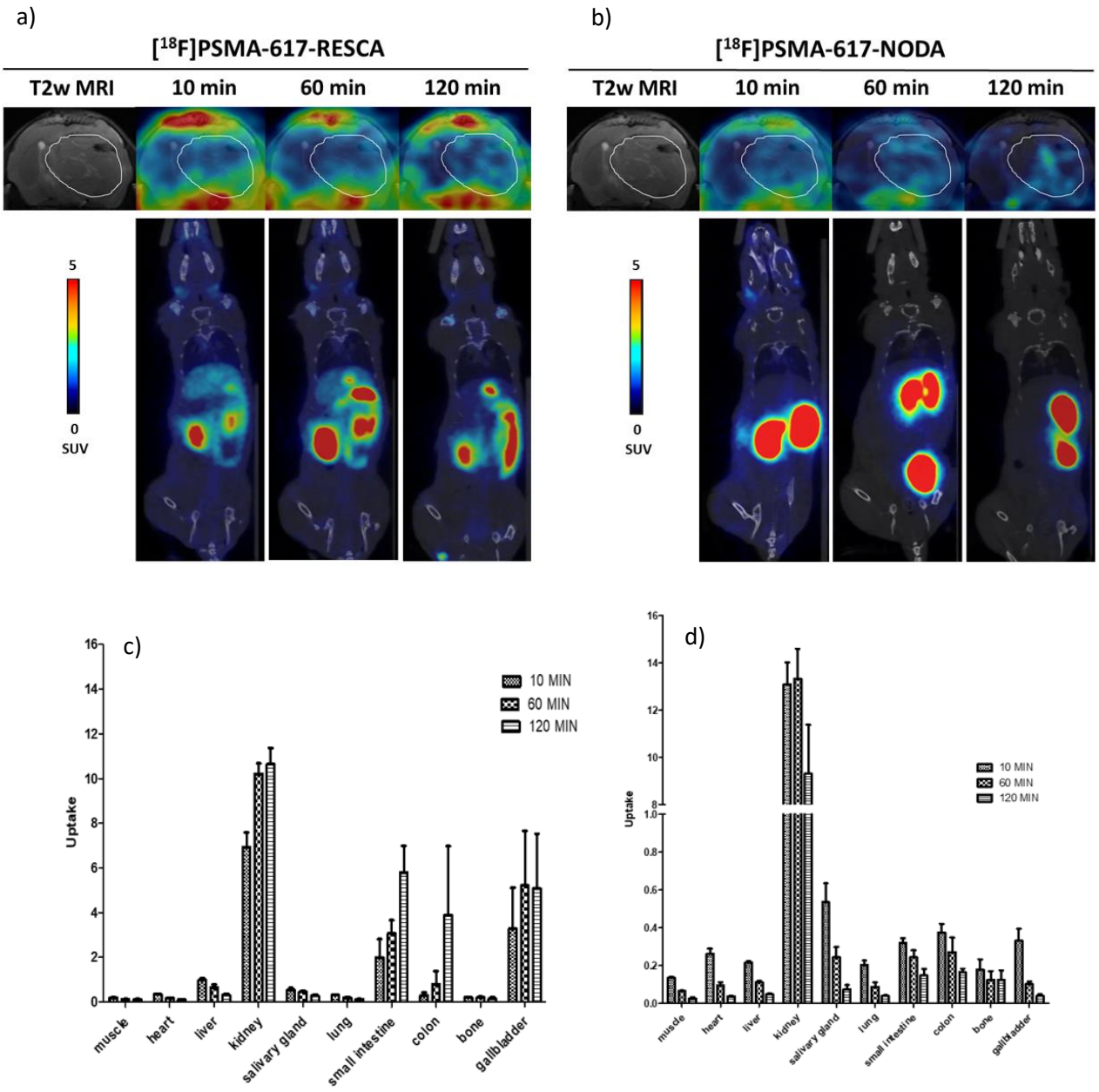

Figure 3.10: *Comparison between PSMA617-NODA derivative (product **[^{18}F]3.20**) and PSMA617-RESCA derivative (product **[^{18}F]3.21**) in human glioblastoma tumor*. a) The relative quantification data of Product **[^{18}F]3.21** expression in GBM tumor compared to contralateral healthy tissue, are reported as ΔΔct, b) The relative quantification data of Product **[^{18}F]3.20** expression in GBM tumor compared to contralateral healthy tissue, are reported as ΔΔct, c) Product **[^{18}F]3.21** uptake in different tissues, d) Product **[^{18}F]3.20** uptake in different tissues.

3.3 CHAPTER CONCLUSION

Novel derivatives of PSMA-617 functionalized with NODA and RESCA chelator were radiolabeled and characterized. Both products were obtained in good yield, purity and molar activity. Moreover, whole radiolabeling procedure was fully automated.

It is important to mention that results showed marked differences in terms of reaction conditions and stability in solution and plasma. NODA derivative (**[^{18}F] 3.20**) showed better stability in solution and

in plasma, but its reaction with [^{18}F]AlF^{2+} requires heating at high temperatures. Moreover, semi-preparative HPLC purification was necessary to obtain a product with suitable radiochemical purity. On the contrary, RESCA derivative (**[^{18}F] 3.21**) showed better radiochemical yield, also due to a shorter preparation time, milder reaction conditions and easy purification on SPE, but on the other hand it also proved to be less stable in solution and plasma.

Overall, automation of radiolabeling procedure via "aluminum-fluoride introduction" was satisfactory, and similar protocols might be applied to the radiolabeling of other potentially interesting biomolecules.

Finally, the two derivatives were tested *in vivo* in mice on human prostate and glioblastoma tumor models. PSMA-617-NODA derivative (**[^{18}F] 3.20**) resulted to have a higher uptake and specificity in PCa model and lower background model than the routinely used[^{18}F]PSMA-1007. Moreover, PSMA-617-NODA derivative (**[^{18}F] 3.20**) showed lower uptake in the peripheral organs and higher uptake in human glioblastoma tumor compared to healthy brain than PSMA-617-RESCA derivative (**[^{18}F] 3.21**).

CHAPTER IV

Synthesis of new PSMA-617 derivatives and radiolabeling with fluorine-18 direct introduction by S_N2 substitution reaction

4.1 ABSTRACT

This Chapter focuses on the radiolabeling with fluorine-18 via a direct S_N2 reaction of two derivatives of PSMA-617 functionalized with 2-trimethylammonium nicotinic amide (**4.1**) and bromoacetic amide (**4.2**) (Figure 4.1). At first, chemical synthesis of precursors was performed with ~22% overall yields for precursor **4.1** and ~10% for precursor **4.2**. Then, radiolabeling of PSMA-617 2-trimethylammonium nicotinic amide derivative was successfully performed (radiochemical purity >99%, synthesis time 63 min, ~20% of not-corrected RCY, >1000 GBq/μmol). Unfortunately, radiolabeling of precursor **4.2** was not successful. In addition, the radiosynthetic process was automated on a suitable Trasis All-in One radiosynthetic module.

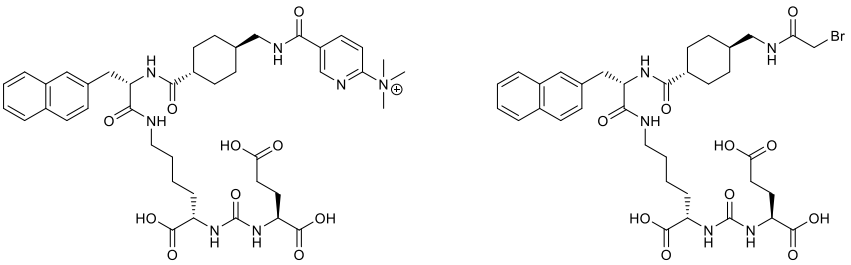

4.1 4.2

Figure 4.1: *Precursor **4.1** or **4.2**.*

4.2 RESULTS AND DISCUSSION

Preparation of "cold" products was implemented in the laboratories of Medical Biotechnology and Translational Medicine Department of Università degli Studi di Milano as well as NMR characterizations, under supervision of prof. Patrizia Ferraboschi and Diego Colombo. Radiolabeled products as well as RP-HPLC analysis and RP-HPLC purifications were performed in the laboratories of the Tecnomed Foundation- Università degli Studi di Milano-Bicocca. MS characterizations were made at Departement of Medicine and Surgery of Università degli Studi di Milano - Bicocca.

4.2.1 Chemistry

The synthesis of precursors **4.1** and **4.2** was designed functionalizing PSMA-617 "core" (compound **2.10**) with suitable leaving groups. In the first case, a 2-trimethyl ammonium nicotinic acid was added to the biomolecule "core", while in the second case compound **2.10** was coupled with bromo-acetic acid.

4.2.1.1 Synthesis of PSMA-617 functionalized by pyridine-2-trimethylammonium

The radiosynthetic strategy started from the preparation of 2-trimethylammonium nicotinic acid activated in the form of highly reactive tetrafluoro-phenol ester. As shown in Scheme 4.1, starting from commercial tetrafluoro-phenol and 2-chloro nicotinic acid, coupling reaction occurred in

presence of dicyclohexylcarbodiimide and ester bond was formed at room temperature [127]. The activated ester was purified by chromatographic column and pure compound **4.3** was obtained.
Then, chlorine at 2 position was substituted by trimethylammonium group as suitable leaving group for fluorine-18 S_N2 direct introduction. Following the procedure of Olberg et al. [128], compound **4.3** was reacted with a 2M solution of trimethyl amine in dry THF. The reaction was conducted under nitrogen atmosphere to prevent potential hydrolyzed byproducts. When the product begins to form, a precipitation occurs. Then, at the end of reaction, the crude mixture was filtered and the crude compound **4.4** with chloride as counter-ion was obtained (**4.4** after reaction b). Reaction progress was monitored by TLC until complete disappearance of compound **4.3**. Finally, chloride counter-ion was substituted by triflate one. As shown in Scheme 4.1 entry c, the obtained crude was suspended in dichloromethane and trimethylsilyl triflate was added. Product **4.4** (after reaction c) was obtained and characterized by NMR and MS spectrometry.

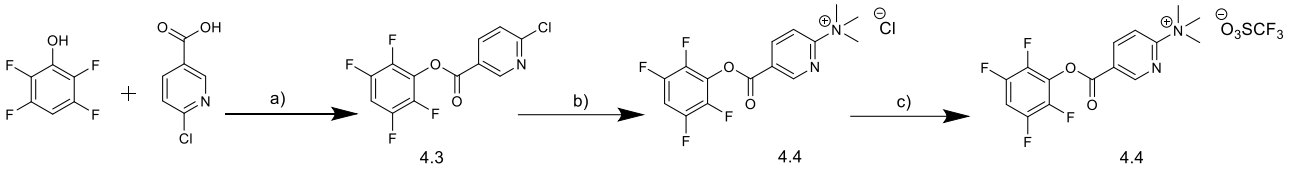

Scheme 4.1: *Synthesis of activated 2-trimethylpyridin ammonium 5-carboxylic acid.* Reagent and conditions: a) DCC, 1,4 dioxane, rt, overnight, (74%); b) 2M NMe_3, THF dry, rt, overnight, c) TMSOTf, dry DCM, rt, 2h, (74%).

Once the 2-trimethyl ammonium nicotinic acid derivative was obtained, activated by reactive tetrafluoro phenyl ester, the functionalization of PSMA-617 "core" (compound **2.10**) was performed. As shown in Scheme 4.2 (entry a), reaction was carried out in DMF in presence of triethylamine in order to activate free primary amine group of compound **2.10**, and compound **4.5** was obtained in good yields. Again, product **4.5** didn't run through the TLC matrix due to the presence of salts, so the reaction progress was monitored based on PSMA-617 "core" disappearance.

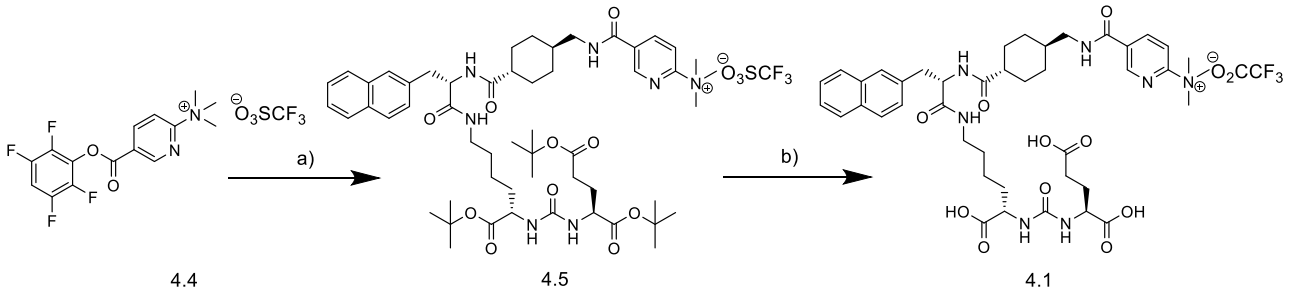

Scheme 4.2: *Synthesis of Precursor **4.1***. Reagent and conditions: a) Compound **2.10**, DMF, rt, overnight, (82%); b) TFA, DCM, rt, 2h, (48%).

At last, the *tert*-butyl protecting groups removal was conducted in the same acidic conditions showed in the previous chapters. Triflate counter ion permitted a better solubility in dichloromethane and compound **4.1** was obtained in good yields. The reaction progress was monitored by NMR until complete disappearance of tert-butyl peak at 1.5 ppm. Finally, a semi-preparative RP-HPLC purification was carried out. Isocratic elution (70:30 of water+0.1% TFA: acetonitrile+0.1% TFA)

was set and the final product was obtained in good yields. The overall synthesis path yields were 21.6%.
The synthesis of the "cold", non-radiolabeled reference standard was performed as follows.
Fluorine introduction with TBAF in THF directly on compound **4.5** was not successful and compound **4.7** was not obtained. For this reason, it was decided to introduce fluorine on activated ester trimethyl ammonium derived **4.4** and then coupling it with PSMA-617 "core", as shown before.

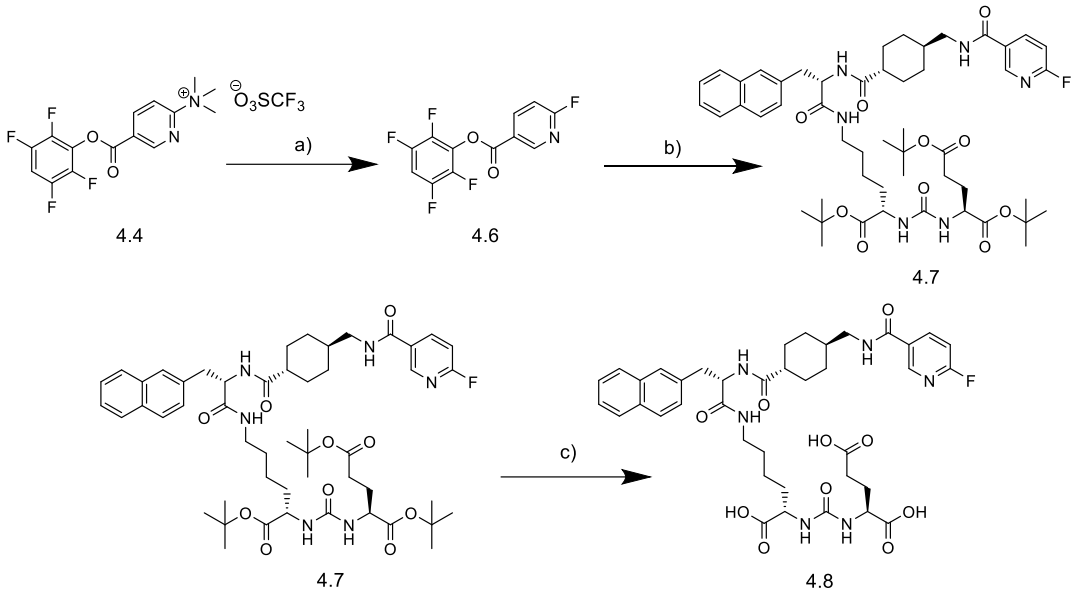

Scheme 4.3: *Synthesis of "cold" standard **4.8***. Reagents and conditions: a) 1M TBAF in THF dry, ACN dry, rt, 1h, (10%); b) Compound **2.10**, TEA, DMF, rt, overnight, (93%); c) TFA, DCM, rt, 2 days, (50%).

Based on Olberg *et al.* work [128], fluorine was introduced on substrate **4.4** using a 1M solution of TBAF in dry THF in acetonitrile as solvent to solubilize the substrate. When compound **4.4** in acetonitrile solution was added, a strong precipitation occurred and reaction progress stopped. Even adding more amount of TBAF or solvent, reaction didn't proceed further. That's the reason of low yield obtained in this step. Moreover, column chromatography was performed and compound **4.6** was obtained with satisfactory purity. The low yield obtained in this passage conditioned the whole synthesis yield.
Then, the obtained 2-fluoro nicotinic acid trifluoro phenyl ester was reacted with PSMA-617 "core" (compound **2.10**) under the same conditions showed above. In this case, product **4.7** was eluted through the TLC and reaction progress could be monitored. Finally, tert-butyl were removed in acidic media and compound **4.8** was purified by semi-preparative RP-HPLC in same conditions showed above.
In conclusion, standard "cold" version product was obtained with satisfactory purity and the whole synthesis yield was 5% calculated on compound **4.4**.

4.2.1.2 Synthesis of PSMA-617 functionalized by bromine

In principle, the bromine-derivative intermediates **3.3** and **3.9**, showed in Chapter III as precursors for NODA or RESCA PSMA-derivatives, could be very interesting substrates to which introduce fluorine-18. Unfortunately, due to the failure of obtaining a PSMA-617 derivative connected to a bromine leaving group by a propyl linker, it was decided to switch on compound **4.2** synthesis. As it

is possible to see in Figure 4.1, the biologically active molecule was functionalized by bromoacetic acid. Given to the proximity of bromine to the electron withdrawing carbonyl group, the subsequent fluorine-18 introduction could be more difficult.
As future perspective, new substrates should be synthetized with different linker lengths and also different functionalization in order to study different reactions for fluorine-18 introducing on sp^3 hybridized carbon (see Chapter I).

The synthesis was set coupling a bromo acetic acid on PSMA-617 "core" (compound **2.10**). As shown in Scheme 4.4 two different attempts were performed and different results in terms of yield were obtained.

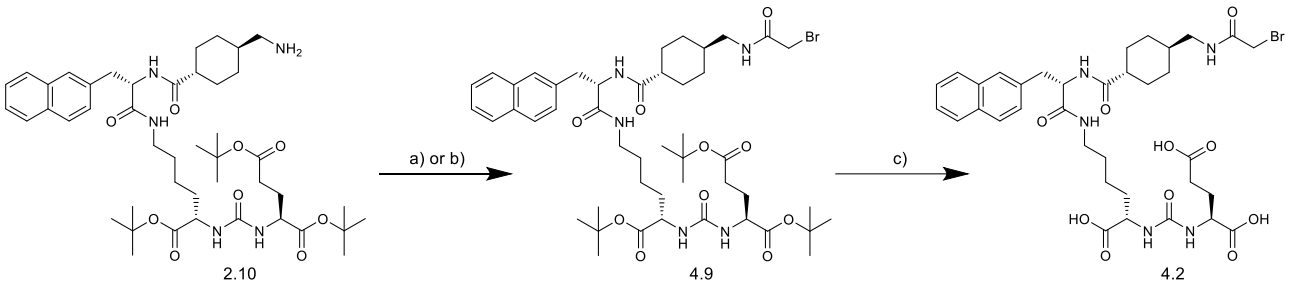

Scheme 4.4: *Synthesis of precursor **4.2***. Reagent and conditions: a) bromoacetic acid, HATU, TEA, DMF, from 0°C to rt, overnight, (20%); b) bromoacetic acid, DCC, DMAP, DCM, rt, 30 min, (83%); c) TFA, DCM, rt, 2h, (57%).

In the first attempt, the coupling reaction was conducted using HATU as condensing agent (Scheme 4.4 entry a). Compound **4.9** was obtained after purification by chromatographic column in low yields (20%). Probably the amount of 2.5 equivalents of triethyl amine gave strong competition effects: precursor **2.10** performed the desired coupling but also substitution of bromine substituent of the acid. It was confirmed by crude mixture where a large number of by-products in TLC were noticed and purification by silica gel had to be performed two times, due to the presence of multiple products co-elution in various fractions. In addition, by NMR characterization analysis gave not completely clear results.
Thus, a different coupling approach was conducted, using dicyclohexylcarbodiimide (DCC) and small amount of dimethyl aminopyridine (DMAP) in dichloromethane (Scheme 4.4 entry b). Even in this case, the product had to be purified by chromatography to remove unreacted reagents and dicyclohexylurea, but yield was much better.
Finally, the obtained compound **4.9** was deprotected from *tert*-butyl in acidic media. As already mentioned several times, trifluoroacetic acid in dichloromethane gave good results. After semi-preparative RP-HPLC purification the precursor **4.2** was obtained with high purity and ready to be radiolabelled with fluorine-18, with an overall yield of ~10%.

In addition, the "cold" standard precursor had to be synthetized. As shown in Scheme 4.5, the same reaction and conditions used for preparation of precursor **4.2** were used. Due to the high yields obtained using DCC as condensing agent, product **4.10** was obtained reacting PSMA-617 "core" with fluoroacetic acid. Purification on silica gel was performed, and high yield and purity were achieved. No significant differences were noticed compared with bromine-precursor strategy.

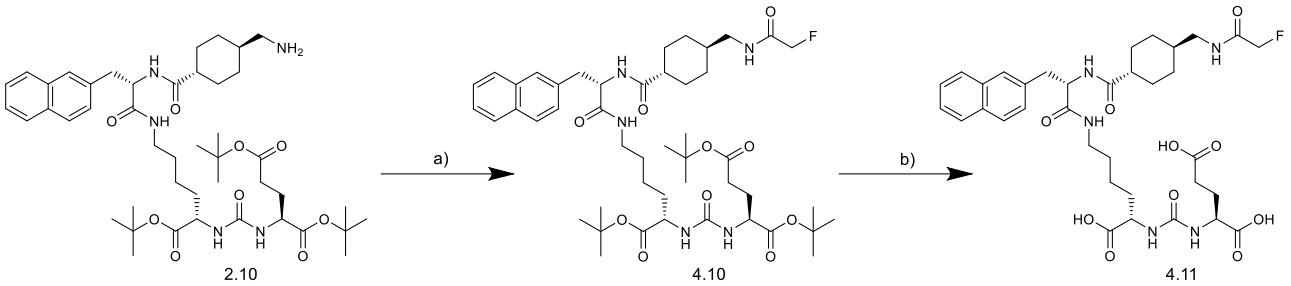

Scheme 4.5: *Synthesis of compound **4.11***. Reagent and conditions: a) fluoroacetic acid, DCC, DMAP, dry DCM, rt, 30 min, (89%); b) TFA, dry DCM, rt, 1h, (42%).

Finally, the standard "cold" final product (**4.11**) was obtained after *tert*-butyl deprotection in acidic media by trifluoroacetic acid. After purification via semi-preparative RP-HPLC, the desired product was obtained with good yield and purity. All the products were characterized by NMR and MS spectroscopy and an analytical HPLC method was implemented to monitor fluorine-18 direct introduction on precursor **4.2**. In addition, the overall synthetic yield was 37%, calculated on compound **2.10**.

Moreover, the direct fluorine S_N2 introduction was tested on compound **4.9**. As shown in the Scheme 4.6, the bromine precursor was heated at high temperature in presence of TBAF in tetrahydrofuran (bringing THF to reflux). The formation of compound **4.10** was monitored by TLC and NMR. Unfortunately, no product was obtained in those conditions and large amount of hydrolyzed byproduct was detected.

Despite of the poor results, the study of this reaction could be useful to have a basis to find the best conditions of direct fluorine-18 introduction in order to switch them to radiosynthesis module. Although various "cold" attempts were made using TBAF and heating, compound **4.10** was not obtained, as mentioned above. However, it was decided to go ahead with the project by testing S_N2 direct fluorine-18 introduction reaction using precursor **4.2**, and using different reagents (Kryptofix 2.2.2 and K_2CO_3 instead of TBAF).

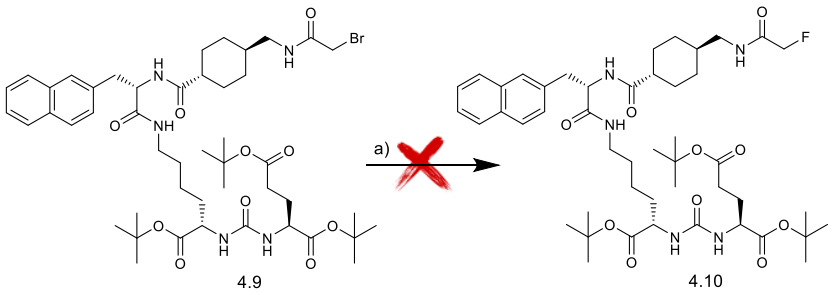

Scheme 4.6: *Compound **4.10** preparation from compound **4.9***. Reagent and conditions: a) 1M TBAF in dry THF, 80°C, 5h.

4.2.2 Radiochemistry

Generally, direct fluorine-18 introduction occurs in "harsh" conditions, for example heating at high temperature (>80°C) and those conditions are not suitable for large macromolecules because of their denaturation and loss of biological properties.

However, in case of PSMA-617, precursor resulted to be stable at high temperatures and an attempt to radiolabel it also with direct fluorine-18 introduction seemed to be feasible.
In this paragraph, direct introduction on aryl precursor **4.1** and alkyl precursor **4.2** is described. The radiosyntheses were performed on a Trasis-All in One automated system.

4.2.2.1 Radiosynthesis with fluorine-18 direct introduction (S_N2) on PSMA-617 pyridine trimethylammonium derivative

Radiosynthesis of product **[^{18}F]4.8** was conducted taking profit of the conditions already established for the preparation of the radiopharmaceutical PSMA-1007, a PSMA ligand used in patient routine for PCa imaging (see Chapter I).
In details, at the end of bombardment (EOB), fluorine-18 was transferred to the radiosynthesis module in form of [^{18}F] hydrofluoric acid solution in water and trapped onto an anionic exchange cartridge (QMA). Then fluorine-18 was eluted with 0.75 ml of a 0.75 mM tetrabutylammonium hydrogen carbonate (TBA) solution. Thanks to counterion exchange, [^{18}F] TBAF was obtained and fluorine-18 in this form was ready to react in S_N2 reaction.
As shown in Scheme 4.7, [^{18}F] TBAF was reacted with precursor **4.1**, functionalized with trimethylammonium bonded on aryl as leaving group. The reaction occurred in dimethylsulfoxide at 105°C.

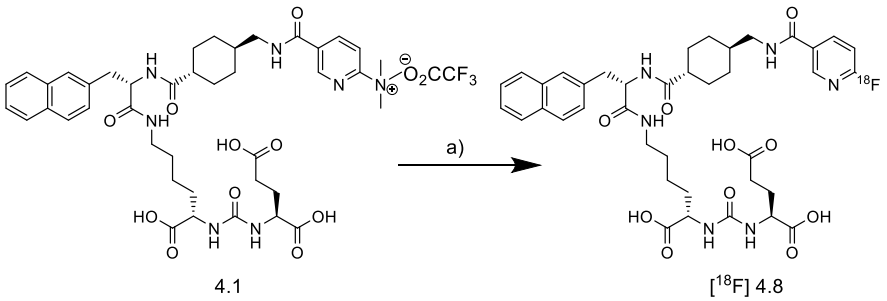

Scheme 4.7: *Radiosynthesis of product **[^{18}F]4.8***. Reagent and conditions: a) [^{18}F] TBAF, DMSO, 105°C, 10 min.

Several attempts were made to achieve a suitable purification. At first, purification with SPE was tested because of shorter time and easier automation.
For this purpose, the mixture after radiosynthesis was loaded on two Oasis (weak cationic exchange, 1 ml hold up volume) and C_{18} Sep-Pak cartridge (0.8ml hold up volume) connected in series.
Then, the SPE cartridge was eluted using different ratio of a water/ethanol solution: at first, the two Sep-Pak cartridges were washed with 20 ml of a solution of 5% ethanol in water and the unreacted fluorine-18 could be successfully removed. Then, several attempts to elute the cartridge with different ratio from 20% to 30% ethanol solution in water were made. 20 ml of solution was passed through the cartridges in steps of 5 ml each, and the obtained fractions were analysed by analytical HPLC to monitor the purification process. The best results were obtained using 30% ethanol solution in water but, as shown in Figure 4.2, purification from by-products was not satisfactory. In addition, product **[^{18}F]4.8** was found in more fractions, thus splitting activity, lowering yields and giving troubles for

final formulations. Cartridges have been chosen based on recommendations of Trasis for [^{18}F] PSMA-1007 automated system preparation [129].

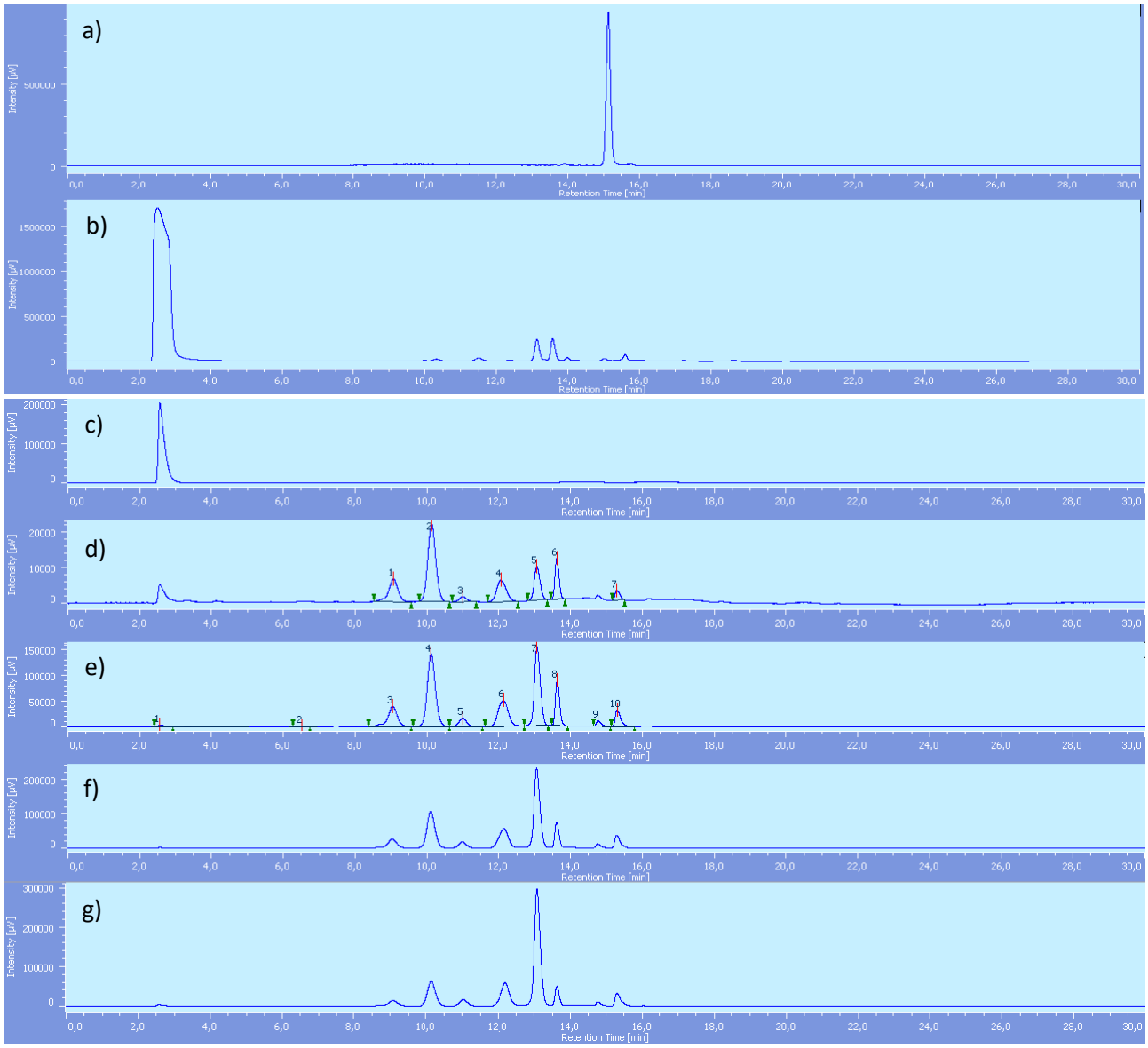

Figure 4.2: *SPE purification of product* ***[^{18}F]4.8***. a) Radiochemical detector: crude mixture, b) UV detector: crude mixture, c) UV detector: washing 5% ethanol in water solution (20 ml), d) UV detector: first 5 ml eluting 30% ethanol in water solution, e) UV detector: second 5 ml eluting 30% ethanol in water solution, f) UV detector: third 5 ml eluting 30% ethanol in water solution, UV detector: g) fourth 5 ml eluting 30% ethanol in water solution. Method: gradient from 70:30 to 20:80 in 25 min buffer phosphate pH=2.55/acetonitrile. Product **[^{18}F]4.8** tr: 14.7 min.

Considering the above findings, it was mandatory to proceed with semi-preparative RP-HPLC purification. In detail, the crude mixture was diluted with water (8 ml) and the obtained solution was injected in HPLC. The method used provided a gradient from 70:30 to 60:40 of water+0.1%TFA/ acetonitrile+0.1%TFA in 20 minutes. The method proved to be effective, and pure **[^{18}F]4.8** product fraction was diluted with 50% water and passed through a C_{18} Sep-Pak cartridge, where it was then washed several times with water.

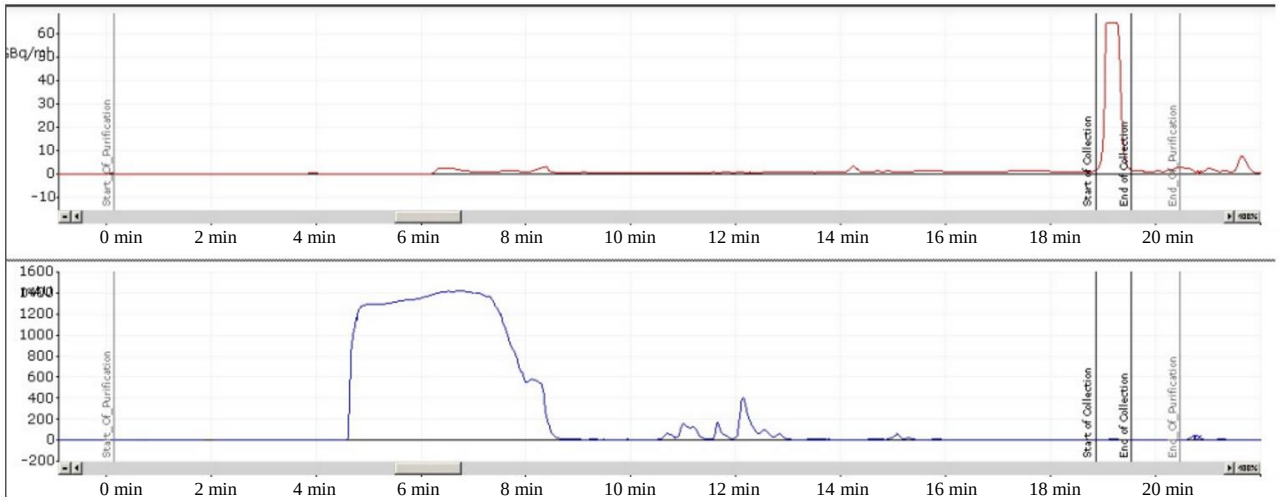

Figure 4.3: *Purification by semi-preparative RP-HPLC of compound* ***[^{18}F]4.8***.

Finally, the pure **[^{18}F]4.8** product was eluted from the C_{18} Sep-Pak cartridge by passing 1 ml of ethanol, followed by 19 ml of physiological solution to obtain the final formulation.
The radiosynthetic procedure took an overall time of 63 min, with a final RCY of ~20 %, not decay correct (molar activity >1000 GBq/μmol), while radiochemical purity was >99%.

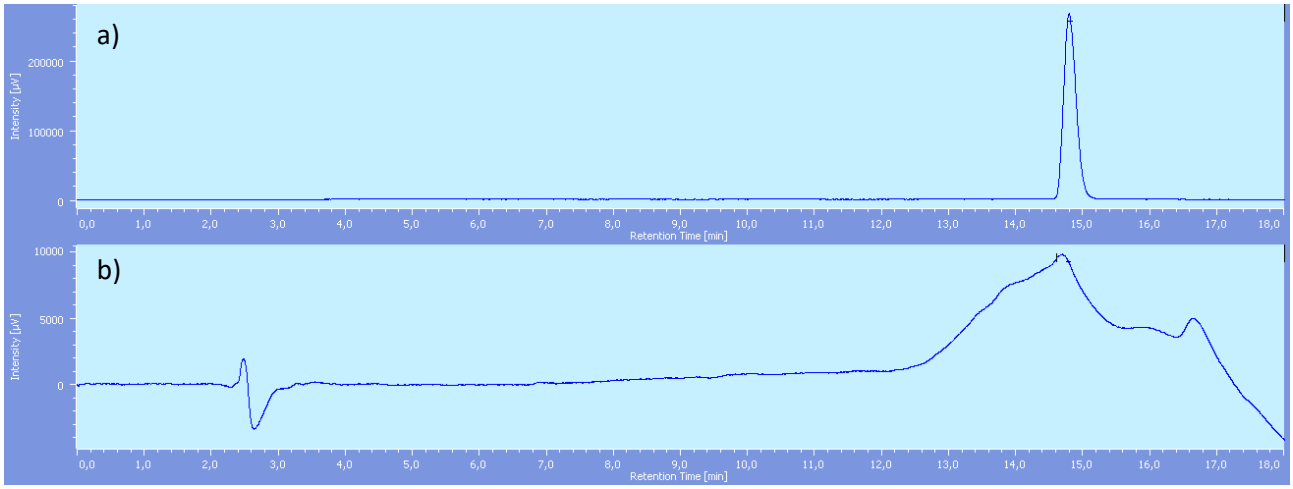

Figure 4.4: *HPLC chromatogram of pure* ***[^{18}F]4.8***. a) Radiochemical detector, b) UV detector. Method: buffer phosphate pH=2.55/ acetonitrile isocratic 75:25 for 2 min, gradient from 75:25 to 70:30 in 6 min, gradient from 70:30 to 60:40 in 5 min, isocratic 60:40 for 5 min. Product **[^{18}F]4.8** tr: 14.7 min.

Chemical and radiochemical stability were tested by analytical HPLC analysis of samples of the purified product up to four hours after the end of radiosynthesis, at time intervals of two hours and storing the vial at room temperature. Stability was monitored both by analytical HPLC and radio-TLC. The chosen method was the same as described in the European Pharmacopoeia monograph for [^{18}F]PSMA-1007 [129] because in those conditions it was possible to detect with more accuracy by-products like the hydrolysis one.
Radiochemical purity was also monitored by radio-TLC (eluent: water/acetonitrile 20:80), using an autoradiography system mod. CYCLONE (Perkin Elmer).

As shown in Figure 4.5, a small and gradual radiolytic degradation was detected. In fact, after two hours in solution, percentage of fluorine-18 increased from 1.2% to 2.1% and after 4 hours increased to 2.7%. In addition, percentage of **[^{18}F] 4.8** decreased to 93.9% after 4 hours. The limit of injectable solution is >95% of radiochemical purity, so the synthetized radiopharmaceutical couldn't be injected after 2 hours, due to radiolytic degradation.

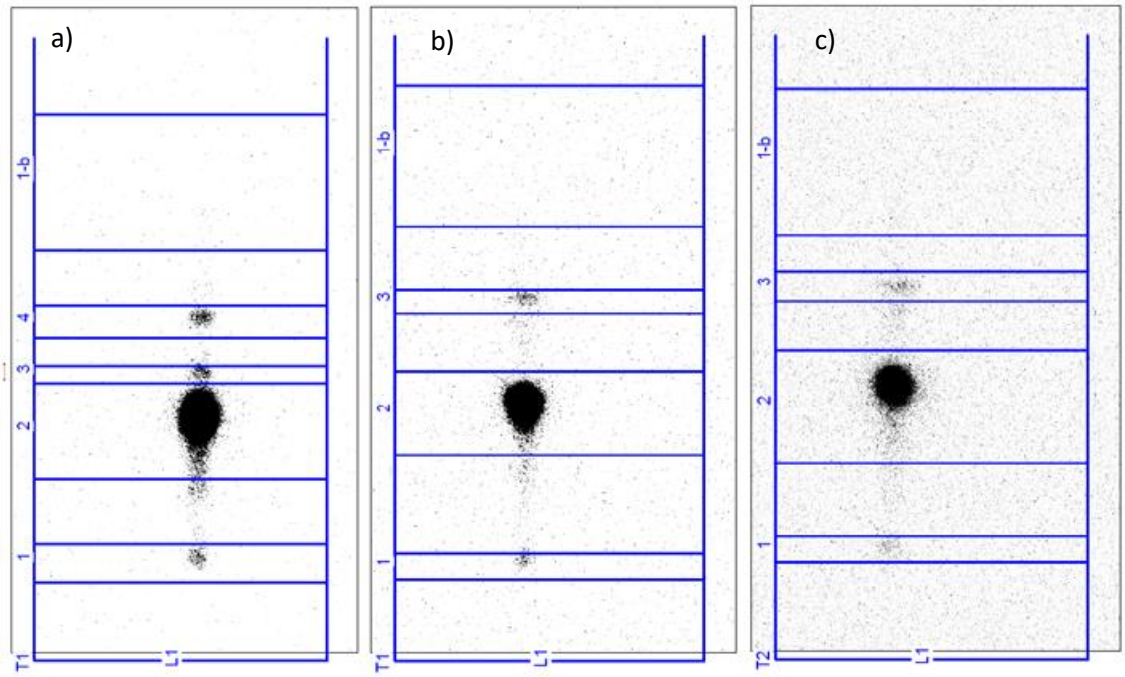

Specie	a)Time t=0	b)Time t=2h	c)Time t=4h
Product **[^{18}F] 4.8** (Rf=0.3) Zone 2	96.6 %	95.6%	93.9%
Fluorine-18 (Rf=0) Zone 1	1.2%	2.1%	2.7%
Unknown radioactive by-product Zone 3-4	2.0%	2.0%	3.5%

Figure 4.5: *Radio-TLC of pure compound [^{18}F]4.8*. Fluorine-18 Rf=0, product **[^{18}F]4.8** Rf= 0.3 (Proof-2). a) cartridge at t=0; b) cartridge at t=2h; c) cartridge at t=4h

Moreover, a study to evaluate the product stability in human plasma was performed. Plasma was obtained by blood centrifugation at 2800 rpm for 15 min. Then, 20µl of the radiopharmaceutical solution were added and the mixture was incubated at 37°C for 2 and 4 hours, respectively. At the end of incubation acetonitrile was added to the mixture, precipitating the plasma proteins. The resulting mixture was monitored in HPLC and Radio-TLC, and no significant differences were found with respect for the stability in solution.

4.2.2.2 Radiosynthesis with fluorine-18 direct introduction (S_N2) on PSMA-617 bromine derivative

After product **[^{18}F] 4.8** was successfully obtained, we attempted to introduce fluorine-18 using aliphatic bromine PSMA-617 derivative in order to compare radiosynthetic conditions, yields, specific activity and the metabolic stability of aromatic sp^2 C-F bond vs aliphatic sp^3 C-F bond.

As shown in Scheme 4.8 the reaction was carried out in same conditions showed above: [^{18}F] TBAF was reacted at high temperature with precursor **4.2** in DMSO.

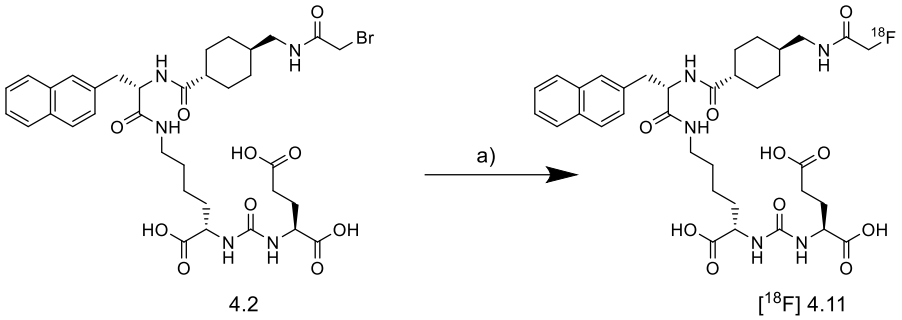

Scheme 4.8: *Radiosynthesis of compound* ***[^{18}F] 4.11***. *Reagent and conditions*: a) [^{18}F] TBAF, DMSO or DMF, 105°C, 10 min.

Unfortunately, using DMSO and small amount of precursor (1.15 µmol) no product was obtained. Other attempts increasing precursor amount (up to 12 µmol) and changing solvent with dimethyl formamide (DMF) didn't bring to satisfactory results.

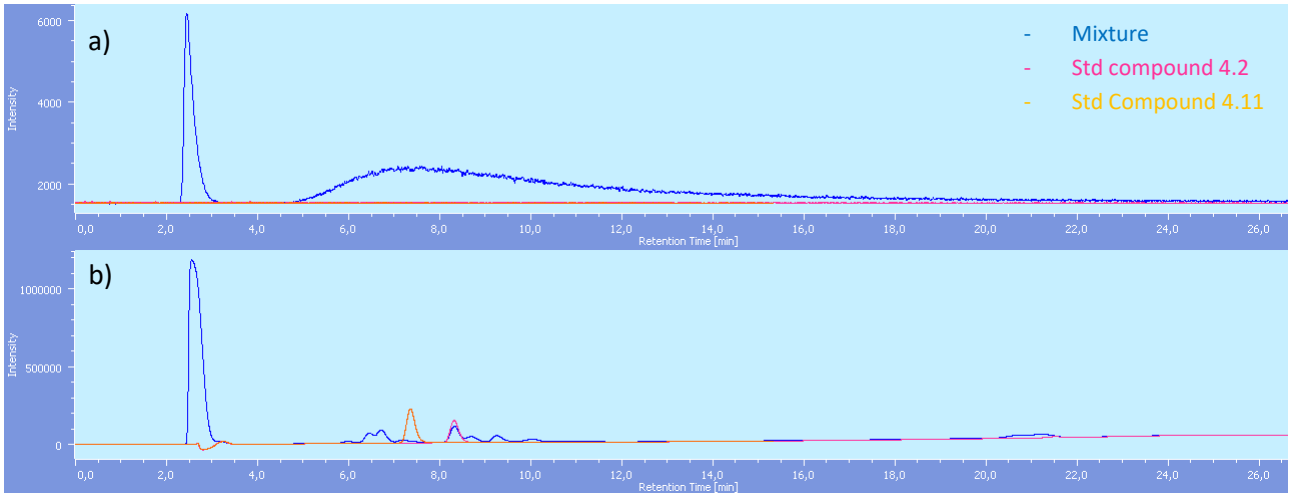

Figure 4.6: *HPLC of crude mixture of* ***[^{18}F] 4.11*** *radiosynthesis*. a) Radiochemical detector, b) UV detector. Method: water +0.1%TFA/acetonitrile +0.1%TFA gradient from 70:30 to 20:80 in 20 min, isocratic 20:80 for 2 min. Rt= 7 min.

As is shown in the Figure 4.6, the final product was not formed, and several impurities were detected.

In literature, the use of the amine 1,8-Diazabicyclo (5.4.0) undec-7-ene (DBU) is very interesting because it can substitute the bromine leaving group giving a higher electrophilic carbon, more suitable for nucleophilic fluorine-18 introduction [73]. Generally, those types of reaction occur on tertiary or secondary amides, better if the carbon is trisubstituted (for example -CF_2Br) but an attempt was performed even in our case.
So, the last attempt was conducted using 1.1 equivalent DBU in a solution of precursor **4.2** in DMF. It was heated at 105°C for 15 min and mixture was monitored by HPLC. Unfortunately, again, no final product **[^{18}F] 4.11** was obtained. Probably the -CH_2Br bond of precursor **4.2** is not so labile leaving group in the conditions used. As future perspective it was planned to synthetize a PSMA-617

derivative, functionalized by difluoro-bromo-acetamide, in order to study fluorine-18 on more reactive substrate, with DBU auxilium.

4.3 CHAPTER CONCLUSION

In summary, novel derivatives of PSMA-617 functionalized with 2-trimethylammonium nicotinic amide (precursor **4.1**) and bromoacetic amide (precursor **4.2**) were synthetized and characterized. Both products were obtained in good yield and purity (>99%). Radiolabeling of **[^{18}F] 4.8** was successful (RCY ~20%, molar activity ~ 1000 GBq/μmol), and final product was obtained with high chemical and radiochemical purity (>99%). Moreover, the compound resulted to be stable in solution and in plasma up to 2 hours and resulted ~94% after 4 hours. The entire procedure was fully automated.
On the contrary, radiosynthesis of **[^{18}F] 4.11** did not yield the desired product, and strategy need to be changed.

CONCLUSIONS

In conclusion, three different methods to introduce fluorine-18 on biologically active molecules were studied and tested. The three approaches consisted on a "click" chemistry reaction (CuAAC), the introduction of $[^{18}F]AlF^{2+}$ specie into suitable NODA and RESCA chelators, and direct fluorine-18 introduction by a S_N2 nucleophilic substitution reaction, respectively.

PSMA-617 ligand derivatives precursors, functionalized by suitable LG or chelators, were synthetized in order to conduct the above radiolabeling procedures. Radiolabeled products were successfully obtained with suitable radiochemical yields and purity, and the radiosynthetic procedures were fully automated.

The "click" method is fully complying with the original aim of the work, as it allowed to link fluorine-18 to a biomolecule following a reaction carried out at room temperature in an aqueous media. The drawback of this method is the need to use copper as a catalyst, whose toxicity in humans requires a careful control of its amount in the final injectable solution. This problem might be overcome with the use of strained alkyne structures, and preliminary tests, not published in the present work have already been successfully performed.

The radiolabeling methods with $[^{18}F]AlF^{2+}$ clearly showed the impact of the chelator choice on the overall outcome. Chelators with a cyclic structure, such as NODA, requires high temperatures to coordinate the aluminum complex, but then they are kinetically stable; on the contrary, "open" chelators such as RESCA are capable to bind the complex at room temperature but they are prone to lose the radionuclide. However, they were both implemented successfully and potentially be used for future purposes also with other molecules than PSMA-617 derivatives.

The last method, with classic S_N2 nucleophilic substitution, proved to be suitable in the introduction of fluorine-18 with a quite stable molecule such as PSMA-617, but still require *harsh* reaction conditions and need to be refined trying to find alternative leaving groups or even different strategies, in case a "heat sensitive" molecule has to be radiolabeled.

So, comparing the approaches shown in chapters above, everyone had particular characteristic and advantages related to fluorine-18 introduction on biologically active molecules in terms of time, temperature, specific activity and radiochemical yields.

Finally, product **[^{18}F] 3.20** and **[^{18}F] 3.21** were also tested in mice and PSMA-617-NODA derivative (**[^{18}F] 3.20**) showed good results in terms of uptake and specificity *in vivo* in mice model of prostatic and glioblastoma tumors, thus prompting for further biological characterization.

EXPERIMENTAL PROCEDURES

Material and Methods

All solvents and reagents were purchased from Sigma-Aldrich, 1 Chem LP, Alfa Aesar, Chematech, Abcr and Carlo Erba.

TLC analyses were performed on silica gel 60 F254 pre-coated plates (Merck) by detection with a 5% phosphomolybdic acid solution in ethanol or 10% ninhydrin in butanol, and heating at 110°C.

Mass spectra were acquired using Impact HD^{TM} UHR-QqToF (Bruker Daltonics, Germany) mass spectrometer and by AmaZon ETD (Bruker Daltonics) ion trap mass spectrometer. Samples were solubilized in methanol and then infused in ESI source at a flow rate of 3 µL/min.

Concerning ion trap instrument, ESI source was used with the following setting: capillary -4500V, end plate offset -500V, nebulizer 20 psi, dry gas 9 l/min at 200°C). Ions from the source were detected in a mass range of 70 to 1000 m/z, with 200000 ICC, and 50 ms as maximum accumulation time. A target mass of 300 m/z and a trap drive of 100% were employed.

For UHR-QqToF spectrometer, parameters for the ESI source were set as follow: capillary 4000 V, end plate offset 500 V, nebulizer 0.3 bar, dry gas 4 l/min at 200 °C. Ions from the source were detected in a mass range from 50 to 3000 m/z. For Mass Spectrometer the following tuning was applied: Funnel 1 radiofrequency (RF) of 400 Vpp, Funnel 2 RF of 400 Vpp, Hexapole RF of 400 Vpp and a prepulse of 12 µs.

Fragmentation spectra were acquired using MRM modality and by optimizing both the isolation window and the fragmentation energy for each analyte.

Data results were processed by DataAnalysis^{TM} 4.0 (Bruker Daltonics) software.

NMR spectra were recorded on a Bruker AVANCE 500 spectrometer equipped with a 5mm broadband reverse probe with field *z*-gradient operating at 500.13 and 125.76 MHz for ^{1}H and ^{13}C, respectively. NMR spectra were recorded at 298 K in $CDCl_3$, CD_3OD or d-6 DMSO (isotopic enrichment 99.95%) solution and the chemical shifts were reported on a δ (ppm) scale. Data were collected and processed by XWIN-NMR software (Bruker) running on a PC with Microsoft Windows 7. The samples were dissolved in the appropriate solvent in a 5 mm NMR tube. Acquisition parameters for 1D were as follows: ^{1}H spectral width of 5000 Hz and 32K data points providing a digital resolution of ca. 0.305 Hz per point, relaxation delay 10 s; ^{13}C spectral width of 29,412 Hz and 64 K data points providing a digital resolution of ca. 0.898 Hz per point, relaxation delay 2 s. Chemical shifts (δ) of the ^{1}H NMR and ^{13}C NMR spectra are reported in ppm using the signal of residual solvent protons resonance as internal standard. ^{1}H NMR: $CDCl_3$ 7.26 ppm, CD_3OD 3.31 ppm and d-6 DMSO 2.50 ppm;^{13}C NMR: $CDCl_3$ 77.16 ppm (central line), CD_3OD 49.00 ppm and d-6 DMSO 39.52 ppm. The splitting pattern abbreviations are as follows: s, singlet; d, doublet; t, triplet; q, quartet; m, multiplet, and br, broad signal. For two-dimensional experiments, Bruker microprograms using gradient selection (gs) were applied. All two-dimensional spectra (COSY, HSQC, HMBC) were acquired with 2048 data points for t_2 and 256 for t_1 increments.

[^{18}F]fluoride was produced by a cyclotron (Cyclone 18/9, IBA) *via* the $^{18}O(p,n)^{18}F$ nuclear reaction, by proton beam irradiation of a target containing 2 mL of >97% enriched [^{18}O]water (Rotem).

Radioactive tests were carried out on a commercially available radiochemistry automated system (Trasis-AllinOne) located in a suitably shielded hot cell (MIP-2, Comecer).

Sep-Pak Light Waters Accel Plus QMA and SepPak tC18 cartridges were from Waters Corp.

Radiolabeled preparations and "cold" references were analyzed by RP-HPLC on a Jasco PU-2089i system equipped with an automated injector, DAD detector, and radiochemical detector Raytest Gabi Star. Semi-preparative purification was carried out on a RP-HPLC equipped with a Perkin Elmer Flexar system quaternary pump and a Knauer WellChrom mod. K-2501 UV detector or on a Knauer P4.1S pump and a TOYDAD400 2Ch UV detector, connected to the automated module for radiosynthesis. Wavelenght was set at 220 nm.
Analytical RP-HPLC column (Xterra C18 250x4.6 mm, 5 μm) was purchased from Waters Corp, while semi-preparative RP-HPLC column (Clarity Oligo-RP C18, 250x10 mm, 5 μm) from Phenomenex.
Radio TLC analyses were performed using a PerkinElmer Cyclone® Plus, equipped with Cyclone® Plus Phosphor Scanner and software OptiQuant™.

CHAPTER II

Chemical Procedures

(S)-2-[(Imidazole-1-carbonyl)amino]pentanedioic acid di-*tert*-butyl ester (2.2)

Under anhydrous conditions, to a suspension of commercial L-di-*tert*-butyl glutamate hydrochloride (1 g, 3.38 mmol) in CH_2Cl_2 (DCM) (9 ml), cooled to 0°C, trimethylamine (TEA) (1.17 ml, 8.45 mmol) and 4-dimethylaminopyridine (DMAP) (15.16 mg, 0.14 mmol) were added. The mixture was stirred for 5 minutes, carbonyldiimidazole (CDI) was added (0.603 g, 3.718 mmol) and the reaction mixture was stirred overnight at room temperature. The reaction progress was monitored by TLC (DCM/MeOH 9:1). The reaction mixture was diluted with DCM (20 ml) and the obtained solution was washed with saturated aqueous sodium bicarbonate (20 ml), water (2 x 20 ml) and brine (20 ml). The organic phase was dried over sodium sulfate, filtered and concentrated at reduced pressure. The product was obtained as a semisolid without purification and used in the next step (1.1 g, 3.11 mmol, 92%).
R_f: 0.63.

^{1}H-NMR, ^{13}C-NMR and MS spectra are in agreement with the reported ones [121].

(S)-2-[3((S)-(5-Benzyloxycarbonylamino)-1-*tert*-butoxycarbonylpentylureido]pentanedioic acid di-*tert*-butyl ester (2.3)

Under anhydrous conditions, to a solution of **2.2** (520 mg, 1.47 mmol) in dichloroethane (DCE) (10 ml) at 0°C, methyl trifluoromethanesulfonate (MeOTf) (0.16 ml, 1.47 mmol) and TEA (0.4 ml, 2.94 mmol) were added. The solution was stirred for 30 min, commercial Cbz-Lys-Ot-Bu (548.4 mg, 1.47 mmol) was added and the solution was heated at 40 °C. The reaction progress was monitored by TLC (DCM/MeOH 9.5:0.5). After 2 h, the reaction mixture was concentrated under reduced pressure and the crude product was purified by silica gel column chromatography (eluents: gradient of DCM/acetone). The desired compound was obtained as a colorless semisolid (733.7 mg, 1.18 mmol, 80%).
R_f: 0.41

^{1}H-NMR, ^{13}C-NMR and MS spectra are in agreement with the reported ones. [121]

(S)-2-[3-(5-Amino-1-*tert*-butoxycarbonylpentyl) ureido]pentanedioic acid di-*tert*-butyl ester (2.4)

To a solution of compound **2.3** (733.7 mg, 1.18 mmol) in EtOH (10 ml) ammonium formate was added (1.12 g, 17.7 mmol) followed by 5% Pd-C (240 mg). The suspension was stirred at room temperature and the reaction progress was monitored by TLC (DCM/MeOH 9:1). After 5 h the reaction was filtered through a Celite pad and solvent was evaporated at reduced pressure. The resulting crude semisolid product was diluted with a sodium hydrogen carbonate saturated aqueous solution (30 ml) and extracted with DCM (3 x 30 ml). The collected organic layers were washed with brine (30 ml) and evaporated to afford the desired product as a yellow semisolid (570 mg, 1.17 mmol, 99 %).

^{1}H-NMR, ^{13}C-NMR and MS spectra are in agreement with the reported ones. [121]

(S)-ethyl-2-amino-3-naphtyl propanoate (2.5)

A solution of commercial (S)- naphtyl alanine (1 g, 4.65 mmol) in EtOH (20 ml) was brought to -5 °C. Thionyl chloride was added (0.54 ml, 7.43 mmol) and the mixture was heated to reflux for 3 h. The reaction progress was monitored by TLC (DCM/MeOH 9.5:0.5). The mixture was evaporated at reduced pressure and the desired product was obtained as a brown liquid (1.1 g, 4.52 mmol, 97%).
R_f: 0.36
^{1}H-NMR (CD_3OD): δ 1.13 (t, 3H), 3.07 (m, 1H), 3.14 (m, 1H), 3.77 (t, 1H), 4.10 (q, 2H), 7.34 (dd, 1H), 7.45 (m, 2H), 7.66 (s, 1H), 7.80 (m, 3H).
^{13}C-NMR (CD_3OD): δ 13.01, 40.65, 55.30, 60.60, 125.28, 125.76, 127.10, 127.19, 127.23, 127.64, 127.78, 132.54, 133.58, 134.52, 174.47.
MS (m/z) (ESI+) 244.1 $[M+H]^+$.

***Trans*-4-[(benzyloxycarbonyl)amino]methyl cyclohexane acid (2.6)**

To a solution of commercial *trans*-4-(aminomethyl)cyclohexane acid (1g, 6.4 mmol) in THF/H_2O (2:1, 30 ml) benzyl chloroformate (Cbz-Cl) (1.31 ml, 1.5 mmol) and 2M NaOH (9 ml) were added. The reaction mixture was stirred overnight at room temperature and the reaction progress was monitored by TLC (DCM/MeOH, 9:1). Then, the mixture was quenched with 1M HCl (30 ml). The aqueous phase was extracted with EtOAc (3 x 30 ml). The collected organic phases were washed with brine (30 ml), dried over sodium sulfate and the solvent was removed at reduced pressure. The crude product was finally purified by silica gel column chromatography (eluents: gradient of DCM/acetone) to afford the pure **2.6** as a white solid (1.79 g, 6.17 mmol, 96%).
R_f: 0.54

^{1}H-NMR, ^{13}C-NMR and MS spectra are in agreement with the reported ones. [130]

(S)-ethyl [2-trans-4- (((benzyloxycarbonyl)amino)methyl)cycloesanecarboxyamido]-3-naphtyl propanoate (2.7)

Under anhydrous conditions, a solution of compound **2.5** (747 mg, 3.07 mmol), compound **2.6** (895 mg, 3.07 mmol) and TEA (1.06 ml, 7.68 mmol) in DMF (10 ml) was cooled to 0°C. (1-

[Bis(dimethylamino)methylene]-1H-1,2,3-triazolo[4,5-b]pyridinium 3-oxide hexafluorophosphate (HATU) (1.29 g, 3.38 mmol) was added dropwise over 5 min and the mixture was stirred at room temperature for 5 h. The reaction progress was monitored by TLC (DCM/MeOH, 9.5:0.5) until the starting material disappeared. The reaction mixture in DMF was dripped in H_2O (100 ml) and extracted with EtOAc (3 x 50 ml). The collected organic phases were washed with brine (50 ml), dried over sodium sulfate and the solvent was removed at reduced pressure. The crude mixture was finally purified by silica gel column chromatography (eluents: gradient of DCM/acetone) to afford the desired product **2.7** as a pale-yellow solid (1.42 g, 2.75 mmol, 90%).
R_f: 0.5
^{1}H-NMR ($CDCl_3$): δ 0.92 (q, 2H), 1.25 (t, 3H), 1.42 (q, 3H), 1.84 (m, 4H), 2.01 (m, 1H), 3.03 (m, 2H), 3.29 (dm, 2H), 4.19 (q, 2H), 4.93 (q, 1H), 5.09 (s, 2H), 5.94 (d, 1H), 7.22 (dd, 1H), 7.33- 7.35 (m, 5H), 7.46 (m, 2H), 7.54 (s, 1H), 7.76 (m, 2H), 7.81 (m, 1H).
^{13}C-NMR ($CDCl_3$): δ 14.16, 28.68, 28.98, 29.61, 29.70, 37.60,37.97, 45.14, 47.01, 52.87, 61.60, 66.69, 125.77, 126.23, 127.43, 127.29, 127.69, 128.14, 128.16, 128.18, 128.54, 132.48, 133.36, 133.51, 136.59, 156.54, 171.75, 175.18.
MS (m/z) (ESI+) 517.1 $[M+H]^+$, 539.1 $[M+Na]^+$.

(S) [2-trans-4- (((benzyloxycarbonyl)amino)methyl)cycloesanecarboxyamido]-3-(naphtyl-2-methyl) propanoic acid (2.8)
A solution of compound **2.7** (674 mg, 1.3 mmol) in THF/H_2O (1:1, 12 ml) was cooled at 0°C. A solution of 1M LiOH·H_2O (4.5 ml, 4.6 mmol) was added dropwise. The mixture was stirred at 0°C for 2 h monitoring the reaction progress by TLC (DCM/MeOH, 9.5:0.5). Then, the solvent was evaporated at reduced pressure. Crude mixture was diluted with water (20 ml) and pH was brought to 1 by dripping 1M HCl. The solution was extracted by EtOAc (3 x 20 ml). Collected organic phases were washed with brine (20 ml) and dried over sodium sulfate. Finally, the solvent was removed affording the desired product as a white solid (605 mg, 1.24 mmol, 95%).
^{1}H-NMR (DMSO-d_6): δ 0.80 (m, 2H), 1.08 (m, 1H), 1.23 (m, 2H), 1.49 (m, 1H), 1.62 (m, 3H), 2.03 (m, 1H), 2.80 (m, 2H), 3.01 (m, 1H), 3.20 (m, 1H), 4.49 (m, 1H), 4.98 (s, 2H), 7.19 (m, 1H), 7.31-7.38 (m, 6H), 7.45 (m, 2H), 7.68 (s, 1H), 7.82 (m, 3H), 8.01 (d, 1H), 12.65 (br, 1H).
^{13}C-NMR (DMSO-d_6): δ 28.91, 29.06, 29.85, 29.92, 37.37, 37.72, 44.09, 46.98, 53.56, 65.57, 125.90, 126.44, 127.53, 127.80, 127.88, 127.93, 128.16, 128.19, 128.79, 128.87, 132.29, 133.39, 135.99, 137.79, 156.72, 173.65, 175.49.
MS (m/z) (ESI+) 511.1 $[M+Na]^+$.

(3S,10S,14S)-tri-*tert*-butyl 1- [trans-4-(((benzyloxycarbonyl)amino)methyl)cycloesanecarboxyamido]-3-(naphtyl-2-methyl)-1,4,12-trioxo-2,5,11,13-tetraazahexadecane-10,14,16-tricarboxylate (2.9)
Under anhydrous conditions, a solution of compound **2.4** (970 mg, 1.99 mmol), compound **2.8** (971 mg, 1.99 mmol) and TEA (0.69 ml, 4.98 mmol) in DMF (10 ml) was cooled to 0°C. HATU (832 mg, 2.19 mmol) was added dropwise over 5 min and the mixture was stirred overnight at room temperature. Reaction was monitored by TLC (DCM/MeOH, 9.5:0.5). After the reaction was complete, the mixture in DMF was dripped into H_2O (100 ml) and the solution was extracted with EtOAc (3 x 50 ml). Collected organic phases were washed with brine (50 ml), dried over sodium sulfate and the solvent was removed at reduced pressure. The crude reaction mixture was purified by

silica gel column chromatography (eluents: gradient of DCM/acetone) to afford the desired product as a pale-yellow solid (1.8 g, 1.88 mmol, 94%).
R_f: 0.31
^{1}H-NMR (DMSO-d_6): δ 0.78 (m, 2H), 1.01 (m, 1H), 1.20 (m, 4H), 1.30 (m, 2H), 1.37 (s, 27H), 1.41-1.57 (m, 4H), 1.63 (m, 3H), 1.85 (m, 1H), 2.04 (t, 1H), 2.21 (m, 2H), 2.79 (t, 2H), 2.93 (m, 2H), 3.06 (m, 2H), 3.91 (m, 1H), 4.02 (m, 1H), 4.51 (m, 1H), 4.97 (s, 2H), 6.22 (d, 1H), 6.27 (d, 1H), 7.18 (t, 1H), 7.31 (m, 5H), 7.37 (m, 1H), 7.43 (m, 2H), 7.66 (s, 1H), 7.77 (m, 2H), 7.83 (d, 1H), 7.89 (m, 2H).
^{13}C-NMR (DMSO-d_6): δ 22.88, 27.30, 28.10, 28.13, 28.20, 28.79, 29.09, 29.21, 29.84, 29.99, 31.36, 32.09, 37.72, 38.64, 38.74, 44.15, 46.99, 52.65, 53.50, 54.16, 65.56, 80.18, 80.70, 81.03, 125.75, 126.33, 127.71, 127.73, 127.87, 127.89, 128.14, 128.17, 128.35, 128.77, 132.23, 133.35, 136.20, 137.78, 156.70, 157.57, 171.44, 171.87, 172.31. 172.71, 175.34.
MS (m/z) (ESI+) 980.6 $[M+Na]^+$, 996.0 $[M+K]^+$.

(3S,10S,14S)-tri-*tert*-butyl 1- [trans-4- (aminomethyl)cycloesanecarboxyamido]-3-(naphtyl-2-methyl)-1,4,12-trioxo-2,5,11,13-tetraazahexadecane-10,14,16-tricarboxylate (2.10)
To a solution of compound **2.9** (500 mg, 0.52 mmol) in MeOH/THF (1:1, 10 ml) ammonium formate (329 mg, 5.21 mmol) was added followed by 5% Pd-C (72.5 mg). The suspension was stirred overnight at room temperature and the reaction progress was monitored by TLC (DCM/MeOH 9:1). Then, the mixture was filtered through Celite pad and the solvent was evaporated at reduced pressure. The resulting crude semisolid was diluted in sodium hydrogen carbonate saturated solution (15 ml) and the obtained solution was extracted with DCM (3 x 20 ml). The collected organic phases were washed with brine (20 ml) and concentrated in order to afford the desired product as yellow oil (390 mg, 0.47 mmol, 91 %).
^{1}H-NMR (DMSO-d_6): δ 0.75 (m, 2H), 1.04 (m, 2H), 1.19 (m, 4 H), 1.28 (m, 1H), 1.36 (s, 27H), 1.43-1.56 (m, 3H), 1.57-1.75 (m, 4H), 1.85 (m, 1H), 2.05 (m, 1H), 2.20 (m, 2H), 2.28 (d, 2H), 2.93 (m, 2H), 3.06 (m, 2H), 3.91 (q, 1H), 4.04 (q, 1H), 4.52 (m, 1H), 6.24 (d, 1H), 6.29 (d, 1H), 7.37 (m, 1H), 7.43 (m, 2H), 7.66 (s, 1H), 7.77 (m, 2H), 7.83 (d, 1H), 7.91 (m, 2H).
^{13}C-NMR (DMSO-d_6): δ 22.88, 28.10, 28.13, 28.19, 28.84, 28.93, 29.09, 29.33, 29.49, 29.89, 30.03, 31.36, 32.09, 38.64, 38.73, 44.32, 48.14, 52.65, 53.50, 54.15, 80.18, 80.69, 81.03, 125.74, 126.33, 127.71, 127.72, 127.86, 127.89, 128.34, 132.23, 133.35, 136.20, 157.56, 171.44, 171.86, 172.31, 172.71, 175.43.
MS (m/z) (ESI+) 824.5 $[M+H]^+$, 846.5 $[M+Na]^+$.

(3S,10S,14S)-tri-*tert*-butyl 1- [trans-4- (hex-5-yn-aminomethyl)cycloesanecarboxyamido]-3-(naphtyl-2-methyl)-1,4,12-trioxo-2,5,11,13-tetraazahexadecane-10,14,16-tricarboxylate (2.11)
Under anhydrous conditions, a solution of compound **2.10** (470 mg, 0.57 mmol), 5-hexynoic acid (0.06 ml, 0.57 mmol) and TEA (0.197 ml, 1.43 mmol) in DMF (10 ml) was cooled to 0°C. HATU (238 mg, 0.63 mmol) was added dropwise over 5 min and the mixture was stirred 3h at room temperature. The reaction progress was monitored by TLC (DCM/MeOH, 9.5:0.5) until starting material disappearance. The mixture was dripped in H_2O (100 ml) and extracted with EtOAc (3 x 30 ml). Collected organic phases were washed with brine (50 ml), dried over sodium sulfate and solvent was removed at reduced pressure. The crude product was finally purified by silica gel column chromatography (eluents: gradient of DCM/acetone) to afford the desired product as a pale-yellow solid (465 mg, 0.51 mmol, 89%).

R_f: 0.48
^{1}H-NMR (DMSO-d_6): δ 0.6 (m, 2H), 1.1 (m, 1H), 1.20 (m, 5H), 1.32 (m, 2H), 1.40 (s, 27H), 1.5 (m, 3H), 1.65 (m, 5H), 1.82 (m, 1H), 2.05 (m, 1H), 2.10 (m, 4H), 2.20 (m, 2H), 2.75 (t, 1H), 2.83 (t, 2H), 2.91 (m, 2H), 3.05 (m, 2H), 3.89 (m, 1H), 4.05 (m, 1H), 4.52 (m, 1H), 6.21 (d, 1H), 6.27 (d, 1H), 7.37 (m, 1H), 7.43 (m, 2H), 7.66 (s, 1H), 7.71 (t, 1H), 7.77 (m, 2H), 7.83 (m, 1H), 7.89 (m, 2H).
^{13}C-NMR (DMSO-d_6): δ 17.88, 22.88, 24.84, 28.11, 28.14, 28.21, 28.83, 29.09, 29.24, 29.99, 30.14, 31.37, 32.11, 34.63, 37.46, 38.63, 38.75, 44.16, 45.09, 52.66, 53.50, 54.13, 71.84, 80.20, 80.72, 81.05, 84.55, 125.75, 126.34, 127.71, 127.74, 127.87, 127.89, 128.34, 132.24, 133.35, 136.19, 157.55, 171.41, 171.76, 171.86, 172.30, 172.70, 175.35.
MS (m/z) (ESI+) 940.9 $[M+Na]^+$.

(3S,10S,14S)-1- [trans-4- (hex-5-yn-aminomethyl)cycloesanecarboxyamido]-3-(naphtyl-2-methyl)-1,4,12-trioxo-2,5,11,13-tetraazahexadecane-10,14,16-tricarboxylic acid (2.1)
Under anhydrous conditions, compound **2.11** (240 mg, 0.261 mmol) was dissolved in DCM (5 ml). Trifluoroacetic acid (TFA) was added dropwise in 2 h (0.32 ml). The solution was stirred for 2 days and the reaction progress was monitored by TLC (DCM/MeOH, 9.5:0.5).

Alternatively, compound **2.11** (500 mg, 0.544 mmol) was dissolved in dioxane (10 ml) and 4M HCl (1.2 ml) was added. The mixture was stirred at 30°C for three days and the reaction progress was monitored by TLC (DCM/MeOH, 9.5:0.5).

Upon reaction completion, the solvent was removed at reduced pressure. The crude mixture was diluted with sodium hydrogen carbonate saturated solution (10 ml) and the solution was extracted with EtOAc (3 x 5 ml). Aqueous phase was acidified to pH 4 with 1M HCl: The precipitate crude white solid (190 mg) was recovered by suction and dried.
Crude mixture was purified by semi-preparative HPLC. Pure precursor **2.1** was obtained as a white solid (First conditions: 67 mg, 0.09 mmol, 34%; second conditions: 89 mg, 0.12 mmol, 22.1%).
Analytical RP-HPLC condition: XTerra C18 5µm, 250x4.6 mm; water +0.1%TFA/acetonitrile +0.1%TFA gradient from 70:30 to 50:50 in 20 min, gradient from 50:50 to 20:80 in 2 min; 1 ml/min, 220 nm, UV detector.
R_t: 11.20 min.
Semi-preparative RP-HPLC condition: column Clarity Oligo RP 5µm, 250x10 mm; isocratic 60:40 water +0.1%TFA/acetonitrile +0.1%TFA; 6 ml/min, 220 nm, UV detector.
R_t: 6 min
^{1}H-NMR (DMSO-d_6): δ 0.77 (m, 2H), 1.01 (m, 1H), 1.21 (m, 4H), 1.30 (m, 2H), 1.45 (m, 2H), 1.51-1.66 (m, 6H), 1.70-1.87 (br, 2H), 2.04 (m, 1H), 2.12 (m, 4H), 2.22 (br, 2H), 2.76 (t, 1H), 2.83 (t, 2H), 2.89-3.11 (m, 4H), 3.99 (m, 1H), 4.05 (m, 1H), 4.50 (m, 1H), 6.29 (br, 2H), 7.37 (m, 1H), 7.43 (m, 2H), 7.66 (s, 1H), 7.77 (m, 1H), 7.77 (m, 2H), 7.83 (m, 1H), 7.93 (m, 2H).
^{13}C-NMR (DMSO-d_6): δ 17.87, 23.03, 24.83, 28.57, 28.80, 29.18, 29.23, 29.98, 30.14, 31.17, 32.18, 34.61, 37.44, 38.61, 38.83, 44.14, 45.09, 52.48, 52.84, 54.15, 71.87, 84.57, 125.76, 126.34, 127.72, 127.73, 127.88, 128.36, 132.22, 133.34, 136.23, 157.72, 171.45, 171.77, 174.36, 174.69, 175.09, 175.36.
MS (m/z) (ESI+) 772.4 $[M+Na]^+$.

(3S,10S,14S)-1- [trans-4-((4-(1-(4-((2-(2-(2-fluoroethoxy)ethoxy)ethoxy)methyl)benzyl)-1H-1,2,3-triazol-4-yl)butanamido)methyl)cyclohexyl]-3-(naphtyl-2-methyl)-1,4,12-trioxo-2,5,11,13-tetraazahexadecane-10,14,16-tricarboxylic acid (2.14)

To a solution of compound **2.13** in acetonitrile (2.5 mg, 0.0084 mmol, 100µl), compound **2.1** in MeOH (7.25 mg, 0.0097 mmol, 200 µl) and sodium L-ascorbate in H_2O (9.03 mg, 0.046 mmol, 100 µl), a solution of copper sulfate pentahydrate in H_2O was added (4.05 mg, 0.016 mmol, 100 µl). Mixture was stirred at room temperature for 20 min and the reaction progress was monitored by analytical RP-HPLC. The reaction was quenched dripping 1M HCl (0.1 ml) and the formed precipitate was dissolved by addition of acetonitrile (400µl). The pure compound **2.14** was obtained as a white solid after final semi-preparative HPLC purification (4.5 mg, 0.004 mmol, 45%).

Analytical RP-HPLC condition: XTerra C18 5µm, 250x4.6 mm; water +0.1%TFA/acetonitrile +0.1%TFA gradient from 70:30 to 20:80 in 25 min; 1 ml/min, 220 nm, UV detector.

R_t: 11 min

Semi-preparative RP-HPLC condition: Clarity Oligo-RP 5µm, 250x10 mm; water +0.1%TFA/acetonitrile +0.1%TFA gradient from 55:45 to 50:50 in 25 min; 6 ml/min, 220 nm, UV detector.

R_t: 12.5 min

^{1}H-NMR (DMSO-d_6): δ 0.80 (m, 2H), 1.03 (m, 1H), 1.13-1.28 (m, 4H), 1.32 (m, 2H), 1.48 (m, 2H), 1.55-1.69 (m, 4H), 1.78 (m, 3H), 1.86 (m, 1H), 2.10 (m, 3H), 2.25 (m, 2H), 2.57 (t, 2H), 2.85 (t, 2H), 2.89-3.15 (m, 4H), 3.55 (m, 8H), 3.61 (t, 1H), 3.67 (t, 1H), 4.02 (m, 1H), 4.09 (m, 1H), 4.46 (t, 1H), 4.48 (s, 2H), 4.50-4.57 (m, 2H), 5.53 (s, 2H), 6.31 (br, 2H), 7.27 (d, 2H), 7.32 (d, 2H), 7.40 (m, 1H), 7.45 (m, 3H), 7.70 (m, 2H), 7.79 (m, 2H), 7.83-7.90 (m, 1H), 12.08-12.98 (br, 3H).

^{13}C-NMR (DMSO-d_6): δ 23.02, 25.16, 25.74, 28.35, 28.81, 29.17, 29.24, 30.01, 30.16, 30.88, 32.17, 35.34, 37.45, 38.62, 38.83, 44.16, 45.10, 52.30, 52.77, 52.92, 54.14, 69.63, 70.06, 70.22, 70.29, 72.07, 82.82, 84.14, 122.42, 125.74, 126.33, 127.71, 127.73, 127.87, 128.24, 128.35, 132.22, 133.34, 135.76, 136.22, 138.89, 147.29, 157.72, 171.43, 172.07, 174.25, 175.01, 175.35.

MS (m/z) (ESI+) 1047.5161 $[M+H]^+$.

Radiochemistry

1-(azidomethyl)-4-4((2-[2-(2-[^{18}F]fluoroethoxy)ethoxy]ethoxy)methyl)benzene ([^{18}F]2.13)

24-82 GBq of [^{18}F]fluoride solution in [^{18}O]H_2O produced by cyclotron were passed through a Sep-Pak light QMA cartridge. A solution of potassium carbonate (2.51 mg, 0.018 mmol) in water (0.5 ml) was then passed through the cartridge eluting the activity in the $K^+[^{18}F]^-$ form directly in the reaction vial. A solution of Kryptofix 2.2.2 (15 mg, 0.04 mmol) in 1 ml acetonitrile was added and the solvent was azeotropically distilled at 85°C at reduced pressure. Then, the reaction vial was cooled down at 60°C and solution of compound **2.12** (10 mg, 0.025 mmol) in anhydrous acetonitrile (1 ml) was added. The reaction mixture was stirred 20 min at 100°C. Then, the reaction vial was cooled down at 50°C. Water (9 ml) was added and the mixture was passed through a tC18 Sep-Pak Plus cartridge previously conditioned with 10 ml ethanol and 10 ml water. The cartridge was washed with 10 ml water/acetonitrile 80:20 and the product **[^{18}F]2.13** was obtained by eluting the cartridge with

acetonitrile (1 ml) into the final container. The average obtained final RCY not corrected for decay was in the range of 25-36%, >99% radiochemical purity. Preparation time was 58 min.
Analytical RP-HPLC condition: XTerra C18 5µm, 250x4.6 mm; water/acetonitrile gradient from 60:40 to 20:80 in 20 min; 1 ml/min, 220 nm, UV detector.
R_t: 10.20 min

(3S,10S,14S)-1- [trans-4-((4-(1-(4-((2-(2-(2-[^{18}F]fluoroethoxy)ethoxy)ethoxy)methyl)benzyl)-1H-1,2,3-triazol-4-yl)butanamido)methyl)cyclohexyl]-3-(naphtyl-2-methyl)-1,4,12-trioxo-2,5,11,13-tetraazahexadecane-10,14,16-tricarboxylic acid ([^{18}F]2.14)

Starting from ~198 GBq of [^{18}F] fluorine produced by cyclotron, **[^{18}F]2.13** was synthetized as previously described and passed through tC18 Sep-Pak Plus cartridge. The product **[^{18}F]2.13** was obtained eluting the cartridge with acetonitrile (1 ml) into the second reactor. Acetonitrile was removed heating up to 85°C for 8 min, then reactor was cooled down to 30°C. A solution of compound **2.1** (7.5 mg, 0.01 mmol in 0.2 ml of 0.5M aqueous NH_3 solution) and freshly-prepared sodium ascorbate (9.11 mg, 0.046 mmol in 0.1 ml of 0.5M aqueous NH_3 solution) was added, followed by copper(II) sulfate pentahydrate in water (3.99 mg, 0.016 mmol, 0.1 ml). The reaction mixture was stirred for 20 min at room temperature. The reaction was quenched with 1M HCl (1 ml) and eluted with of water /acetonitrile +0.1%TFA 70:30 (8 ml). Then, in order to purify product **[^{18}F]2.14**, the mixture was submitted to semi-preparative RP-HPLC. The collected fraction was diluted with water (10 ml) and passed through a tC18 Sep-Pak Plus cartridge previously conditioned with ethanol (10 ml) and water (10 ml). The cartridge was washed with water (10 ml) and the final product was obtained by elution with EtOH (1 ml) and saline physiological solution (20 ml) into the final container.
The final activity was 12.1 GBq (6.1% RCY not decay correct, >99% radiochemical purity). Total synthesis time was 112 min (Molar activity >650 GBq/µmol).
Semi-preparative RP-HPLC condition: column Clarity Oligo-RP 5µm, 250x10 mm; water +0.1%TFA/acetonitrile +0.1%TFA gradient from 70:30 to 60:40 in 20 min, isocratic 60:40 for 5 min, gradient from 60:40 to 20:80 in 2 min; 6 ml/min, 220 nm, UV detector.
R_t: 17 min
Analytical RP-HPLC condition: column XTerra C18 5µm, 250x4.6 mm; water +0.1%TFA/acetonitrile +0.1%TFA gradient from 70:30 to 20:80 in 25 min; 1 ml/min, 220 nm, UV detector.
R_t: 11 min

CHAPTER III

Chemical Procedures

Di-tert-butyl (((S)-1-(tert-butoxy)-6-((S)-2-((1r,4S)-4-((4-hydroxybutanamido) methyl)cyclohexane-1-carboxamido)-3-(naphthalen-2-yl)propanamido)-1-oxohexan-2-yl)carbamoyl)-L-glutamate (3.5)

A solution of commercial compound **2.10** (390 mg, 0.473 mmol) and δ-butyric lactone (0.39 ml, 0.520 mmol) in toluene (5 ml) was heated to reflux (130°C). The reaction was stirred for three days. The reaction progress was monitored by TLC (DCM/MeOH 9:1). The mixture was evaporated at reduced pressure. The crude reaction mixture was purified by silica gel column chromatography (eluents: gradient of DCM/acetone) to afford the desired product as a pale-yellow solid (310 mg, 0.34 mmol, 72%).

R_f: 0.40

^{1}H-NMR (DMSO-d_6): δ 0.69-0.85 (m, 2H), 1.00 (m, 1H), 1.13-1.24 (m, 5H), 1.28 (m, 2H), 1.35 (s, 27H), 1.39-1.52 (m, 3H), 1.52-1.68 (m, 5H), 1.84 (m, 1H), 1.04 (m, 3H), 1.17 (m, 2H), 2.82 (t, 2H), 2.86-2.97 (m, 2H), 2.97-3.12 (m, 2H), 3.33 (m, 2H), 3.89 (q, 1H), 4.01 (q, 1H), 4.42 (t, 1H), 4.49 (m, 1H), 6.21 (d, 1H), 6.26 (d, 1H), 7.33-7.48 (m, 3H), 7.66 (m, 2H), 7.76 (m, 2H), 7.83 (m, 1H), 7.90 (m, 2H).

Ethyl (1R,4R)-4-(aminomethyl)cyclohexane-1-carboxylate (3.7)

A solution of commercial *trans*-4-(aminoethyl) cyclohexane carboxylic acid (500 mg, 3.18 mmol) in EtOH (10 ml) was brought to -5 °C. Thionyl chloride was added (0.30 ml, 4.13 mmol) and the mixture was heated to reflux overnight. The reaction progress was monitored by TLC (DCM/MeOH 9.5:0.5). The mixture was evaporated at reduced pressure and the desired product was obtained as a colorless liquid (583 mg, 3.17 mmol, >99%).

R_f: 0.45

^{1}H-NMR (DMSO-d_6): δ 0.95 (m, 2H), 1.15 (t, 3H), 1.29 (m, 2H), 1.51 (m, 1H), 1.75-1.95 (dd, 4H), 2.21 (t, 1H), 2.61 (d, 2H), 4.02 (q, 2H), 7.79 (br, 3H).

ethyl (1R,4R)-4-((4-bromobutanamido)methyl)cyclohexane-1-carboxylate (3.9)

A solution of compound **3.7** (100 mg, 0.54 mmol) and 4-bromine butyric acid (95 mg, 0.57 mmol) in dry dichloromethane (3 ml) was brought to 0°C. Then, dicyclohexyl carcodiimmide (117 mg, 0.57 mmol) was added and at last DMAP (2.5 mg, 0.02 mmol). Then reaction was stirred at room temperature for three days. The reaction progress was monitored by TLC (DCM/MeOH 9.5:0.5). The mixture was evaporated at reduced pressure. The crude reaction mixture was purified by silica gel column chromatography (eluents: gradient of DCM/acetone) to afford the desired product as a pale-yellow solid (70 mg, 0.21 mmol, 40%).

R_f: 0.50

^{1}H-NMR (DMSO-d_6): δ 0.88 (m, 2H), 1.15 (t, 3H), 1.20-1.29 (m, 3H), 1.68 (d, 2H), 1.84 (d, 2H), 1.97 (m, 2H), 2.16 (m, 1H), 2.35 (t, 2H), 2.88 (t, 2H), 4.01 (q, 2H), 4.58 (t, 2H) 7.85 (m, 1H).

^{13}C-NMR (DMSO-d_6): δ 14.58, 24.32, 28.69, 29.75, 31.43, 37.40, 42.91, 45.02, 60.07, 81.19, 171.47, 175.47.
MS (m/z) (ESI+) 334.1098 $[M+H]^+$, 356.0821 $[M+Na]^+$.

di-tert-butyl 2,2'-(7-(4-((((1r,4r)-4-(ethoxycarbonyl)cyclohexyl)methyl)amino)-4-oxobutyl)-1,4,7-triazonane-1,4-diyl)diacetate (3.11)

Under nitrogen atmosphere, to a solution of compound **3.9** (70 mg, 0.21 mmol) and NO_2AtBu (68 mg, 0.19 mmol) in dry acetonitrile (3 ml) was added DIPEA (0.1 ml, 0.63 mmol). Then reaction was stirred at room temperature overnight. The reaction progress was monitored by TLC (DCM/MeOH +3 drops 30% ammonium hydroxide solution 9.5:0.5). The mixture was evaporated at reduced pressure obtaining a crude pale-yellow solid (114 mg, 0.18 mmol, 99%).
R_f: 0.49
^{1}H-NMR (DMSO-d_6): δ 0.88 (m, 2H), 1.13 (t, 3H), 1.18-1.34 (m, 3H), 1.38 (s, 18H), 1.69 (d, 2h), 1.86 (m, 4H), 2.09-2.22 (m, 3H), 2.61 (br, 2H), 2.71-2.83 (m, 4H), 2.88 (m, 1H), 3.02 (br, 2H), 3.16 (br, 5H), 3.44 (m, 4H), 4.00 (q, 2H).

(1r,4r)-4-((4-(4,7-bis(2-(tert-butoxy)-2-oxoethyl)-1,4,7-triazonan-1-yl)butanamido)methyl) cyclohexane-1-carboxylic acid (3.12)

A solution of compound **3.11** (83 mg, 0.14 mmol) in THF/H_2O (1:1, 2 ml) was cooled at 0°C. A solution of 1M LiOH·H_2O (0.48 ml, 0.48 mmol) was added dropwise. The mixture was stirred at 0°C for 3 h monitoring the reaction progress by TLC (DCM/MeOH +3 drops 30% ammonium hydroxide solution 9.5:0.5). Then, the solvent was evaporated at reduced pressure. Crude mixture was diluted with water (10 ml) and pH was brought to 1 by dripping 1M HCl. The solution was extracted by EtOAc (3 x 10 ml). Collected organic phases were washed with brine (10 ml) and dried over sodium sulfate. Finally, the solvent was removed affording the desired product as a white semi-solid (78 mg, 0.13 mmol, 99%).
^{1}H-NMR (CD_3OD): δ 0.94 (m, 2H), 1.37-1.48 (m, 3H), 1.78 (d, 2H), 1.87 (m, 2H), 1.93 (d, 2H), 2.04 (m, 1H), 2.20 (t, 2H), 2.46-2.64 (m, 10H), 2.77 (m, 4H), 3.16 (m, 2H), 3.27 (m, 2H).

di-tert-butyl 2,2'-(7-(4-ethoxy-4-oxobutyl)-1,4,7-triazonane-1,4-diyl)diacetate (3.15)

Under anhydrous conditions, a suspension of commercial NO_2AtBu (52 mg, 0.16 mmol) and potassium carbonate (40 mg; 0.29 mmol) in dry acetonitrile (1 ml) was stirred at room temperature. Then a solution of ethyl 4-bromo butanoate (31 mg; 0.16 mmol) in dry acetonitrile (2 ml) was added and the mixture was stirred overnight at room temperature. The reaction progress was monitored by TLC (DCM/MeOH + 3 drops 30% ammonium hydroxide solution 9:1). The reaction was filtered through a folded paper filter and acetonitrile was evaporated to afford the desired product as a yellow semisolid (50 mg, 0.11 mmol, 76%).
R_f: 0.25
^{1}H-NMR ($CDCl_3$): δ 1.22 (t, 3H), 1.87 (br, 2H), 2.34 (t, 2H), 2.64-3.20 (m, 14H), 3.32 (s, 4H), 4.09 (q, 2H).
^{13}C-NMR ($CDCl_3$): δ 14.09, 21.77, 31.90, 54.16, 55.04, 56.66, 59.40, 60.44, 81.00, 171.23, 173.20.

di-tert-butyl 2,2'-(7-(4-(benzyloxy)-4-oxobutyl)-1,4,7-triazonane-1,4-diyl)diacetate (3.17)

Under anhydrous conditions, a suspension of commercial NO_2AtBu (50 mg, 0.14 mmol) and potassium carbonate (57.9 mg; 0.419 mmol) in dry acetonitrile (1 ml) was stirred at room temperature. Then a solution of benzyl 4-bromo butanoate (53.9 mg; 0.21 mmol) in dry acetonitrile (2 ml) was added and the mixture was stirred overnight at room temperature. The reaction progress was monitored by TLC (DCM/MeOH + 3 drops 30% ammonium hydroxide solution 9:1). The reaction was filtered through a folded paper filter and acetonitrile was evaporated to afford the desired product as a yellow semisolid (94 mg, 0.18 mmol, 79%).
R_f: 0.25
^{1}H-NMR ($CDCl_3$): δ 1.42 (s, 18H), 1.91 (br, 2H), 2.42 (t, 2H), 2.79 (s, 6H), 2.87-3.10 (br, 7H), 3.20-3.36 (m, 5H), 5.08 (d, 2H), 7.27-7.36 (m, 5H).
^{13}C- NMR ($CDCl_3$): δ 21.73, 28.19, 31.58, 54.37, 56.73, 58.97, 66.31, 81.08, 128.19, 128.24, 128.26, 128.57, 135.88, 171.14, 172.87.
MS (m/z) (ESI+) 534.3530 $[M+H]^+$.

4-(4,7-bis(2-(tert-butoxy)-2-oxoethyl)-1,4,7-triazonan-1-yl)butanoic acid (3.16)
A suspension of Compound **3.17** (92 mg, 0.17 mmol), 10% Pd-C (49 mg) in ethanol (3 ml) was stirred overnight at room temperature under hydrogen flow. The reaction progress was monitored by TLC (DCM/MeOH + 3 drops 30% ammonium hydroxide solution 8:2). After completion, the reaction was filtered through a Celite pad and solvent was evaporated at reduced pressure. The desired crude product was obtained as a yellow semisolid (71.8 mg, 0.16 mmol, 94%).
^{1}H-NMR ($CDCl_3$): δ 1.42 (s, 18H), 2.06 (br, 2H), 2.48 (m, 2H), 2.58-2.90 (m, 3H), 2.91-3.29 (m, 5H), 3.29-3.62 (m, 8H).
^{13}C- NMR ($CDCl_3$): δ 21.17, 28.23, 31.59, 48.28, 51.68, 52.27, 55.06, 57.13, 170.81.
MS (m/z) (ESI+) 444.3070 $[M+H]^+$.

di-tert-butyl (((S)-6-((S)-2-((1R,4S)-4-((4-(4,7-bis(2-(tert-butoxy)-2-oxoethyl)-1,4,7-triazonan-1-yl)butanamido)methyl)cyclohexane-1-carboxamido)-3-(naphthalen-2-yl)propanamido)-1-(tert-butoxy)-1-oxohexan-2-yl)carbamoyl)-L-glutamate (3.14)
Under anhydrous conditions, a solution of compound **3.16** (36 mg, 0.08 mmol), "PSMA-617" core **2.10** (67 mg, 0.08 mmol) and HATU (34 mg, 0.09 mmol) in DMF (3 ml) was cooled to 0°C. TEA (0.03 ml, 0.20 mmol) was added dropwise over 5 min and the mixture was stirred 3h at room temperature. Reaction was monitored by TLC (DCM/MeOH + 3 drops 30% ammonium hydroxide solution, 8.5:1.5). After the reaction was complete, the mixture in DMF was dripped into H_2O (30 ml) and the solution was extracted with EtOAc (3 x 30 ml). Collected organic phases were washed with brine (90 ml), dried over sodium sulfate and the solvent was removed at reduced pressure. The crude product **3.14** was obtained as brown semisolid (100.5 mg, 0.08 mmol, >99%).
R_f: 0.5
^{1}H-NMR (CD_3OD): δ 0.83-1.02 (m, 3H), 1.20-1.37 (m, 8H), 1.44 (s, 45H), 1.52-1.65 (m, 3H), 1.65-1.84 (m, 4H), 2.03 (m, 3H), 2.15 (m, 1H), 2.31 (m, 4H), 2.71 (m, 1H), 2.90 (m, 9H), 3.02-3.13 (m, 3H), 3.22 (m, 5H), 3.30 (m, 4H), 3.46 (m, 2H), 4.05 (q, 1H), 4.19 (q, 1H), 4.65 (m, 1H), 7.35-7.47 (m, 3H), 7.67 (s, 1H), 7.74-7.83 (m, 3H).
^{13}C-NMR (CD_3OD): δ 20.25, 22.22, 26.91, 26.95, 26.98, 27.05, 27.71, 28.24, 28.38, 28.88, 29.54, 29.65, 31.12, 31.45, 31.77, 37.16, 38.02, 38.48, 44.50, 45.17, 46.55, 50.02, 50.81, 51.44, 52.79, 53.37,

54.52, 55.76, 80.37, 81.11, 81.30, 81.50, 125.25, 125.71, 127.12, 127.17, 127.26, 127.59, 127.64, 132.51, 133.52, 134.57, 158.52, 171.28, 172.21, 172.34, 172.54, 172.65, 177.09, 177.30.
MS (m/z) (ESI+) 1049.8066 $[M+H]^+$.

(((S)-5-((S)-2-((1R,4S)-4-((4-(4,7-bis(carboxymethyl)-1,4,7-triazonan-1-yl)butanamido)methyl)cyclohexane-1-carboxamido)-3-(naphthalen-2-yl)propanamido)-1-carboxypentyl)carbamoyl)-L-glutamic acid (3.1)

Compound **3.14** (200 mg, 0.16 mmol) was dissolved in dioxane (5 ml). HCl 4M (1.4 ml) was added dropwise in 2 h. The solution was stirred for 2h and the reaction progress was monitored by analytical RP-HPLC. Upon reaction completion, the solvent was removed at reduced pressure.
Crude mixture was purified by semi-preparative HPLC. Pure precursor **3.1** was obtained as a white solid (50 mg, 0.05 mmol, 45%).
Analytical RP-HPLC condition: column XTerra C18 5µm, 250x4.6 mm; water +0.1%TFA/acetonitrile +0.1%TFA isocratic at 80:20 for 1 min, gradient from 80:20 to 60:40 in 30 min, gradient from 60:40 to 20:80 in 2 min; 1 ml/min, 220 nm, UV detector.
R_t: 19 min
Semi-preparative RP-HPLC condition: column Clarity Oligo-RP 5µm, 250x10 mm; water +0.1%TFA/acetonitrile +0.1%TFA gradient from 80:20 to 60:40 in 30 min; 5 ml/min, 220 nm, UV detector.
R_t: 18 min
^{1}H-NMR (CD_3OD): δ 0.92 (m, 2H), 1.18-1.30 (m, 5H), 1.31-1.44 (m, 4H), 1.51 (m, 1H), 1.59 (m, 1H), 1.64-1.73 (m, 2H), 1.78 (m, 2H), 1.88 (m, 1H), 2.04 (m, 2H), 2.13 (m, 2H), 2.32 (t, 2H), 2.40 (m, 2H), 2.78 (m, 2H), 2.85 (m, 2H), 2.92-3.02 (m, 4H), 3.02-3.18 (m, 6H), 3.18-3.28 (m, 6H), 3.56 (d, 4H), 4.16 (m, 1H), 4.30 (m, 1H), 4.64 (t, 1H), 7.35-7.47 (m, 3H), 7.67 (s, 1H), 7.74-7.83 (m, 3H).
^{13}C-NMR (CD_3OD): δ 20.06, 22.20, 27.54, 28.19, 28.38, 28.82, 29.53, 29.63, 29.73, 31.43, 31.79, 37.18, 37.94, 38.43, 44.48, 45.16, 46.76, 50.23, 51.47, 52.12, 52.51, 54.53, 54.69, 54.85, 125.25, 125.71, 127.09, 127.15, 127.25, 127.57, 127.63, 132.51, 133.51, 134.53, 158.73, 172.23, 172.73, 173.48, 174.56, 175.01, 172.42.
MS (m/z) (TOF MS ESI-) 967.4794 $[M-H]^-$.

((1S,4r)-4-(((S)-1-(((S)-5-carboxy-5-(3-((S)-1,3-dicarboxypropyl)ureido)pentyl)amino)-3-(naphthalen-2-yl)-1-oxopropan-2-yl)carbamoyl)cyclohexyl)methanaminium (3.18)

Under anhydrous conditions, PSMA-617 "core" **2.10** (172.5 mg, 0.21 mmol) was dissolved in dichloromethane (4 ml). TFA was added dropwise (1 ml) and stirred at room temperature overnight. Reaction progress was monitored by analytical RP-HPLC. Upon reaction completion, the solvent was removed at reduced pressure.
Crude mixture was purified by semi-preparative HPLC. Pure precursor **3.18** was obtained as a white solid (81 mg, 0.12 mmol, 59%).
Analytical RP-HPLC condition: column XTerra C18 5µm, 250x4.6 mm; water +0.1%TFA/acetonitrile +0.1%TFA isocratic at 80:20 for 1 min, gradient from 80:20 to 60:40 in 30 min; 1 ml/min, 220 nm, UV detector.
R_t: 14.3 min

Semi-preparative RP-HPLC condition: column Clarity Oligo-RP 5µm, 250x10 mm; water +0.1%TFA/acetonitrile +0.1%TFA gradient from 80:20 to 60:40 in 30 min; 5 ml/min, 220 nm, UV detector.
R_t: 12.5 min
^{1}H-NMR (DMSO-d_6): δ 0.80 (m, 2H), 1.02 (m, 1H), 1.20 (m, 3H), 1.28 (m, 2H), 1.34-1.52 (m, 3H), 1.57 (m, 1H), 1.67 (m, 4H), 1.89 (m, 1H), 2.06 (m, 1H), 2.21 (m, 2H), 2.59 (t, 2H), 2.89-3.13 (m, 4H), 4.00 (m, 1H), 4.07 (m, 1H), 4.52 (m, 1H), 6.28 (dd, 2H), 7.33-7-48 (m, 3H), 7.61 (br, 3H), 7.66 (s, 1H), 7.70-7.86 (m, 3H), 7.95 (m, 2H), 12.00-12.71 (br, 3H).
^{13}C-NMR (DMSO-d_6): δ 23.04, 28.02, 28.41, 28.81, 29.18, 29.37, 30.37, 32.19, 35.49, 38.69, 38.83, 43.63, 44.81, 52.14, 52.74, 54.08, 122.71, 126.00, 126.37, 127.71, 127.75, 127.92, 128.38, 132.24, 133.35, 136.22, 157.75, 171.44, 174.18, 174.62, 175.01, 175.11.
MS (m/z) (ESI+) 656.3288 $[M+H]^+$.

(((S)-5-((S)-2-((1R,4S)-4-((2-(4-((((1R,2R)-2-(bis(carboxymethyl)amino)cyclohexyl)(carboxymethyl)amino)methyl)phenyl)acetamido)methyl)cyclohexane-1-carboxamido)-3-(naphthalen-2-yl)propanamido)-1-carboxypentyl)carbamoyl)-L-glutamic acid (3.2)

In a 0.05M sodium bicarbonate buffer solution, pH~8.6 (2 ml), a solution of compound **3.18** (24.5 mg, 0.04 mmol) in DMSO (0.3 ml) was added. After pH correction to ~8.6 adding dropwise a 2M sodium carbonate buffer solution, a solution of commercial (±)-H_3RESCA-TFP (23.1 mg, 0.04 mmol) in DMSO (0.2 ml) was added. pH was corrected to ~8.6 and solution was stirred at room temperature for 3h.
Crude solution mixture was purified by semi-preparative HPLC. Pure precursor **3.2** was obtained as a white solid (18 mg, 0.02 mmol, 42 %).
Analytical RP-HPLC condition: column XTerra C18 5µm, 250x4.6 mm; water +0.1%TFA/acetonitrile +0.1%TFA isocratic at 80:20 for 1 min, gradient from 80:20 to 50:50 in 40 min, gradient from 50:50 to 20:80 in 2 min; 1 ml/min, 220 nm, UV detector.
R_t: 23.5 min
Semi-preparative RP-HPLC condition: column Clarity Oligo-RP 5µm, 250x10 mm; water +0.1%TFA/acetonitrile +0.1%TFA gradient from 80:20 to 50:50 in 40 min; 5 ml/min, 220 nm, UV detector.
R_t: 25 min
^{1}H-NMR (CD_3OD): δ 1.15-1.45 (m, 11H), 1.45-1.62 (m, 3H), 1.62-1.83 (m, 5H), 1.82-1.92 (m, 2H), 2.05-2.20 (m, 3H), 2.30 (d, 1H), 2.40 (m, 2H), 2.84-3.02 (m, 4H), 3.02-3.14 (m, 4H), 3.22 (m, 2H), 3.38 (m, 1H), 3.52 (m, 3H), 3.84 (d, 1H), 4.17 (m, 1H), 4.20-4.35 (m, 3H), 4.55 (d, 1H), 4.65 (t, 1H), 7.31-7.39 (m, 3H), 7.42 (m, 2H), 7.61 (m, 2H), 7.67 (s, 1H), 7.73-7.82 (m, 3H).
^{13}C-NMR (CD_3OD): δ 22.20, 23.87, 24.04, 25.06, 27.54, 28.19, 28.35, 28.84, 29.45, 29.59, 29.74, 31.44, 37.18, 37.96, 38.46, 42.08, 44.49, 45.25, 49.36, 52.14, 52.51, 53.83, 54.54, 57.32, 60.00, 63.85, 117.79, 125.26, 125.72, 127.10, 127.15, 127.25, 127.59, 127.64, 129.72, 131.29, 132.51, 133.51, 134.53, 138.09, 158.73, 161.11, 161.38, 168.06, 172.13, 172.24, 174.58, 175.03, 177.43.
MS (m/z) (TOF MS ESI-) 1079.4899 $[M-H]^-$.

Radiochemistry

(((S)-5-((S)-2-((1R,4S)-4-((4-(4,7-bis(carboxymethyl)-1,4,7-triazonan-1-yl)butanamido)methyl)cyclohexane-1-carboxamido)-3-(naphthalen-2-yl)propanamido)-1-carboxypentyl)carbamoyl)-L-glutamic acid [^{18}F] aluminium fluoride ([^{18}F] 3.20)

An activity in the range of 40-50 GBq of aqueous [^{18}F]fluoride was passed through a Sep-Pak light QMA cartridge pre-conditioned with NaCl solution (10 ml). The cartridge was washed with 10 ml of ultrapure water. Then, 300 µl of sodium acetate buffer 0.1M pH=4 solution were passed through the cartridge eluting the activity in the $Na^+[^{18}F]^-$ form directly in the reaction vial, where 50 µl of $AlCl_3$ 2mM solution were previously loaded (0.1 µmol, 24 µg). The reaction mixture was bubbled by nitrogen for 5 min at room temperature. Then, a 2mM solution of Precursor **3.1** (0.2 µmol, 0.2 mg) in 100 µl of sodium acetate buffer 0.1M pH=4 and 350 µl ethanol was added and reaction mixture was heated at 110°C for 15 min. Then, in order to purify product **[^{18}F] 3.20**, the mixture was diluted with 8 ml of 80:20 water+0.1% TFA/ acetonitrile+0.1% TFA and submitted to semi-preparative RP-HPLC. The fraction containing the desired product was collected, diluted with water (10 ml) and passed through a C_{18} Sep-Pak Plus cartridge previously conditioned with ethanol (10 ml) and water (10 ml). The cartridge was washed with water (10 ml) and the final product was obtained by elution with EtOH (1 ml) and saline physiological solution (19 ml) into the final container. The average obtained final RCY not corrected for decay was in the range of ~23%, >99% radiochemical purity (Molar activity >170 GBq/µmol). Preparation time was 59 min.

Semi-preparative RP-HPLC condition: column Clarity Oligo-RP 5µm, 250x10 mm; water +0.1%TFA/acetonitrile +0.1%TFA gradient from 80:20 to 60:40 in 30 min; 5 ml/min, 220 nm, UV detector.

R_t: 20 min

Analytical RP-HPLC condition: column XTerra C18 5µm, 250x4.6 mm; water +0.1%TFA/acetonitrile +0.1%TFA isocratic at 80:20 for 1 min, gradient from 80:20 to 60:40 in 30 min, gradient from 60:40 to 20:80 in 2 min; 1 ml/min, 220 nm, UV detector.

R_t: 14.9 min

(((S)-5-((S)-2-((1R,4S)-4-((2-(4-((((1R,2R)-2-(bis(carboxymethyl)amino)cyclohexyl)(carboxymethyl)amino)methyl)phenyl)acetamido)methyl)cyclohexane-1-carboxamido)-3-(naphthalen-2-yl)propanamido)-1-carboxypentyl)carbamoyl)-L-glutamic acid [^{18}F] aluminium fluoride ([^{18}F] 3.21)

An activity in the range of 40-50 GBq of aqueous [^{18}F]fluoride solution was passed through a Sep-Pak light QMA cartridge pre-conditioned with NaCl solution (10 ml). The cartridge was washed with 10 ml of ultrapure water. Then, 300 µl of sodium acetate buffer 0.1M pH=4 solution were passed through the cartridge eluting the activity in the $Na^+[^{18}F]^-$ form directly in the reaction vial, where 50 µl of $AlCl_3$ 2mM solution were previously loaded (0.1 µmol, 24 µg). The reaction mixture was bubbled by nitrogen for 5 min at room temperature. Then, a 2mM solution of Precursor **3.2 (**0.2 µmol, 0.21 mg) in 100 µl of sodium acetate buffer 0.1M pH=4 and 350 µl ethanol was added and reaction mixture bubbled with nitrogen for 15 min at room temperature. Then, in order to purify product **[^{18}F] 3.21**, the mixture was diluted with 15 ml of water and passed through C_{18} Sep-Pak Plus cartridge previously conditioned with ethanol (10 ml) and water (10 ml). The cartridge was washed with water (30 ml) and the final product was obtained by elution with EtOH (1 ml) and saline physiological solution (19 ml) into the final container. The average obtained final RCY not corrected for decay was

in the range of 40%, >95% radiochemical purity (Molar activity >90 GBq/μmol). Preparation time was 42 min.
Analytical RP-HPLC condition: column XTerra C18 5μm, 250x4.6 mm; water +0.1%TFA/acetonitrile +0.1%TFA isocratic at 80:20 for 1 min, gradient from 80:20 to 60:40 in 30 min, gradient from 60:40 to 20:80 in 2 min; 1 ml/min, 220 nm, UV detector.
R_t: 18.6 min

CHAPTER IV

Chemical Procedures

2,3,5,6-tetrafluorophenyl 6-chloronicotinate (4.3)

A solution of commercial tetrafluorophenol (742 mg, 4.47 mmol), 6-chloronicotinic acid (704 mg, 4.47 mmol) and DCC (1.014 gr, 4.918 mg) in 1,4 dioxane (20 ml) was stirred at room temperature overnight. The reaction progress was monitored by TLC (DCM/acetone 9.5:0.5). After completion, the mixture filtered and solvent was evaporated at reduced pressure. The crude reaction mixture was purified by silica gel column chromatography (eluents: gradient of DCM/acetone) to afford the desired product as a white solid (1.01 gr, 3.31 mmol, 74%).
R_f: 0.95
^{1}H-NMR, ^{13}C-NMR and MS spectra are in agreement with the reported ones [127].

N,N,N-Trimethyl-5-((2,3,5,6-tetrafluorophenoxy)- carbonyl)pyridin-2-aminium Trifluoromethanesulfonate (4.4)

To solution of compound **4.3** (170 mg, 0.56 mmol) in THF dry (4 ml), a solution of 2M trimethyl amine in THF (2.11 ml, 4.2 mmol) was added and the mixture was stirred vigorously at room temperature overnight. After completion, the mixture was filtered. The filtered white solid was washed twice with diethyl ether (20 ml) and once with DCM (20 ml). The obtained crude product N,N,N-Trimethyl-5-((2,3,5,6-tetrafluorophenoxy)- carbonyl)pyridin-2-aminium chloride was afforded as a white solid (174 mg).
Then, crude product chloride salt was suspended in dry dichloromethane (8 ml) and TMFOTf was added dropwise (0.246 mg, 1.36 mmol). The reaction was stirred for 2h at room temperature. At completion, the solvent was evaporated at reduced pressure and the crude product was triturated with diethyl ether (20 ml) for three time. Product 4.4 was obtained as white solid (198 mg, 0.414 mmol, 74%)
^{1}H-NMR, ^{13}C-NMR and MS spectra are in agreement with the reported ones [128].

5-((((1S,4r)-4-(((7S,11S,18S)-7,11-bis(tert-butoxycarbonyl)-2,2-dimethyl-19-(naphthalen-2-yl)-4,9,17-trioxo-3-oxa-8,10,16-triazanonadecan-18-yl)carbamoyl)cyclohexyl)methyl)carbamoyl)-N,N,N-trimethylpyridin-2-aminium triflate (4.5)

Under nitrogen atmosphere, to a solution of compound **2.10** (100 mg, 0.12 mmol) and compound **4.4** (58 mg, 0.12 mmol) in DMF (3 ml), triethyl amine was added (0.07 ml, 0.49 mmol) and reaction was stirred overnight at room temperature. The reaction completion was monitored by compound **2.10**

disappearance in TLC (DCM:MeOH 9:1 + 3 drops 30% ammonium hydroxide solution). After the reaction was complete, the mixture in DMF was dripped into H_2O (30 ml) and the solution was extracted with EtOAc (3 x 30 ml). Collected organic phases were washed with brine (30 ml), dried over sodium sulfate and the solvent was removed at reduced pressure. The crude reaction mixture was obtained with a satisfactory purity grade as a white solid (113 mg, 0.1 mmol, 82.2%).
^{1}H-NMR (DMSO-d_6): δ 0.87 (m, 2H), 1.03 (m, 1H), 1.20 (m, 4H), 1.30 (m, 2H), 1.36 (s, 27H), 1.40-1.54 (m, 2H), 1.59-1.75 (m, 5H), 1.84 (m, 1H), 2.08 (m, 1H), 2.20 (m, 2H), 2.89-2.98 (m, 2H), 2.99-3.13 (m, 4H), 3.58 (s, 9H), 3.90 (q, 1H), 4.01 (m, 1H), 4.50 (m, 1H), 6.24 (d, 1H), 6.28 (d, 1H), 7.34-7.47 (m, 3H), 7.66 (s, 1H), 7.73-7.78 (m, 2H), 7.82 (m, 1H), 7.89-7.97 (br, 3H), 8.17 (d, 1H), 8.54 (dd, 1H), 8.85 (br, 1H), 8.98 (m, 1H).
MS (m/z) (ESI+) 1158.5431 $[M+Na]^+$.

5-((((1S,4r)-4-(((S)-1-(((S)-5-carboxy-5-(3-((S)-1,3-dicarboxypropyl)ureido)pentyl)amino)-3-(naphthalen-2-yl)-1-oxopropan-2-yl)carbamoyl)cyclohexyl)methyl)carbamoyl)-N,N,N-trimethylpyridin-2-aminium trifluoroacetate(4.1)

To solution of compound **4.4** (56 mg, 0.05 mmol) in dry dichloromethane (2 ml) was added TFA (1 ml) and was stirred at room temperature for 2h. Then, solvent was evaporated at reduced pressure and crude product was purified by semi-preparative RP-HPLC. Crude mixture was purified by semi-preparative HPLC. Pure precursor **4.1** was obtained as a white solid (15 mg, 0.02 mmol, 48%).
Analytical RP-HPLC condition: XTerra C18 5µm, 250x4.6 mm; water +0.1%TFA/acetonitrile +0.1%TFA isocratic 75:25 for 15 min, gradient from 75:25 to 20:80 in 2 min; 1 ml/min, 220 nm, UV detector.
R_t: 14.3 min.
Semi-preparative RP-HPLC condition: column Clarity Oligo RP 5µm, 250x10 mm; isocratic 75:25 water +0.1%TFA/acetonitrile +0.1%TFA for 15 min; 6 ml/min, 220 nm, UV detector.
R_t: 10 min
^{1}H-NMR (DMSO-d_6): δ 0.87 (m, 2H), 1.06 (m, 1H), 1.22 (m, 3H), 1.32 (m, 2H), 1.37-1.54 (m, 3H), 1.58 (m, 1H), 1.63-1.78 (m, 4H), 1.91 (m, 1H), 2.08 (m, 1H), 2.24 (m, 2H), 2.88-2.99 (m, 2H), 3.01-3.09 (m, 2H), 3.09-3.13 (m, 2H), 3.60 (s, 9H), 4.01 (q, 1H), 4.09 (q, 1H), 4.52 (q, 1H), 6.29 (d, 1H), 6.33 (d, 1H), 7.39-7.50 (m, 3H), 7.66 (s, 1H), 7.74-7.86 (m, 3H), 7.90-7.99 (br, 2H), 8.19 (d, 1H), 8.56 (dd, 1H), 8.84 (br, 1H), 8.92 (m, 1H), 12.43 (br, 3H).
^{13}C-NMR (DMSO-d_6): δ 23.02, 28.02, 28.83, 29.17, 29.20, 30.06, 30.20, 30.37, 32.12, 37.40, 38.64, 38.83, 44.09, 45.95, 52.14, 52.74, 54.14, 55.10, 115.52, 125.76, 126.34, 127.72, 127.86, 127.89, 128.36, 132.22, 132.59, 133.34, 136.22, 140.23, 147.93, 157.74, 158.43, 163.51, 171.44, 174.15, 174.59, 174.97, 175.31.
MS (m/z) (ESI+) 818.4094 $[M+H]^+$.

2,3,5,6-tetrafluorophenyl 6-fluoronicotinate (4.6)

Under nitrogen atmosphere, to a solution of 1M of TBAF in dry THF (0.7 ml, 0.67 mmol) was added a solution of compound **4.4** (213 mg, 0.45 mmol) in ACN dry (6 ml). The mixture was stirred at room temperature for 1 hour. Reaction progress was monitored by TLC (DCM:acetone 9.8:0.2). Then, after reaction completion, the mixture was filtered and solvent was evaporated under reduced pressure. The crude reaction mixture was purified by silica gel column chromatography (eluents: gradient of DCM/acetone) to afford the desired product **4.6** as a brown semi-solid (13 mg, 0.05 mmol, 10%).

R_f: 0.90
^{1}H-NMR, ^{13}C-NMR and MS spectra are in agreement with the reported ones [128].

di-tert-butyl (((S)-1-(tert-butoxy)-6-((S)-2-((1r,4S)-4-((6-fluoronicotinamido)methyl)cyclohexane-1-carboxamido)-3-(naphthalen-2-yl)propanamido)-1-oxohexan-2-yl)carbamoyl)-L-glutamate (4.7)

Under nitrogen atmosphere, to a solution of compound **4.6** (13 mg, 0.05 mmol) and compound **2.10** (37 mg, 0.05 mmol) in DMF (1.5 ml) was added triethylamine (0.02 ml, 0.11 mmol). The reaction mixture was stirred overnight at room temperature. Reaction progress was monitored by TLC (DCM:MeOH 9.5:0.5). After the reaction was complete, the mixture in DMF was dripped into H_2O (15 ml) and the solution was extracted with EtOAc (3 x 15 ml). Collected organic phases were washed with brine (15 ml), dried over sodium sulfate and the solvent was removed at reduced pressure. The crude reaction mixture was obtained with a satisfactory purity grade as a white solid (40 mg, 0.046 mmol, 93.3%).

R_f: 0.50

^{1}H-NMR (DMSO-d_6): δ 0.81 (m, 2H), 1.05 (m, 1H), 1.15-1.24 (m, 5H), 1.29 (m, 2H), 1.37 (s, 27H), 1.45-1.55 (m, 2H), 1.58-1.76 (m, 4H), 1.84 (m, 1H), 2.07 (m, 1H), 2.20 (m, 2H), 2.92 (m, 2H), 2.98-3.11 (m, 4H), 3.90 (m, 1H), 4.01 (m, 1H), 4.50 (m, 1H), 6.20 (d, 1H), 6.26 (m, 1H), 7.26 (m, 1H), 7.36-7.46 (m, 3H), 7.65 (s, 1H), 7.74-7.84 (m, 3H), 7.88 (m, 2H), 8.34 (m, 1H), 8.56 (t, 1H), 8.65 (d, 1H).

^{13}C-NMR (DMSO-d_6): δ 22.89, 28.13, 28.20, 28.84, 29.10, 29.23, 30.08, 30.23, 31.35, 32.10, 37.39, 38.64, 38.74, 44.13, 45.86, 52.64, 53.49, 54.15, 80.20, 80.72, 81.05, 109.62, 109.92, 125.77, 126.36, 127.73, 127.91, 128.36, 129.13, 129.34, 132.00, 132.24, 133.36, 136.21, 141.78, 141.85, 147.65, 147.77, 157.57, 163.62, 164.07, 165.53, 171.44, 171.88, 172.34, 171.73, 175.35.

MS (m/z) (ESI+) 947.5221 $[M+H]^+$, 969.5036 $[M+Na]^+$.

(((S)-1-carboxy-5-((S)-2-((1r,4S)-4-((6-fluoronicotinamido)methyl)cyclohexane-1-carboxamido)-3-(naphthalen-2-yl)propanamido)pentyl)carbamoyl)-L-glutamic acid (4.8)

Under nitrogen atmosphere, to a solution of compound **4.7** (39 mg, 0.04 mmol) in DCM dry (5 ml), TFA was added dropwise (0.02 ml, 0.26 mmol) and the mixture was stirred for 2 days at room temperature. Reaction progress was monitored by TLC (DCM:MeOH 9.5:0.5) until the compound **4.7** disappearance. Then, after reaction completion, the solvent was evaporated under reduced pressure and the crude mixture was washed three times with hexane (3x 20 ml). Crude mixture was purified by semi-preparative HPLC. Pure precursor **4.8** was obtained as a white solid (15 mg, 0.02 mmol, 50%).

Analytical RP-HPLC condition: XTerra C18 5µm, 250x4.6 mm; water +0.1%TFA/acetonitrile +0.1%TFA isocratic 80:20 for 1 min, gradient from 80:20 to 60:40 in 30 min, gradient from 60:40 to 20:80 in 2 min; 1 ml/min, 220 nm, UV detector.

R_t: 28.1 min.

Semi-preparative RP-HPLC condition: column Clarity Oligo RP 5µm, 250x10 mm; isocratic 75:25 water +0.1%TFA/acetonitrile +0.1%TFA for 15 min; 6 ml/min, 220 nm, UV detector.

R_t: 9 min

^{1}H-NMR (DMSO-d_6): δ 0.88 (m, 2H), 1.04 (m, 1H), 1.22 (m, 3H9, 1.30 (m, 2H), 1.36-1.53 (m, 3H), 1.57 (m, 1H), 1.66 (m, 2H), 1.72 (m, 2H), 1.86 (m, 1H), 2.08 (t, 1H), 2.23 (m, 2H), 2-87-3.05 (m,

3H), 3.08 (m, 3H), 4.00 (m, 1H), 4.08 (m, 1H), 4.52 (m, 1H), 6.28 (m, 2H), 7.28 (dd, 1H), 7.36-7.48 (m, 3H), 7.68 (s, 1H), 7.78 (m, 2H), 7.84 (m, 1H), 7.94 (m, 2H), 8.35 (m, 1H), 8.59 (t, 1H), 8.66 (d, 1H), 12.53 (br, 3H).
^{13}C-NMR (DMSO-d_6): δ 23.02, 28.25, 28.82, 29.17, 29.23, 30.08, 30.23, 30.67, 32.16, 37.37, 38.63, 38.82, 44.13, 45.87, 52.25, 52.76, 54.14, 109.62, 109.92, 125.78, 126.37, 127.74, 127.88, 127.91, 128.38, 129.34, 129.37, 132.23, 133.36, 136.24, 141.79, 141.86, 147.64, 147.77, 157.74, 163.61, 164.09, 165.51, 171.46, 174.27, 174.66, 175.04, 175.37.
MS (m/z) (ESI+) 779.3411 $[M+H]^+$.

di-tert-butyl (((S)-6-((S)-2-((1r,4S)-4-((2-bromoacetamido)methyl)cyclohexane-1-carboxamido)-3-(naphthalen-2-yl)propanamido)-1-(tert-butoxy)-1-oxohexan-2-yl)carbamoyl)-L-glutamate (4.9)

Under nitrogen atmosphere, to a solution of compound **2.10** (200 mg, 0.24 mmol), bromoacetic acid (35 mg, 0.25 mmol) and DCC (52 mg, 0.25 mmol) in dichloromethane (8 ml) was added DMAP (1 mg, 0.01 mmol). The reaction was stirred at room temperature for 30 min. Reaction progress was monitored by TLC (DCM:MeOH 8.5:1.5). After completion, the mixture was filtered to remove the dicyclohexylurea and the solvent was evaporated at reduced pressure. The crude reaction mixture was purified by silica gel column chromatography (eluents: gradient of DCM/acetone) to afford the desired product **4.9** as a white solid (191 mg, 0.20 mmol, 83%).
R_f: 0.65
^{1}H-NMR (DMSO-d_6): δ 0.94 (m, 2H), 1.24 (m, 3H), 1.34 (m, 3H), 1.44 (s, 27 H), 1.59 (m ,3H), 1.66-1.85 (m, 5H), 2.01 (m, 1H), 2.14 (m, 1H), 2.29 (m, 2H), 3.02 (m, 3H), 3.09 (m, 2H), 3.22 (m, 1H), 3.79 (s, 2H), 4.04 (m, 1H), 4.18 (m, 1H), 4.64 (m, 1H), 7.36-7.47 (m, 3H), 7.67 (s, 1H), 7.78 (m, 3H).
^{13}C-NMR (DMSO-d_6): δ 22.15, 26.89, 26.94, 26.96, 27.36, 27.69, 28.19, 28.34, 28.85, 29.39, 29.49, 31.11, 31.39, 37.11, 37.95, 38.43, 44.48, 45.45, 52.78, 53.35, 54.53, 80.37, 81.10, 81.49, 125.23, 125.70, 127.10, 127.15, 127.24, 127.58, 127.63, 132.52, 133.52, 134.56, 158.54, 165.87, 168.19, 172.21, 172.36, 172.55, 177.36.
MS (m/z) (ESI+) 946.4393 $[M+H]^+$, 968.4214 $[M+Na]^+$.

(((S)-5-((S)-2-((1r,4S)-4-((2-bromoacetamido)methyl)cyclohexane-1-carboxamido)-3-(naphthalen-2-yl)propanamido)-1-carboxypentyl)carbamoyl)-L-glutamic acid (4.2)

Under nitrogen atmosphere, to a solution of compound **4.9** (191 mg, 0.20 mmol) in DCM (8 ml) was added TFA (1.5 ml, 19.6 mmol). The reaction was stirred at room temperature for 2 hours. Reaction progress was monitored by TLC (DCM:MeOH 8.5:1.5) until complete compound **4.9** disappearance. Then, after reaction completion, the solvent was evaporated under reduced pressure and the crude mixture was washed three times with hexane (3x 20 ml). Crude mixture was purified by semi-preparative HPLC. Pure precursor **4.2** was obtained as a white solid (90 mg, 0.12 mmol, 57%).
Analytical RP-HPLC condition: XTerra C18 5µm, 250x4.6 mm; water +0.1%TFA/acetonitrile +0.1%TFA gradient from 70:30 to 20:80 in 20 min, isocratic 20:80 for 2 min; 1 ml/min, 220 nm, UV detector.
R_t: 8.2 min.
Semi-preparative RP-HPLC condition: column Clarity Oligo RP 5µm, 250x10 mm; isocratic 60:40 water +0.1%TFA/acetonitrile +0.1%TFA; 6 ml/min, 220 nm, UV detector.
R_t: 6 min

^{1}H-NMR (DMSO-d_6): δ 0.95 (m, 2H), 1.26 (m, 3H), 1.38 (m, 4H), 1.56 (m, 2H), 1.70 (m, 2H), 1.79 (m, 2H), 1.90 (m, 1H), 2.15 (m, 2H), 2.41 (m, 2H), 3.02 (d, 2H), 3.05-3.15 (m, 3H), 3.24 (m, 1H), 3.80 (s, 2H), 4.18 (m, 1H), 4.31 (m, 1H), 4.66 (m, 1H), 7.36-7.48 (m, 3H), 7.68 (s, 1H), 7.74-7.84 (m, 3H).
^{13}C-NMR (DMSO-d_6): δ 22.18, 27.36, 27.53, 28.19, 28.31, 28.84, 29.38, 29.48, 29.73, 31.42, 37.09, 37.95, 38.45, 44.47, 45.46, 52.12, 52.48, 54.52, 125.23, 125.70, 127.09, 127.14, 127.23, 127.59, 127.63, 132.51, 133.51, 134.54, 158.73, 168.22, 172.24, 174.57, 175.02, 177.41.
MS (m/z) (ESI+) 777.5973 $[M+H]^+$.

di-tert-butyl (((S)-1-(tert-butoxy)-6-((S)-2-((1r,4S)-4-((2-fluoroacetamido)methyl)cyclohexane-1-carboxamido)-3-(naphthalen-2-yl)propanamido)-1-oxohexan-2-yl)carbamoyl)-L-glutamate (4.10)

Under nitrogen atmosphere, to a solution of compound **2.10** (106 mg, 0.13 mmol), fluoroacetic acid (10 µl, 0.14 mmol) and DCC (28 mg, 0.14 mmol) in dichloromethane (4 ml) was added DMAP (0.63 mg, 0.005 mmol). The reaction was stirred at room temperature for 30 min. Reaction progress was monitored by TLC (DCM:MeOH 8.5:1.5). After completion, the mixture was filtered to remove the dicyclohexylurea and the solvent was evaporated at reduced pressure. The crude reaction mixture was purified by silica gel column chromatography (eluents: gradient of DCM/acetone) to afford the desired product **4.10** as a white solid (102 mg, 0.11 mmol, 89%).
R_f: 0.75
^{1}H-NMR (CD_3OD): δ 0.92 (m, 2H), 1.19-1.37 (m, 7H), 1.44 (s, 28H), 1.60 (m, 2H), 1.70 (m, 1H), 1.78 (m, 3H), 2.02 (m, 1H), 2.15 (m, 1H), 2.30 (m, 2H), 3.02-3.12 (m, 5H), 3.22 (m, 1H), 4.04 (m, 1H), 4.18 (m, 1H), 4.64 (m, 1H), 4.70-4.83 (d, 2H, J=45.59 Hz), 7.34-7.47 (m, 3H), 7.67 (s, 1H), 7.74-7.82 (m, 3H).
^{13}C-NMR (CD_3OD): δ 22.16, 26.87, 26.89, 26.91, 26.93, 26.96, 26.98, 27.70, 28.20, 28.35, 28.84, 29.43, 29.53, 31.12, 31.39, 37.14, 37.96, 38.43, 44.44, 44.50, 52.79, 53.35, 54.53, 78.84, 80.29, 80.36, 81.11, 81.49, 125.23, 125.70, 127.10, 127.15, 127.24, 127.58, 127.63, 132.52, 133.52, 134.56, 158.54, 169.07, 169.10, 172.21, 172.36, 172.55, 177.37.
MS (m/z) (ESI+) 946.4393 $[M+H]^+$, 968.4214 $[M+Na]^+$.

(((S)-1-carboxy-5-((S)-2-((1r,4S)-4-((2-fluoroacetamido)methyl)cyclohexane-1-carboxamido)-3-(naphthalen-2-yl)propanamido)pentyl)carbamoyl)-L-glutamic acid (4.11)

Under nitrogen atmosphere, to a solution of compound **4.10** (102 mg, 0.20 mmol) in DCM (7 ml) TFA (1 ml, 13.1 mmol) was added. The reaction was stirred at room temperature for 1 hours. Reaction progress was monitored by TLC (DCM:MeOH 8.5:1.5) until complete compound **4.10** disappearance. Then, after reaction completion, the solvent was evaporated under reduced pressure and the crude mixture was washed three times with hexane (3x 20 ml). Crude mixture was purified by semi-preparative HPLC. Pure precursor **4.11** was obtained as a white solid (35 mg, 0.05 mmol, 42%).
Analytical RP-HPLC condition: XTerra C18 5µm, 250x4.6 mm; water +0.1%TFA/acetonitrile +0.1%TFA gradient from 70:30 to 20:80 in 20 min, isocratic 20:80 for 2 min; 1 ml/min, 220 nm, UV detector.
R_t: 7 min.

Semi-preparative RP-HPLC condition: column Clarity Oligo RP 5µm, 250x10 mm; isocratic 60:40 water +0.1%TFA/acetonitrile +0.1%TFA; 6 ml/min, 220 nm, UV detector.
R_t: 5 min
^{1}H-NMR (DMSO-d_6): δ 0.78 (m, 2H), 1.00 (m, 1H), 1.19 (m ,3H), 1.29 (m, 3H), 1.45 (m, 2H), 1.53-1.73 (m, 5H), 1.90 (m, 1H), 2.05 (m, 1H), 2.22 (m, 2H), 2.85-2.93 (m, 3H), 2.93-2.99 (m, 1H), 2.99-3.11 (m, 2H), 3.99 (m, 1H), 4.07 (m, 1H), 4.50 (m, 1H), 4.70-4.99 (d, 2H, J=46.59 Hz), 6.25 (d, 1H), 6.29 (d, 1H), 7.34-7.48 (m, 3H), 7.66 (s, 1H), 7.73-7.80 (m, 2H), 7.83 (m, 1H), 7.91 (m, 2H), 8.06 (t, 1H), 12.01-12.65 (br, 3H).
^{13}C-NMR (DMSO-d_6): δ 23.02, 28.02, 28.76, 29.18, 29.92, 30.07, 30.37, 32.17, 37.30, 38.64, 38.83, 44.12, 44.63, 52.13, 52.73, 54.12, 79.74, 81.17, 125.78, 126.37, 127.73, 127.88, 127.91, 128.38, 133.36, 132.24, 136.24, 157.74, 167.36, 167.49, 171.44, 174.17, 174.62, 175.00, 175.35.
MS (m/z) (ESI+) 716.3304 $[M+H]^+$.

Radiochemistry

(((S)-1-carboxy-5-((S)-2-((1r,4S)-4-((6-fluoronicotinamido)methyl)cyclohexane-1-carboxamido)-3-(naphthalen-2-yl)propanamido)pentyl)carbamoyl)-L-glutamic acid ([^{18}F]4.8)
An activity of ~70 GBq of aqueous [^{18}F]fluoride was passed through a Sep-Pak light QMA cartridge pre-conditioned with NaCl solution (10 ml). The cartridge was eluted by 0.75 ml of a 75 mM solution of tetrabutylammonium hydrogen carbonate (TBA) in water directly into the reactor. Then, solution was evaporated heating at 130°C for 5 min. After evaporation, a solution of Precursor **4.1** (1.10 mg, 1.4 µmol) in DMSO (1.6 ml) was added and reaction mixture was heated at 105°C for 10 min. Then, in order to purify product **[^{18}F] 4.8**, the mixture was diluted with 8 ml water and submitted to semi-preparative RP-HPLC. The fraction containing the desired product was collected, diluted with water (10 ml) and passed through a C_{18} Sep-Pak Plus cartridge previously conditioned with ethanol (10 ml) and water (10 ml). The cartridge was washed with water (30 ml) and the final product was obtained by elution with EtOH (1 ml) and saline physiological solution (19 ml) into the final container. The average obtained final RCY not corrected for decay was in the range of ~20%, >99% radiochemical purity (Molar activity >1000 GBq/µmol). Preparation time was 63 min.
Semi-preparative RP-HPLC condition: column Clarity Oligo-RP 5µm, 250x10 mm; water +0.1%TFA/acetonitrile +0.1%TFA gradient from 70:30 to 60:40 in 20 min; 5 ml/min, 220 nm, UV detector.
R_t: 19 min
Analytical RP-HPLC condition: column XTerra C18 5µm, 250x4.6 mm; buffer phosphate pH=2.55/ acetonitrile isocratic 75:25 for 2 min, gradient from 75:25 to 70:30 in 6 min, gradient from 70:30 to 60:40 in 5 min, isocratic 60:40 for 5 min; 1 ml/min, 220 nm, UV detector.
R_t: 14.7 min

GLOSSARY

- ACTIVITY: Often used term for "Radioactivity". It refers to the number of nuclear transformations occurring in a unit of time.
- ALPHA DECAY: Process where an instable radionuclide emits an alpha (α) particle during a nuclear transformation, disintegration or radioactive decay. The alpha particle consists in two neutrons and two protons ($^{4}He^{2+}$ ion).
- ANNIHILATION: The radiation produced by reaction between a particle and its anti-particle. It consists in production of two photons with same direction, opposite verse and total energy equivalent to the masses of particles annihilated.
- ATOMIC NUMBER: Number of photons in a nucleus. Symbol Z.
- BEQUEREL (Bq): The SI unit of radioactivity. An activity of 1 Bq implies an average disintegration rate of 1 disintegration per second.
- BETA DECAY: Process where an instable radionuclide emits a beta (β) particle during a nuclear transformation, disintegration or radioactive decay. The atom nucleus raises atomic number if the emitted particle is negatively charged (electron, β^-) or lowers atomic number if the particle is positively charged (positron, β^+). In addition, during beta decay, another no-charged and vanishingly small mass particle is emitted: a neutrino for positron emission or an antineutrino for electron emission.
- BIODISTRIBUTION: Distribution of a pharmaceutical or radiopharmaceutical in the body of a living being.
- Bq: Abbreviation for Bequerel
- CHELATOR: An organic compound which is able to form a complex with a metal. It consists in a formation of closed ring of atoms to a central metal ion.
- CuAAC: Cu(I)-catalyzed Huisgen [3+2] cycloaddition between an azide and a terminal alkyne. It is the most used reaction type in the "click chemistry" reactions family.
- CYCLOTRON: A machine which accelerates charged particles is a spiral or circular path and deflects them onto a target.
- DCM: Abbreviation for dichloromethane
- DECAY: Radioactive decay. Spontaneous transformation of a radioactive atom nucleus into a new nuclear form, accompanied by emission of radiation.
- DFT: Density Functional Theory calculation. Computational quantum mechanical modelling to investigate the electronic structure (or nuclear structure) of many-body systems, like atoms and molecules.
- DMF: Abbreviation for dimethyl formamide
- DMSO: Abbreviation for dimethyl sulfoxide
- ELECTRONIC CAPTURE (EC): A beta decay process, where radionuclides with excess of protons get stability by capturing an orbital electron (generally from a K shell) and convert a proton into a neutron.
- ESI: Electrospray ionization, associated to a Mass Spectrometry (MS) analysis. It consists in bringing to a gaseous phase analytes in the form of charged species, without damaging.
- FUNCTIONAL GROUP: A part of the structure of a molecule characterized by specific elements and well-defined and precise structure, which gives to the compound a typical reactivity, similar to other molecules containing the same group.

- GAMMA DECAY: Process where an instable radionuclide emits a gamma (γ) particle during a nuclear transformation, disintegration or radioactive decay. It consists in high-energy photons emission with no change of atomic and mass numbers.
- GENERATOR: A device where a short-lived daughter radionuclide is separated physically and periodically from longer-lived radionuclide adsorbed onto a column. It is very used for obtaining Gallium-68 from Germanium-68.
- HALF-LIFE: Time required for the amount of a substance's radioactivity to be reduced to one-half.
- HOT CELL: Terms to indicate Shielded nuclear radiation containment chambers. Hot cells are used in both the nuclear-energy and the nuclear-medicines industries. They are required to protect individuals from radioactive isotopes by providing a safe containment box in which they can control and manipulate the equipment required.
- HPLC: High Performance Liquid Chromatography. Technique used to test chemical and radiochemical purity or to separate two or more substances very efficiently.
- IN VITRO: Outside the living body. Term used to indicate a test outside living body, usually using isolated tissues, organs or cells.
- IN VIVO: Test performed on people or animals.
- ISOTOPES: Nuclides having the same atomic number but different mass number.
- LABELLED COMPOUND: A molecule in which one or more atoms are replaced with radionuclides, either isotopes or foreign elements.
- LEAVING GROUP (LG): An atom or group of atoms which detaches from the main or residual part of a substrate during a reaction.
- LIGAND: Any molecules that bind to another. For example for a little molecule which bind a large protein, the little molecule will be classed as ligand.
- MASS NUMBER: Sum of protons and neutrons inside a nucleus. Symbol is A.
- MeOH: Abbreviation for methanol.
- MS: Abbreviation for Mass Spectrometry. Analytical technique used to measure the mass-to-charge ratio of ions. The results are presented in a mass-spectrum.
- NMR: Abbreviation for Nuclear Magnetic Resonance. Analytical technique used to determine the molecular structure and chemical composition of a sample. It is based on the analysis of the spin behaviour of nuclei in presence of a strong magnetic field.
- NODA: Abbreviation for IUPAC 1,4,7-triazonane-1,4-diyl)diacetic acid. Important chelator for gallium-68 and [^{18}F] aluminum fluoride complexation.
- PET: Abbreviation for Positron Emission Tomography.
- POSITRON DECAY: Emission of positron during a radioactive decay (β^+). In addition, another no-charged and vanishingly small mass neutrino particle is emitted.
- PROSTETIC GROUP: A molecule of a non- protein nature closely linked to a protein. In general it indicates a molecule without biological activity closely linked to a biomolecule.
- PSMA: Abbreviation for Prostetic Specific Membrane Antigen. Moreover, PSMA ligands are abbreviated with initials "PSMA" followed by a number.
- RADIOCHEMICAL PURITY: The proportion of the total radioactivity in a stated chemical form.
- RADIOCHEMICAL YIELD (RCY): The fraction of percentage of the original radionuclide incorporated into the radiochemical at the end of the synthesis, corrected for decay after synthesis and processing to the time of measurement.

- RADIOCHEMICAL YIELD NOT DECAY CORRECTED (RCYndc): The fraction of percentage of the original radionuclide incorporated into the radiochemical at the end of the synthesis, without correcting for decay after synthesis and processing to the time of measurement.
- RADIOCHEMISTRY: The chemistry of radioactive materials, including the production and purification of radionuclides, synthesis of labelled compounds and the use of these materials in chemical studies.
- RADIOLYSIS: The decomposition of a material by radiations.
- RADIONUCLIDE: An unstable or radioactive nuclide that decays by spontaneous fission, alpha, beta and gamma radiations.
- RADIOPHARMACEUTICAL: Any pharmaceutical preparation which includes a radionuclide in its composition. It can be used for imaging or therapy purposes.
- RADIOSYNTHESIS: A chemical synthesis which include radionuclides.
- RADIOSYNTHETIC MODULE: Automated equipment that is used for perform radiosynthesis
- RESCA: Abbreviation for IUPAC 2,2'-(((1R,2R)-2-((carboxymethyl)(4-(carboxymethyl) benzyl) amino)cyclohexyl)azanediyl)diacetic acid. Important chelator for [^{18}F] aluminum fluoride complexation.
- SPECT: Abbreviation for Single-photon Emission Computed Tomography.
- SPECIFIC ACTIVITY: Represent the activity per unit of mass. Generally, it is indicated as Bq/µmol.
- TARGET: The material which is bombarded by an accelerated beam of charged particles to produce a radionuclide.
- TRACER: A labelled molecule used to trace a chemical reaction or to follow the passage of a substance through a biological or physical system.
- TLC: Abbreviation for Thin Layer Chromatography. It is a technique used to separate compounds is a mixture based on their affinity. It is an extremely versatile method, widely used for qualitative and quantitative analyses.
- YIELD: The fraction of amount of final product produced from raw materials at the end of a chemical synthesis.

PUBLICATIONS AND PRESENTATIONS

PUBLICATIONS

- Synthesis of new PSMA-617 NODA and RESCA derivatives and radiolabeling with fluorine-18 by [^{18}F]AlF^{2+} complexation approach; *About to be published* **2022/2023**.
- Synthesis and automatedfluorine-18 radiolabeling of new PSMA-617derivatives with a CuAAC radiosynthetic approach; MN Iannone, S Stucchi, EA Turolla, C Beretta, S Ciceri, C Chinello, L Pagani, S Todde, P Ferraboschi; *J. Label. Compd. Radiopharm.*; **2022**; 1-15.
- A novel versatile precursor suitable for 18F-radiolabeling via "click chemistry"; B Lugato, S Stucchi, S Ciceri, MN Iannone, EA Turolla, L Giuliano, C Chinello, S Todde, P Ferraboschi; *J. Label. Compd. Radiopharm.*; **2017**; 60, 466-480.

ABSTRACT PRESENTATION

- "A comparison of different approaches aimed to introduce fluorine-18 in biologically active molecules". MN Iannone, S Stucchi, EA Turolla, S Todde; IX National congress GICR, Napoli, May **2022**

REFERENCES

[1] C. Nicolau, N. Antunes, B. Paño, and C. Sebastia, "Imaging characterization of renal masses," *Med.*, vol. 57, no. 1, pp. 1–19, 2021, doi: 10.3390/medicina57010051.

[2] V. Valotassiou *et al.*, "SPECT and PET imaging in Alzheimer's disease," *Ann. Nucl. Med.*, vol. 32, no. 9, pp. 583–593, 2018, doi: 10.1007/s12149-018-1292-6.

[3] S. H. Jafari *et al.*, "Breast cancer diagnosis: Imaging techniques and biochemical markers," *J. Cell. Physiol.*, vol. 233, no. 7, pp. 5200–5213, 2018, doi: 10.1002/jcp.26379.

[4] G. Crișan, N. S. Moldovean-cioroianu, D. G. Timaru, G. Andrieș, C. Căinap, and V. Chiș, "Radiopharmaceuticals for PET and SPECT Imaging: A Literature Review over the Last Decade," *Int. J. Mol. Sci.*, vol. 23, no. 9, 2022, doi: 10.3390/ijms23095023.

[5] L. Evangelista *et al.*, "PET/MRI in prostate cancer: a systematic review and meta-analysis," *Eur. J. Nucl. Med. Mol. Imaging*, vol. 48, no. 3, pp. 859–873, 2021, doi: 10.1007/s00259-020-05025-0.

[6] V. Duclos, A. Iep, L. Gomez, L. Goldfarb, and F. L. Besson, "Pet molecular imaging: A holistic review of current practice and emerging perspectives for diagnosis, therapeutic evaluation and prognosis in clinical oncology," *Int. J. Mol. Sci.*, vol. 22, no. 8, 2021, doi: 10.3390/ijms22084159.

[7] Tony Theobald, Ed., *Sampson's Textbook of Radiopharmacy*, Fourth Edi. Pharmaceutical Press, 2011.

[8] T. Beyer *et al.*, "What scans we will read: Imaging instrumentation trends in clinical oncology," *Cancer Imaging*, vol. 20, no. 1, pp. 1–38, 2020, doi: 10.1186/s40644-020-00312-3.

[9] M. Pfützner, M. Karny, L. V. Grigorenko, and K. Riisager, "Radioactive decays at limits of nuclear stability," *Rev. Mod. Phys.*, vol. 84, no. 2, pp. 567–619, 2012, doi: 10.1103/RevModPhys.84.567.

[10] S. Todde and S. Boschi, *Compendio di Radiochimica e Radiofarmacia*. 2020.

[11] M. Guillaume, A. Luxen, B. Nebeling, M. Argentini, J. C. Clark, and V. W. Pike, "Recommendations for fluorine-18 production," *Int. J. Radiat. Appl. Instrumentation. Part*, vol. 42, no. 8, pp. 749–762, 1991, doi: 10.1016/0883-2889(91)90179-5.

[12] F. Bray, J. Ferlay, I. Soerjomataram, R. L. Siegel, L. A. Torre, and A. Jemal, "Global cancer statistics 2018: GLOBOCAN estimates of incidence and mortality worldwide for 36 cancers in 185 countries," *CA. Cancer J. Clin.*, vol. 68, no. 6, pp. 394–424, 2018, doi: 10.3322/caac.21492.

[13] N. Mottet *et al.*, "EAU-ESTRO-SIOG Guidelines on Prostate Cancer. Part 1: Screening, Diagnosis, and Local Treatment with Curative Intent," *Eur. Urol.*, vol. 71, no. 4, pp. 618–629, 2017, doi: 10.1016/j.eururo.2016.08.003.

[14] R. J. Rebello *et al.*, "Prostate cancer," *Nat. Rev. Dis. Prim.*, vol. 7, no. 1, 2021, doi: 10.1038/s41572-020-00243-0.

[15] H. U. Ahmed *et al.*, "Diagnostic accuracy of multi-parametric MRI and TRUS biopsy in prostate cancer (PROMIS): a paired validating confirmatory study," *Lancet*, vol. 389, no. 10071, pp. 815–822, 2017, doi: 10.1016/S0140-6736(16)32401-1.

[16] S. Bednarova, M. L. Lindenberg, M. Vinsensia, C. Zuiani, P. L. Choyke, and B. Turkbey, "Positron emission tomography (PET) in primary prostate cancer staging and risk assessment," *Transl. Androl. Urol.*, vol. 6, no. 3, pp. 413–423, 2017, doi: 10.21037/tau.2017.03.53.

[17] R. Manafi-Farid *et al.*, "Molecular imaging in primary staging of prostate cancer patients: Current aspects and future trends," *Cancers (Basel).*, vol. 13, no. 21, pp. 1–29, 2021, doi: 10.3390/cancers13215360.

[18] C. L. Welle *et al.*, "C-choline PET/CT in recurrent prostate cancer and nonprostatic neoplastic processes," *Radiographics*, vol. 36, no. 1, pp. 279–292, 2016, doi: 10.1148/rg.2016150135.

[19] F. E. von Eyben and K. Kairemo, "Acquisition with 11C-choline and 18F-fluorocholine PET/CT for patients with biochemical recurrence of prostate cancer: a systematic review and meta-analysis," *Ann. Nucl. Med.*, vol. 30, no. 6, pp. 385–392, 2016, doi: 10.1007/s12149-016-1078-7.

[20] K. M. Xu, R. C. Chen, D. M. Schuster, and A. B. Jani, "Role of novel imaging in the management of prostate cancer," *Urol. Oncol. Semin. Orig. Investig.*, vol. 37, no. 9, pp. 611–618, 2019, doi: 10.1016/j.urolonc.2019.04.008.

[21] C. Nanni *et al.*, "18F-FACBC (anti1-amino-3-18F-fluorocyclobutane-1-carboxylic acid) versus 11C-choline PET/CT in prostate cancer relapse: results of a prospective trial," *Eur. J. Nucl. Med. Mol. Imaging*, vol. 43, no. 9, pp. 1601–1610, 2016, doi: 10.1007/s00259-016-3329-1.

[22] J. Lau, E. Rousseau, D. Kwon, K. S. Lin, F. Bénard, and X. Chen, "Insight into the development of PET radiopharmaceuticals for oncology," *Cancers (Basel).*, vol. 12, no. 5, 2020, doi: 10.3390/cancers12051312.

[23] M. Benesová *et al.*, "Preclinical evaluation of a tailor-made DOTA-conjugated PSMA inhibitor with optimized linker moiety for imaging and endoradiotherapy of prostate cancer," *J. Nucl. Med.*, vol. 56, no. 6, pp. 914–920, 2015, doi: 10.2967/jnumed.114.147413.

[24] C. S. Rowe SP, Gorin MA, Allaf ME, Pienta KJ, Tran PT, Pomper MG, Ross AE, "PET imaging of prostate-

specific membrane antigen in prostate," *Prostate Cancer Prostatic Dis.*, vol. 19, no. 3, pp. 223–230, 2016, doi: 10.1038/pcan.2016.13.PET.
[25] M. I. Davis, M. J. Bennett, L. M. Thomas, and P. J. Bjorkman, "Crystal structure of prostate-specific membrane antigen, a tumor marker and peptidase," *Proc. Natl. Acad. Sci. U. S. A.*, vol. 102, no. 17, pp. 5981–5986, 2005, doi: 10.1073/pnas.0502101102.
[26] A. X. Zhang *et al.*, "A Remote arene-binding site on prostate specific membrane antigen revealed by antibody-recruiting small molecules," *J. Am. Chem. Soc.*, vol. 132, no. 36, pp. 12711–12716, Sep. 2010, doi: 10.1021/ja104591m.
[27] C. Barinka *et al.*, "Interactions between human glutamate carboxypeptidase II and urea-based inhibitors: Structural characterization," *J. Med. Chem.*, vol. 51, no. 24, pp. 7737–7743, 2008, doi: 10.1021/jm800765e.
[28] C. Barinka, C. Rojas, B. Slusher, and M. Pomper, "Glutamate Carboxypeptidase II in Diagnosis and Treatment of Neurologic Disorders and Prostate Cancer," *Curr. Med. Chem.*, vol. 19, no. 6, pp. 856–870, 2012, doi: 10.2174/092986712799034888.
[29] A. Afshar-Oromieh *et al.*, "The rise of PSMA ligands for diagnosis and therapy of prostate cancer," *J. Nucl. Med.*, vol. 57, pp. 79S-89S, 2016, doi: 10.2967/jnumed.115.170720.
[30] S. P. Rowe *et al.*, "18F-DCFBC PET/CT for PSMA-Based Detection and Characterization of Primary Prostate Cancer," *J Nuc Med*, vol. 56, no. 7, pp. 1003–1010, 2015, doi: 10.2967/jnumed.115.154336.18.
[31] V. Cuccurullo, G. D. Di Stasio, and L. Mansi, "Nuclear Medicine in Prostate Cancer: A New Era for Radiotracers.," *World J. Nucl. Med.*, vol. 17, no. 2, pp. 70–78, 2018, doi: 10.4103/wjnm.WJNM_54_17.
[32] T. Kawada *et al.*, "Diagnostic Performance of Prostate-specific Membrane Antigen Positron Emission Tomography–targeted biopsy for Detection of Clinically Significant Prostate Cancer: A Systematic Review and Meta-analysis," *Eur. Urol. Oncol.*, no. xxxx, 2022, doi: 10.1016/j.euo.2022.04.006.
[33] M. McCarthy, T. Langton, D. Kumar, and A. Campbell, "Comparison of PSMA-HBED and PSMA-I&T as diagnostic agents in prostate carcinoma," *Eur. J. Nucl. Med. Mol. Imaging*, vol. 44, no. 9, pp. 1455–1462, 2017, doi: 10.1007/s00259-017-3699-z.
[34] S. P. Rowe *et al.*, "Prostate-specific membrane antigen-targeted radiohalogenated PET and therapeutic agents for prostate cancer," *J. Nucl. Med.*, vol. 57, no. 10, pp. 90S-96S, 2016, doi: 10.2967/jnumed.115.170175.
[35] X. Di Han *et al.*, "64Cu-PSMA-617: A novel PSMA-targeted radio-tracer for PET imaging in gastric adenocarcinoma xenografted mice model," *Oncotarget*, vol. 8, no. 43, pp. 74159–74169, 2017, doi: 10.18632/oncotarget.18276.
[36] S. Lütje *et al.*, "PSMA ligands for radionuclide imaging and therapy of prostate cancer: Clinical status," *Theranostics*, vol. 5, no. 12, pp. 1388–1401, 2015, doi: 10.7150/thno.13348.
[37] A. Wurzer *et al.*, " Synthesis and Preclinical Evaluation of 177 Lu-labeled Radiohybrid PSMA Ligands (rhPSMAs) for Endoradiotherapy of Prostate Cancer ," *J. Nucl. Med.*, p. jnumed.121.263371, 2022, doi: 10.2967/jnumed.121.263371.
[38] S. Lütje *et al.*, "In vitro and in vivo characterization of an 18F-ALF-labeled PSMA ligand for imaging of PSMA-expressing xenografts," *J. Nucl. Med.*, vol. 60, no. 7, pp. 1017–1022, 2019, doi: 10.2967/jnumed.118.218941.
[39] G. W. Gordon E. Wynant M.S.,Gerald P. Murphy,Julius S. Horoszewicz,Charles E. Neal,B. David Collier,Edith Mitchell,Gary Purnell,Ian Tyson,Albert Heal,Hani Abdel-Nabi, "Immunoscintigraphy of prostatic cancer: Preliminary results with 111in-labeled monoclonal antibody 7E11-C5.3 (CYT-356)," *Prostate*, 1991.
[40] M. Eder *et al.*, "68Ga-complex lipophilicity and the targeting property of a urea-based PSMA inhibitor for PET imaging," *Bioconjug. Chem.*, vol. 23, no. 4, pp. 688–697, 2012, doi: 10.1021/bc200279b.
[41] S. Zang *et al.*, "68Ga-PSMA-11 PET/CT for prostate cancer staging and risk stratification in Chinese patients," *Oncotarget*, vol. 8, no. 7, pp. 12247–12258, 2017, doi: 10.18632/oncotarget.14691.
[42] M. Benešová *et al.*, "Linker Modification Strategies to Control the Prostate-Specific Membrane Antigen (PSMA)-Targeting and Pharmacokinetic Properties of DOTA-Conjugated PSMA Inhibitors," *J. Med. Chem.*, vol. 59, no. 5, pp. 1761–1775, 2016, doi: 10.1021/acs.jmedchem.5b01210.
[43] J. Cardinale *et al.*, "Preclinical evaluation of 18F-PSMA-1007, a new prostate-specific membrane antigen ligand for prostate cancer imaging," *J. Nucl. Med.*, vol. 58, no. 3, pp. 425–431, 2017, doi: 10.2967/jnumed.116.181768.
[44] I. Rauscher *et al.*, "Matched-pair comparison of 68Ga-PSMA-11 PET/CT and 18F-PSMA-1007 PET/CT: Frequency of pitfalls and detection efficacy in biochemical recurrence after radical prostatectomy," *J. Nucl. Med.*, vol. 61, no. 1, pp. 51–57, Jan. 2020, doi: 10.2967/jnumed.119.229187.
[45] F. L. Giesel *et al.*, "F-18 labelled PSMA-1007: biodistribution, radiation dosimetry and histopathological validation of tumor lesions in prostate cancer patients," *Eur. J. Nucl. Med. Mol. Imaging*, vol. 44, no. 4, pp. 678–688, 2017, doi: 10.1007/s00259-016-3573-4.
[46] K. Rahbar *et al.*, "Response and tolerability of a single dose of 177Lu-PSMA-617 in patients with metastatic castration-resistant prostate cancer: A multicenter retrospective analysis," *J. Nucl. Med.*, vol. 57, no. 9, pp. 1334–1338, 2016, doi: 10.2967/jnumed.116.173757.
[47] A. Adnan and S. Basu, "Comparison of Dual-Tracer PET and CT Features to Conventional Risk Categories in

Assessing Response to 177Lu-PSMA-617 Therapy for Metastatic Prostate Adenocarcinoma with Urinary Bladder Involvement," *J. Nucl. Med. Technol.*, vol. 48, no. 2, pp. 148–153, 2020, doi: 10.2967/jnmt.119.235960.
[48] INTERNATIONAL ATOMIC ENERGY AGENCY, *Production and Quality Control of Fluorine-18 Labelled Radiopharmaceuticals*. 2021.
[49] A. Sanchez-Crespo, "Comparison of Gallium-68 and Fluorine-18 imaging characteristics in positron emission tomography," *Appl. Radiat. Isot.*, vol. 76, pp. 55–62, 2013, doi: 10.1016/j.apradiso.2012.06.034.
[50] J. Ajenjo, G. Destro, B. Cornelissen, and V. Gouverneur, "Closing the gap between 19F and 18F chemistry," *EJNMMI Radiopharm. Chem.*, vol. 6, no. 1, 2021, doi: 10.1186/s41181-021-00143-y.
[51] A. F. Brooks, K. J. Makaravage, M. S. Sanford, and P. J. H. Scott, "Fluorine-18 Radiochemistry."
[52] A. Knöchel and O. Zwernemann, "Development of a no-carrier-added method for 18F-labelling of aromatic compounds by fluorodediazonation," *J. Label. Compd. Radiopharm.*, 1996.
[53] S. Preshlock, M. Tredwell, and V. Gouverneur, "18F-Labeling of Arenes and Heteroarenes for Applications in Positron Emission Tomography," *Chem. Rev.*, vol. 116, no. 2, pp. 719–766, 2016, doi: 10.1021/acs.chemrev.5b00493.
[54] M. K. Narayanam, G. Ma, P. A. Champagne, K. N. Houk, and J. M. Murphy, "Synthesis of [18F]Fluoroarenes by Nucleophilic Radiofluorination of N-Arylsydnones," *Angew. Chemie - Int. Ed.*, vol. 56, no. 42, pp. 13006–13010, 2017, doi: 10.1002/anie.201707274.
[55] Y. Yamada, K. Kashima, and M. Okawara, " Substituent Effect in the Nucleophilic Attack by the Bromide Ion on the p -Tolyl-Substituted Phenyliodonium Ions ," *Bulletin of the Chemical Society of Japan*, vol. 47, no. 12. pp. 3179–3180, 1974, doi: 10.1246/bcsj.47.3179.
[56] S. H. Liang, L. Wang, N. A. Stephenson, B. H. Rotstein, and N. Vasdev, "Facile 18 F labeling of non-activated arenes via a spirocyclic iodonium(III) ylide method and its application in the synthesis of the mGluR 5 PET radiopharmaceutical [18 F]FPEB," *Nat. Protoc.*, vol. 14, no. 5, pp. 1530–1545, 2019, doi: 10.1038/s41596-019-0149-3.
[57] N. W. Goldberg, X. Shen, J. Li, and T. Ritter, "AlkylFluor: Deoxyfluorination of Alcohols," *Org. Lett.*, vol. 18, no. 23, pp. 6102–6104, 2016, doi: 10.1021/acs.orglett.6b03086.
[58] R. Halder and T. Ritter, "18F-Fluorination: Challenge and Opportunity for Organic Chemists," *J. Org. Chem.*, vol. 86, no. 20, pp. 13873–13884, 2021, doi: 10.1021/acs.joc.1c01474.
[59] J. Cardinale, J. Ermert, F. Kügler, A. Helfer, M. R. Brandt, and H. H. Coenen, "Carrier-effect on palladium-catalyzed, nucleophilic 18F- fluorination of aryl triflates," *J. Label. Compd. Radiopharm.*, vol. 55, no. 12, pp. 450–453, 2012, doi: 10.1002/jlcr.2973.
[60] B. D. Zlatopolskiy *et al.*, "A Practical One-Pot Synthesis of Positron Emission Tomography (PET) Tracers via Nickel-Mediated Radiofluorination," *ChemistryOpen*, vol. 4, no. 4, pp. 457–462, 2015, doi: 10.1002/open.201500056.
[61] N. J. Taylor *et al.*, "Derisking the Cu-Mediated 18F-Fluorination of Heterocyclic Positron Emission Tomography Radioligands," *J. Am. Chem. Soc.*, vol. 139, no. 24, pp. 8267–8276, 2017, doi: 10.1021/jacs.7b03131.
[62] J. Wu, "Review of recent advances in nucleophilic C-F bond-forming reactions at sp3 centers," *Tetrahedron Lett.*, vol. 55, no. 31, pp. 4289–4294, 2014, doi: 10.1016/j.tetlet.2014.06.006.
[63] Y. Pan, "The dark side of fluorine," *ACS Med. Chem. Lett.*, vol. 10, no. 7, pp. 1016–1019, 2019, doi: 10.1021/acsmedchemlett.9b00235.
[64] M. Kuchar and C. Mamat, "Methods to increase the metabolic stability of 18F-radiotracers," *Molecules*, vol. 20, no. 9, pp. 16186–16220, 2015, doi: 10.3390/molecules200916186.
[65] M. 0 Straatmannand and M. Welch, "(DAST): An F-for-OH Fluorinating Agent," pp. 151–158, 1976.
[66] R. P. Singh and J. M. Shreeve, "Recent advances in nucleophilic fluorination reactions of organic compounds using Deoxofluor and DAST," *Synthesis (Stuttg).*, no. 17, pp. 2561–2578, 2002, doi: 10.1055/s-2002-35626.
[67] M. K. Nielsen, C. R. Ugaz, W. Li, and A. G. Doyle, "PyFluor: A low-cost, stable, and selective deoxyfluorination reagent," *J. Am. Chem. Soc.*, vol. 137, no. 30, pp. 9571–9574, 2015, doi: 10.1021/jacs.5b06307.
[68] F. Sladojevich, S. I. Arlow, P. Tang, and T. Ritter, "Late-stage deoxyfluorination of alcohols with phenofluor," *J. Am. Chem. Soc.*, vol. 135, no. 7, pp. 2470–2473, 2013, doi: 10.1021/ja3125405.
[69] C. Hollingworth *et al.*, "Palladium-catalyzed allylic fluorination," *Angew. Chemie - Int. Ed.*, vol. 50, no. 11, pp. 2613–2617, 2011, doi: 10.1002/anie.201007307.
[70] M. Suehiro *et al.*, "Radiosynthesis of the tumor hypoxia marker [18F]TFMISO via O-[18F]trifluoroethylation reveals a striking difference between trifluoroethyl tosylate and iodide in regiochemical reactivity toward oxygen nucleophiles," *Bioorganic Med. Chem.*, vol. 19, no. 7, pp. 2287–2297, 2011, doi: 10.1016/j.bmc.2011.02.026.
[71] J. Prabhakaran *et al.*, "Synthesis and in vivo evaluation of [18F]-4-[5-(4-methylphenyl)-3-(trifluoromethyl)-1H-pyrazol-1-yl]benzenesulfonamide as a PET imaging probe for COX-2 expression," *Bioorganic Med. Chem.*, vol. 15, no. 4, pp. 1802–1807, 2007, doi: 10.1016/j.bmc.2006.11.033.

[72] S. Verhoog *et al.*, “Silver-Mediated 18F-Labeling of Aryl-CF3 and Aryl-CHF2 with 18F-Fluoride,” *Synlett*, vol. 27, no. 1, pp. 25–28, 2016, doi: 10.1055/s-0035-1560592.
[73] A. B. Gómez *et al.*, “Efficient DBU accelerated synthesis of 18F-labelled trifluoroacetamides,” *Chem. Commun.*, vol. 52, no. 97, pp. 13963–13966, 2016, doi: 10.1039/c6cc08535k.
[74] S. Mizuta *et al.*, “Catalytic decarboxylative fluorination for the synthesis of Tri- and difluoromethyl arenes,” *Org. Lett.*, vol. 15, no. 11, pp. 2648–2651, 2013, doi: 10.1021/ol4009377.
[75] A. Pees *et al.*, “Evaluating N-difluoromethyltriazolium triflate as a precursor for the synthesis of high molar activity [18F]fluoroform,” *J. Label. Compd. Radiopharm.*, vol. 64, no. 12, pp. 466–476, 2021, doi: 10.1002/jlcr.3939.
[76] H. C. Kolb, M. G. Finn, and K. B. Sharpless, “Click Chemistry: Diverse Chemical Function from a Few Good Reactions,” *Angew. Chemie - Int. Ed.*, vol. 40, no. 11, pp. 2004–2021, 2001, doi: 10.1002/1521-3773(20010601)40:11<2004::AID-ANIE2004>3.0.CO;2-5.
[77] A. A. H. Ahmad Fuaad, F. Azmi, M. Skwarczynski, and I. Toth, “Peptide conjugation via CuAAC ‘click’ chemistry,” *Molecules*, vol. 18, no. 11, pp. 13148–13174, 2013, doi: 10.3390/molecules181113148.
[78] G. A. et al Aragao-Leoneti V, Campo V L, “Application of Copper(I)-catalysed azide/alkyne cycloaddition (CuAAC) ‘click chemistry’ in carbohydrate drug and neo glycopolymer synthesis.,” *Tetrahedron*, pp. 9475–9492, 2010.
[79] B. T. Worrell, J. A. Malik, and V. V. Fokin, “Direct evidence of a dinuclear copper intermediate in Cu(I)-catalyzed azide-alkyne cycloadditions,” *Science (80-.).*, vol. 340, no. 6131, pp. 457–460, 2013, doi: 10.1126/science.1229506.
[80] J. E. Hein and V. V. Fokin, “Copper-catalyzed azide-alkyne cycloaddition (CuAAC) and beyond: new reactivity of copper(i) acetylides,” *Chem. Soc. Rev.*, vol. 39, no. 4, pp. 1302–1315, 2010, doi: 10.1039/b904091a.
[81] V. V. Rostovtsev, L. G. Green, V. V. Fokin, and K. B. Sharpless, “A stepwise huisgen cycloaddition process: Copper(I)-catalyzed regioselective ‘ligation’ of azides and terminal alkynes,” *Angew. Chemie - Int. Ed.*, vol. 41, no. 14, pp. 2596–2599, 2002, doi: 10.1002/1521-3773(20020715)41:14<2596::AID-ANIE2596>3.0.CO;2-4.
[82] M. Ahlquist and V. V. Fokin, “Enhanced reactivity of dinuclear copper(I) acetylides in dipolar cycloadditions,” *Organometallics*, vol. 26, no. 18, pp. 4389–4391, 2007, doi: 10.1021/om700669v.
[83] B. F. Straub, “μ-Acetylide and μ-alkenylidene ligands in ‘click’ triazole syntheses,” *Chem. Commun.*, no. 37, pp. 3868–3870, 2007, doi: 10.1039/b706926j.
[84] V. O. Rodionov, V. V. Fokin, and M. G. Finn, “Mechanism of the ligand-free CuI-catalyzed azide-alkyne cycloaddition reaction,” *Angew. Chemie - Int. Ed.*, vol. 44, no. 15, pp. 2210–2215, 2005, doi: 10.1002/anie.200461496.
[85] P. M. E. Gramlich, C. T. Wirges, J. Gierlich, and T. Carell, “Synthesis of modified DNA by PCR with alkyne-bearing purines followed by a click reaction,” *Org. Lett.*, vol. 10, no. 2, pp. 249–251, 2008, doi: 10.1021/ol7026015.
[86] L. M. Gaetke and C. K. Chow, “Copper toxicity, oxidative stress, and antioxidant nutrients,” *Toxicology*, vol. 189, no. 1–2, pp. 147–163, 2003, doi: 10.1016/S0300-483X(03)00159-8.
[87] Z. Wang *et al.*, “Post-synthetic modification of metal-organic framework thin films using click chemistry: The importance of strained C-C triple bonds,” *Langmuir*, vol. 29, no. 51, pp. 15958–15964, 2013, doi: 10.1021/la403854w.
[88] C. D. Smith and M. F. Greaney, “Zinc Mediated Azide À Alkyne Ligation to,” *Org. Lett.*, vol. 15, no. c, pp. 3–6, 2013.
[89] B. C. Boren *et al.*, “Ruthenium-catalyzed azide-alkyne cycloaddition: Scope and mechanism,” *J. Am. Chem. Soc.*, vol. 130, no. 28, pp. 8923–8930, 2008, doi: 10.1021/ja0749993.
[90] C. Remzi Becer, R. Hoogenboom, and U. S. Schubert, “Click chemistry beyond metal-catalyzed cycloaddition,” *Angew. Chemie - Int. Ed.*, vol. 48, no. 27, pp. 4900–4908, 2009, doi: 10.1002/anie.200900755.
[91] M. Glaser and E. Årstad, “‘Click labeling’ with 2-[18F]fluoroethylazide for positron emission tomography,” *Bioconjug. Chem.*, vol. 18, no. 3, pp. 989–993, 2007, doi: 10.1021/bc060301j.
[92] U. Sirion *et al.*, “An efficient F-18 labeling method for PET study: Huisgen 1,3-dipolar cycloaddition of bioactive substances and F-18-labeled compounds,” *Tetrahedron Lett.*, vol. 48, no. 23, pp. 3953–3957, 2007, doi: 10.1016/j.tetlet.2007.04.048.
[93] S. Maschauer and O. Prante, “A series of 2-O-trifluoromethylsulfonyl-d-mannopyranosides as precursors for concomitant 18F-labeling and glycosylation by click chemistry,” *Carbohydr. Res.*, vol. 344, no. 6, pp. 753–761, 2009, doi: 10.1016/j.carres.2009.02.001.
[94] S. Maschauer *et al.*, “Labeling and glycosylate of peptides using click chemistry: a general approach to18F-glycopeptides as effective imaging probes for positron emission tomography,” *Angew. Chemie - Int. Ed.*, vol. 49, no. 5, pp. 976–979, 2010, doi: 10.1002/anie.200904137.
[95] H. Schieferstein and T. L. Ross, “A polar 18F-labeled amino acid derivative for click labeling of biomolecules,” *European J. Org. Chem.*, vol. 2014, no. 17, pp. 3546–3550, 2014, doi: 10.1002/ejoc.201400071.
[96] W. J. McBride *et al.*, “A novel method of 18F radiolabeling for PET,” *J. Nucl. Med.*, vol. 50, no. 6, pp. 991–

998, 2009, doi: 10.2967/jnumed.108.060418.
[97] C. Fersing, A. Bouhlel, C. Cantelli, P. Garrigue, V. Lisowski, and B. Guillet, “A comprehensive review of non-covalent radiofluorination approaches using aluminum [18F]fluoride: Will [18F]AlF Replace 68Ga for metal chelate labeling?,” *Molecules*, vol. 24, no. 16, 2019, doi: 10.3390/molecules24162866.
[98] B. Antonny and M. Chabre, “Characterization of the aluminum and beryllium fluoride species which activate transducin. Analysis of the binding and dissociation kinetics,” *J. Biol. Chem.*, vol. 267, no. 10, pp. 6710–6718, 1992, doi: 10.1016/s0021-9258(19)50484-7.
[99] M. S. Corbillon, M. A. Olazabal, and J. M. Madariaga, “Potentiometric study of aluminium-fluoride complexation equilibria and definition of the thermodynamic model,” *J. Solution Chem.*, vol. 37, no. 4, pp. 567–579, 2008, doi: 10.1007/s10953-008-9257-3.
[100] W. J. McBride, R. M. Sharkey, and D. M. Goldenberg, “Radiofluorination using aluminum-fluoride (Al18F),” *EJNMMI Res.*, vol. 3, no. 1, pp. 1–11, 2013, doi: 10.1186/2191-219X-3-36.
[101] C. A. D’Souza, W. J. McBride, R. M. Sharkey, L. J. Todaro, and D. M. Goldenberg, “High-yielding aqueous 18F-labeling of peptides via Al 18F chelation,” *Bioconjug. Chem.*, vol. 22, no. 9, pp. 1793–1803, 2011, doi: 10.1021/bc200175c.
[102] S. J. Archibald and L. Allott, “The aluminium-[18F]fluoride revolution: simple radiochemistry with a big impact for radiolabelled biomolecules,” *EJNMMI Radiopharm. Chem.*, vol. 6, no. 1, 2021, doi: 10.1186/s41181-021-00141-0.
[103] D. Shetty *et al.*, “Stable aluminium fluoride chelates with triazacyclononane derivatives proved by X-ray crystallography and 18F-labeling study,” *Chem. Commun.*, vol. 47, no. 34, pp. 9732–9734, 2011, doi: 10.1039/c1cc13151f.
[104] K. L. S. Chatalic *et al.*, “Preclinical comparison of Al18F- and 68Ga-labeled gastrin-releasing peptide receptor antagonists for PET imaging of prostate cancer,” *J. Nucl. Med.*, vol. 55, no. 12, pp. 2050–2056, 2014, doi: 10.2967/jnumed.114.141143.
[105] E. A. Turolla *et al.*, “Study of the tissue distribution of TLQP-21 in mice using [18F]JMV5763, a radiolabeled Analog prepared via [18F]aluminum fluoride chelation chemistry,” *Front. Pharmacol.*, vol. 9, no. NOV, pp. 1–11, 2018, doi: 10.3389/fphar.2018.01274.
[106] L. Allott, C. Da Pieve, D. R. Turton, and G. Smith, “A general [18F]AlF radiochemistry procedure on two automated synthesis platforms,” *React. Chem. Eng.*, vol. 2, no. 1, pp. 68–74, 2017, doi: 10.1039/c6re00204h.
[107] F. Cleeren, J. Lecina, E. M. F. Billaud, M. Ahamed, A. Verbruggen, and G. M. Bormans, “New Chelators for Low Temperature Al18F-Labeling of Biomolecules,” *Bioconjug. Chem.*, vol. 27, no. 3, pp. 790–798, 2016, doi: 10.1021/acs.bioconjchem.6b00012.
[108] F. Cleeren *et al.*, “Direct fluorine-18 labeling of heat-sensitive biomolecules for positron emission tomography imaging using the Al 18 F-RESCA method,” *Nat. Protoc.*, vol. 13, no. 10, pp. 2330–2347, 2018, doi: 10.1038/s41596-018-0040-7.
[109] F. Cleeren *et al.*, “Al18F-labeling of heat-sensitive biomolecules for positron emission tomography imaging,” *Theranostics*, vol. 7, no. 11, pp. 2924–2939, 2017, doi: 10.7150/thno.20094.
[110] N. Malik, B. Baur, G. Winter, S. N. Reske, A. J. Beer, and C. Solbach, “Radiofluorination of PSMA-HBED via Al18F2+ Chelation and Biological Evaluations In Vitro,” *Mol. Imaging Biol.*, vol. 17, no. 6, pp. 777–785, 2015, doi: 10.1007/s11307-015-0844-6.
[111] S. Boschi *et al.*, “Synthesis and preclinical evaluation of an Al18F radiofluorinated GLU-UREA-LYS(AHX)-HBED-CC PSMA ligand,” *Eur. J. Nucl. Med. Mol. Imaging*, vol. 43, no. 12, pp. 2122–2130, 2016, doi: 10.1007/s00259-016-3437-y.
[112] N. Lenzo, D. Meyrick, and J. Turner, “Review of Gallium-68 PSMA PET/CT Imaging in the Management of Prostate Cancer,” *Diagnostics*, vol. 8, no. 1, p. 16, 2018, doi: 10.3390/diagnostics8010016.
[113] E. Al-Momani, I. Israel, and S. Samnick, “Validation of a [Al18F]PSMA-11 preparation for clinical applications,” *Appl. Radiat. Isot.*, vol. 130, no. June, pp. 102–108, 2017, doi: 10.1016/j.apradiso.2017.09.003.
[114] A. Afshar-Oromieh *et al.*, “Diagnostic performance of 68Ga-PSMA-11 (HBED-CC) PET/CT in patients with recurrent prostate cancer: evaluation in 1007 patients,” *Eur. J. Nucl. Med. Mol. Imaging*, vol. 44, no. 8, pp. 1258–1268, 2017, doi: 10.1007/s00259-017-3711-7.
[115] M. Perera *et al.*, “Sensitivity, Specificity, and Predictors of Positive 68Ga–Prostate-specific Membrane Antigen Positron Emission Tomography in Advanced Prostate Cancer: A Systematic Review and Meta-analysis,” *Eur. Urol.*, vol. 70, no. 6, pp. 926–937, 2016, doi: 10.1016/j.eururo.2016.06.021.
[116] N. Malik, B. Zlatopolskiy, H. J. Machulla, S. N. Reske, and C. Solbach, “One pot radiofluorination of a new potential PSMA ligand [Al 18F]NOTA-DUPA-Pep,” *J. Label. Compd. Radiopharm.*, vol. 55, no. 9, pp. 320–325, 2012, doi: 10.1002/jlcr.2944.
[117] T. Liu *et al.*, “Preclinical evaluation and pilot clinical study of Al18F-PSMA-BCH for prostate cancer PET imaging,” *J. Nucl. Med.*, vol. 60, no. 9, pp. 1284–1292, 2019, doi: 10.2967/jnumed.118.221671.
[118] O. Sartor *et al.*, “Lutetium-177–PSMA-617 for Metastatic Castration-Resistant Prostate Cancer,” *N. Engl. J. Med.*, vol. 385, no. 12, pp. 1091–1103, 2021, doi: 10.1056/nejmoa2107322.
[119] B. M. Privé *et al.*, “Lutetium-177-PSMA-617 in low-volume hormone-sensitive metastatic prostate cancer: A

prospective pilot study," *Clin. Cancer Res.*, vol. 27, no. 13, pp. 3595–3601, 2021, doi: 10.1158/1078-0432.CCR-20-4298.
[120] B. Lugato *et al.*, "A novel versatile precursor suitable for 18F-radiolabeling via 'click chemistry,'" *J. Label. Compd. Radiopharm.*, vol. 60, no. 10, pp. 466–480, 2017, doi: 10.1002/jlcr.3529.
[121] K. P. Maresca *et al.*, "A series of halogenated heterodimeric inhibitors of prostate specific membrane antigen (PSMA) as radiolabeled probes for targeting prostate cancer," *J. Med. Chem.*, vol. 52, no. 2, pp. 347–357, 2009, doi: 10.1021/jm800994j.
[122] S. Y. Han and Y. A. Kim, "Recent development of peptide coupling reagents in organic synthesis," *Tetrahedron*, vol. 60, no. 11, pp. 2447–2467, 2004, doi: 10.1016/j.tet.2004.01.020.
[123] O. Jacobson, D. O. Kiesewetter, and X. Chen, "Fluorine-18 radiochemistry, labeling strategies and synthetic routes," *Bioconjug. Chem.*, vol. 26, no. 1, pp. 1–18, 2015, doi: 10.1021/bc500475e.
[124] P. Ji, J. H. Atherton, and M. I. Page, "Copper catalysed azide-alkyne cycloaddition (CuAAC) in liquid ammonia," *Org. Biomol. Chem.*, vol. 10, no. 39, pp. 7965–7969, 2012, doi: 10.1039/c2ob26213d.
[125] S. Wang, Y. Gai, M. Li, H. Fang, G. Xiang, and X. Ma, "Synthesis of a new bifunctional NODA for bioconjugation with PSMA ligand and one-step Al18F labeling," *Bioorganic Med. Chem.*, vol. 60, no. February, p. 116687, 2022, doi: 10.1016/j.bmc.2022.116687.
[126] R. B. Martin, "The chemistry of aluminum as related to biology and medicine," *Clin. Chem.*, vol. 32, no. 10, pp. 1797–1806, 1986, doi: 10.1093/clinchem/32.10.1797.
[127] I. V. J. Feiner *et al.*, "Pre-targeting with ultra-small nanoparticles: Boron carbon dots as drug candidates for boron neutron capture therapy," *J. Mater. Chem. B*, vol. 9, no. 2, pp. 410–420, 2021, doi: 10.1039/d0tb01880e.
[128] D. E. Olberg *et al.*, "One step radiosynthesis of 6-[18F]fluoronicotinic acid 2,3,5,6-tetrafluorophenyl ester ([18F]F-Py-TFP): A new prosthetic group for efficient labeling of biomolecules with fluorine-18," *J. Med. Chem.*, vol. 53, no. 4, pp. 1732–1740, 2010, doi: 10.1021/jm9015813.
[129] "European Pharmacopoeia last version, monograph 3116, "PSMA-1007 (18F) Injection"." .
[130] F. Xue and C. T. Seto, "Structure-activity studies of cyclic ketone inhibitors of the serine protease plasmin: Design, synthesis, and biological activity," *Bioorganic Med. Chem.*, vol. 14, no. 24, pp. 8467–8487, 2006, doi: 10.1016/j.bmc.2006.08.040.